Dark Energy
in
Scalar-Tensor Theories

Diploma thesis

Jan Möller

Hamburg, March 2007

Abstract

We investigate several aspects of dynamical dark energy in the framework of scalar-tensor theories of gravity. We provide a classification of scalar-tensor coupling functions admitting cosmological scaling solutions. In particular, we recover that Brans-Dicke theory with inverse power-law potential allows for a sequence of background dominated scaling regime and scalar field dominated, accelerated expansion. Furthermore, we compare minimally and non-minimally coupled models, with respect to the small redshift evolution of the dark energy equation of state. We discuss the possibility to discriminate between different models by a reconstruction of the equation-of-state parameter from available observational data. The non-minimal coupling characterizing scalar-tensor models can - in specific cases - alleviate fine tuning problems, which appear if (minimally coupled) quintessence is required to mimic a cosmological constant. Finally, we perform a phase-space analysis of a family of biscalar-tensor models characterized by a specific type of $\sigma-$model metric, including two examples from recent literature. In particular, we generalize an axion-dilaton model of Sonner and Townsend, incorporating a perfect fluid background consisting of (dark) matter and radiation.

Zusammenfassung

Thema dieser Diplomarbeit sind dynamische Modelle dunkler Energie im Rahmen von Skalar-Tensor Theorien. Die in diesen Gravitationstheorien auftretenden Kopplungsfunktionen werden klassifiziert im Hinblick auf die Möglichkeit sogenannter "scaling" Lösungen. Der Ansatz führt insbesondere auf den bekannten Fall von Brans-Dicke Theorie, kombiniert mit einem Potential von der Form eines inversen Potenzgesetzes. In Modellen dieser Klasse folgt einer Phase, während der sich die dunkle Energie verhält wie die jeweils vorherrschende Fluidkomponente, eine Phase beschleunigter Expansion, die von dem skalaren Feld dominiert wird.

Verschiedene, sowohl minimal wie auch nicht-minimal gekoppelte Modelle werden verglichen hinsichtlich des Verhaltens ihrer Zustandsgleichung im Bereich kleiner Rotverschiebungen. Von besonderem Interesse ist hierbei die Frage, inwieweit es möglich ist, einzelne Modelle zu falsifizieren, indem man die Zustandsgleichung der dunklen Energie aus Beobachtungsdaten rekonstruiert. Es stellt sich heraus, dass gekoppelte Modelle unter Umständen "fine tuning"-Probleme mildern können, mit denen minimal gekoppelte Quintessenz-Modelle konfrontiert sind, die das Verhalten einer kosmologischen Konstanten nachahmen.

Schliesslich werden Modelle mit zwei skalaren Feldern behandelt. Zwei Beispiele aus der jüngeren Literatur, darunter ein Axion-Dilaton-Modell von Sonner und Townsend, werden im Phasenraum analysiert und auf phenomenologische Konsequenzen untersucht. Das Axion-Dilaton-Modell kann durch Berücksichtigung von Strahlung und Materie verallgemeinert werden.

Contents

Chapter 1

Introduction

Our knowledge of the universe is based on two very different, but in their respective domains equally convincing theoretical frameworks: on small scales, the standard model of particle physics, and on large scales, Einstein's theory of gravity. Focusing on the hot early universe, modern cosmology has, on the one hand, established an overlap between both domains. On the other hand, it has revealed the limits of the current theoretical understanding. As an entirely classical theory, general relativity breaks down at Planck scale and has to be replaced by a - yet unknown - quantum theory of gravity. The hierarchy between the Planck and the electroweak scale is furthermore one of the outstanding conceptual problems of the standard model.

Recent cosmological observations [41, 87, 90] have procured overwhelming evidence that, even in the low-energy regime, our theoretical picture of the universe is strikingly incomplete: the particle content of the standard model merely accounts for four percent of the present energy density, to a small amount in visible form (stars), but mostly as interstellar and intergalactic gas. Rotation curves of spiral galaxies imply the existence of extended halos, composed of a smoothly distributed, clustering component called dark matter - which is eventually not dark but transparent, since it interacts only gravitationally [65].

Observations of type Ia supernovae [6, 71, 79, 80, 81, 97] have led to the conclusion, that our universe is not only expanding, but accelerating. Successively, another yet unknown - but actually dominating - contribution to the universe's energy budget has been proposed: dark energy, which can be characterized as a perfect fluid with negative pressure. While high-energy physics beyond the standard model have already come up with a class of reasonable dark matter candidates (in the framework of supersymmetry), the task of including dark energy provides more of a challenge.

The easiest way to explain both the accelerated expansion and the missing 70 percent of the present energy density is provided by a cosmological constant. But to match the order of magnitude of the effect, its value requires an extreme amount of fine tuning with respect to the Planck scale. Alternatively, the dark energy density can be regarded as a dynamical quantity. In this case, its present value would naturally be small, if it is ultimately relaxing to zero, and need not be subject to fine tuning at all.

Within a huge set of different proposals, models featuring a homogeneous, canonical scalar field stand out as exceptionally simple: The evolution of the so-called quintessence field is determined only by the Hubble expansion and a self-interaction potential; interactions with the fermion and gauge sectors of the standard model (and its possible extensions) are excluded.

On the other hand, the scalar field may be regarded as part of the gravitational sector of a fundamental theory. Brans and Dicke [18] originally suggested to modify Einstein gravity by substituting the gravitational constant with a scalar field. In general, scalar-tensor theories of gravity are characterized by the appearance of a specific, "non-minimal" coupling between scalar field and spacetime curvature in the Jordan frame; while in the conformally equivalent Einstein frame description the scalar field couples universally to the trace of the matter energy-momentum tensor. In this thesis, we will focus on dynamical models based on minimally or non-minimally coupled scalar fields, and investigate their phenomenological differences.

Renewed interest in scalar-tensor theories of gravity has also been triggered by the perception, that they naturally appear in the low-energy limit of higher-dimensional physics [46]. The length scale of the compactifying internal space reappears as an additional scalar degree of freedom in the four-dimensional world, offering a connection between the dynamics of the compactification process and observationally verifiable effects. If the number of extra dimensions is larger than one, additional degrees of freedom related to the shape of the internal manifold can be included [38, 70]: these "breathing modes" may be dynamically relevant, even if the overall volume of the compactification space is considered to be stabilized already. This set-up naturally leads us to study dark energy models featuring more than one scalar field.

To provide a satisfactory solution of the dark energy puzzle, a dynamical model is not only required to reproduce the observed acceleration. Complete agreement with observational data has to be achievable without refering to any kind of fine tuning. In comparison to the cosmological constant, which is a one-parameter model, any dynamical model increases complexity. To provide promising dark energy candidates, particle physics or modified gravity theories are faced with the challenge to infer model parameters from fundamental principles. At the level of model building, the list of additional parameters should be kept short, though it might be tempting to hide a possible need of fine tuning by introducing more degrees of freedom.

Scalar field models of dark energy are exceptionally promising, if they admit attractor solutions, which naturally ensure independence of initial conditions. A special class of attractor solutions is considered to be particularly interesting: so-called "scaling solutions" exhibit a fixed relation of background fluid and dark energy densities, and a constant dark energy equation of state. By offering this kind of solution, a dynamical model might be able to explain, why matter and dark energy densities are roughly of the same order at present. More generally, a sequence of scaling solutions should be able to reproduce the sequence of radiation, matter and dark energy dominated stages of expansion, which has been established by standard cosmology.

Within the framework of scalar-tensor theories, dark energy model building does not require to specify a priori an underlying fundamental theory. Families of dynamical models are typically described in terms of a few unspecified functions: a potential and one or two non-canonical couplings. In the simple cases we are interested in, this freedom reduces to a set of constant parameters, determining e.g. potential slope and coupling strength. Phenomenological studies are useful to constrain the allowed range of those parameters. In this thesis, we will analyze and compare models in terms of the fixed point set of the respective dynamical system, using dimensionless density parameters as dynamical variables. We intend to classify viable models with respect to specific attractive properties, like the existence of (sequences of) scaling solutions.

During the course of the forthcoming decade, observational cosmologists hope to realize

a model independent reconstruction of the dark energy equation of state in the low redshift regime. Supposed this task will be successfully completed one day, the important question remains to be addressed, how to discriminate between different dark energy models. While the cosmological constant will undoubtedly be ruled out, if the slightest evolution is positively detected, certain dynamical models might not even be falsified by the equation-of-state diagnostic alone.

The thesis is organized as follows:
In chapter 2 we confront the cosmological constant with basic ideas of dynamical dark energy. In particular, we introduce quintessence, review its phenomenological properties, and give some examples of quintessence candidates within particle or gravitational physics. We comment on the current observational status of the dark energy equation of state, and cite an example of its reconstruction from recent observational data. Presently, the cosmological constant seems to be mildly favoured by the data, while a slight redshift evolution cannot yet be excluded.

Scalar-tensor theories of gravity are introduced in chapter 3. We present a specific form of biscalar-tensor action, which features three yet unspecified functions: the characteristic non-minimal coupling, a non-canonical kinetic term, and an interaction potential. The set-up is general enough to include all the different models we investigate in later chapters. We derive the general form of the coupled equations of motion, which govern the evolution of the two scalar fields. Furthermore, we review observational and experimental results on scalar-tensor gravity, and in some detail the issue of covergence towards general relativity [35].

In chapter 4 we provide a classification of coupling functions, which admit scaling solutions in scalar-tensor cosmology. We are particularly interested in the possibility of scaling solutions with large basins of attraction. We correct - as well as generalize - the findings of [73], and obtain consistency with earlier results on quintessence potentials [59]. We identify a special class of models - including original Brans-Dicke theory combined with inverse power-law potential -, which eventually allow for scaling attractor solutions during matter dominated epoch. Unfortunately, the scaling attractor does not coincide with Einstein gravity. In consequence, the coupling function is already subject to strong constraints, which pose limits on the viability of the models.

Chapter 5 addresses the issue of attractor solutions in a more general way. Within the autonomous system approach of [31], solutions with specific, phenomenologically relevant properties are represented by fixed points in phase-space. We use this method to analyze and compare several classes of quintessence and scalar-tensor models, focusing on modifications induced by the presence of the non-minimal coupling, with respect to quintessence case. To realize a sequence of background dominated scaling solutions, followed by a dark energy dominated attractor, coexistence of the corresponding fixed points is required. This is possible only in the non-minimally coupled case. Furthermore, we numerically investigate the evolution of the dark energy equation of state in the low redshift regime. We thereby hope to be able to discriminate between the different models.

In chapter 6 we generalize the phase-space method used in the preceding chapter to the case of biscalar-tensor theories. Our main interest is to discover, how the introduction of the second field modifies the phenomenological behaviour of single field models. We investigate an axion-dilaton model, which was recently proposed in [86]. While the authors neglected the background fluid contributions to the total energy density, and found recurrent acceleration to be possible, we extend the model by including (dark) matter and radiation. In our version

of the model, recurrent acceleration no longer constitutes the generic case. Furthermore, in a wide range of parameter space the model effectively reduces to a single field model, which is conformally equivalent to Brans-Dicke theory.

Additionally, we specify a subclass of models featuring a periodic potential with saddle points and minima. We show that, under certain assumptions regarding initial conditions, the phenomenologically relevant properties can be reproduced by a single field model with Gaussian potential. To give an example, we discuss a proposal of Peloso and Poppitz [70], realizing quintessence in terms of a complex shape modulus, within the framework of six-dimensional supergravity. The shape moduli potential, determined by the Casimir energy of bulk fields, is of the prescribed form.

Finally, in chapter 7 we summarize our main results and conclude.

Chapter 2

Dark Energy

Over the last few years, observational cosmologists have gathered mounting evidence, that our universe - apart from being flat - expands accelerated, confirmed by several independent observations including those of type Ia supernovae [6, 71, 79, 80, 81, 97], the cosmic microwave background (CMB) [87] and the large scale structure of the universe (LSS) [41, 90]. On the other hand, it became clear that the total amount of all known types of matter-energy, including dark matter, does not account for the critical energy density, being necessary to render the universe flat. It is widely accepted by now, that a new form of energy, the so-called dark energy (DE), presently amounts to about 70 to 75 percent of the total energy density of the universe, and is responsible for the observed acceleration. To give a precise meaning to the terminus, we consider the Einstein equations of gravity,

$$R_{\mu\nu} - \frac{1}{2} g_{\mu\nu} R = \sum_a T^a_{\mu\nu} + T^{DE}_{\mu\nu}, \tag{2.1}$$

where we have adjusted the reduced Planck mass multiplying the LHS,

$$M_p^2 := \frac{1}{8\pi G_0} \equiv 1,$$

by choice of units, and the sum on the RHS runs over all known types of relativistic and nonrelativistic (including dark) matter species.

In most cosmological applications, it is appropriate to neglect particle interactions, as well as non-equilibrium effects, and treat the different components in the approximation of a perfect fluid, characterized by its energy density ρ, pressure p and 4-velocity u^μ. In this case, the energy-momentum tensor takes the form,

$$g^{\mu\rho} T_{\rho\nu} = -(\rho + p) u^\mu u_\nu + p \delta^\mu_\nu \approx diag(-\rho, p, p, p), \tag{2.2}$$

where the second expression applies, if we neglect peculiar velocities. In the perfect fluid approximation, dark matter is just pressureless dust, while radiation (consisting of photons and relativistic particles, e.g. light neutrinos) is characterized by $p = \frac{1}{3}\rho$.

Specializing to a homogeneous and isotropic Robertson-Walker metric,

$$ds^2 = g_{\mu\nu} dx^\mu dx^\nu = -dt^2 + a^2(t)(d\chi^2 + S^2(\chi) d\Omega^2), \tag{2.3}$$

where

$$d\chi^2 = \frac{dr^2}{1 - kr^2},$$

and

$$S^2(\chi) = \begin{cases} \sinh^2\chi, & k=-1, \\ \chi^2, & k=0, \\ \sin^2\chi, & k=1, \end{cases}$$

corresponds to hyperbolic, flat and spheric geometry respectively, the Einstein equations reduce to two ordinary differential equations (ODE), governing the time evolution of the scale factor $a(t)$, the Friedmann equations:

$$H^2 := \frac{\dot{a}^2}{a^2} = \frac{1}{3}(\sum_a \rho_a + \rho_{DE}) - \frac{k}{a^2}, \tag{2.4}$$

$$\frac{\ddot{a}}{a} = -\frac{1}{6}(\sum_a \rho_a + 3p_a + \rho_{DE} + 3p_{DE}). \tag{2.5}$$

Deviding the first equation by H^2,

$$1 = \sum_a \Omega_a + \Omega_{DE} + \Omega_k, \tag{2.6}$$

we introduce the density parameters

$$\Omega_a := \frac{\rho_a}{\rho_{crit}} := \frac{\rho_a}{3H^2},$$

which measure the energy densities in terms of the critical density. We have formally defined:

$$\Omega_k := -\frac{k}{\dot{a}^2}. \tag{2.7}$$

If the corresponding energy-momentum tensor is covariantly conserved, each perfect fluid component separately obeys a continuity equation,

$$\dot{\rho_a} = -3H(\rho_a + p_a) =: -3H(1+w_a)\rho_a, \tag{2.8}$$

where we have introduced the equation of state parameter w_a, which is specified to $w_a = 0$ or $w_a = \frac{1}{3}$, if the subscript a refers to (dark) matter or radiation respectively. From (2.8) we deduce the following scaling behaviour,

$$\rho_{DM} \sim a^{-3}, \quad \rho_{rad} \sim a^{-4},$$

which indicates that radiation must have been the dynamically dominant component in the early universe. This stage is followed by a (dark) matter dominated epoch, which is crucial to the "standard model" of cosmology, since perturbation growth and structure formation is only possible in a background with $|w_{fluid}| < \frac{1}{3}$ [63].

In the following, we will always assume the universe to be flat, corresponding to Ω_k, as defined in (2.7), being exactly zero. This assumption is justified by recent observational data [90]:

$$1 - \Omega_k = 1.003^{+0.010}_{-0.009}.$$

The second Friedmann equation tells us, that accelerated expansion is only possible, if DE has negative pressure; neglecting the present contribution of radiation, we specify this condition as follows:

$$w_{DE} := \frac{p_{DE}}{\rho_{DE}} < -\frac{1}{3}\left(1 + \frac{\Omega_{DM}}{\Omega_{DE}}\right).$$

The simplest possibility to realize a perfect fluid with negative equation of state parameter ($w_{DE} = -1$) is a cosmological constant:

$$g^{\mu\lambda} T^{DE}_{\lambda\nu} = -\delta^{\mu}_{\nu}\Lambda.$$

At present, all existing observational data are in agreement with Dark Energy being a constant with [33]:

$$\rho_{DE} = \Lambda \simeq 10^{-47}(GeV)^4.$$

2.1 A brief history of the cosmological constant

Einstein's field equations of gravity can be derived from an action principle, namely by varying the Einstein-Hilbert action,

$$S = S_{geom} + S_{mat} = \frac{1}{2}\int d^4x\sqrt{-g}R + S_{mat}, \tag{2.9}$$

with respect to the metric. The Lagrangian R, called Ricci or curvature scalar, is just the simplest possible scalar to be constructed from the metric, and leading to field equations linear in its second derivatives. The most general choice with the same property includes a constant,

$$S_{geom} = \frac{1}{2}\int d^4x\sqrt{-g}(R - 2\Lambda), \tag{2.10}$$

and leads to field equations, which do not reduce to Newton's law in the weak field limit. But given the smallness of Λ, the deviation is not in conflict with experimental tests of general relativity (GR).

The vacuum solution with positive and negative cosmological constant is called de Sitter and anti-de Sitter space respectively. A representation of the de Sitter metric can be given in the form of an eponentially expanding Friedmann-Robertson-Walker (FRW) universe with constant Hubble parameter $H = \sqrt{\frac{\Lambda}{3}}$:

$$ds^2 = -dt^2 + e^{Ht}(dr^2 + r^2 d\Omega^2).$$

In 1917, yet before the FRW cosmological solutions to his field equations were discovered, Einstein [40] had introduced the cosmological constant, to guarantee the existence of a closed, static universe ($k = 1$) with a constant energy density. The corresponding Friedmann equations take the following form:

$$\frac{\dot{a}^2}{a^2} = \frac{1}{3}(\rho_{tot} + \Lambda) - \frac{1}{a^2} = 0,$$

$$\frac{\ddot{a}}{a} = -\frac{1}{6}(\rho_{tot} + 3p_{tot} - 2\Lambda) = 0,$$

with $w_{tot} = -1 + \frac{2}{a^2\rho_{tot}}$. When 1929 Edwin Hubble's observations verified the expansion of the universe [54], Einstein discarded the cosmological constant as "the biggest blunder he ever made in his life" [47].

Nevertheless it reappeared, when Zel'dovich [99] realized, that zero-point quantum vacuum fluctuations at one loop level can give rise to an energy momentum tensor of the form:

$$\langle T_{\mu\nu}\rangle_{vac} = \Lambda g_{\mu\nu}.$$

The contribution of vacuum fluctuations to a cosmological constant is formally divergent [82]:

$$\langle T_{00}\rangle_{vac} =: \rho_{vac} \sim \int_0^\infty k^2 dk \sqrt{k^2+m^2} \quad \sim \lim_{k\to\infty} k^4.$$

Assuming that the Planck scale provides the natural ultraviolet cutoff to all quantum field theoretical processes the integral can be be performed with the result,

$$\frac{\rho_{DE}}{\rho_{vac}} = 10^{-123},$$

stating the celebrated and infamous "cosmological constant problem".

An alternative approach, invented to avoid the extreme fine tuning of Λ, is to regard it as a dynamical quantity, which eventually relaxes to zero during cosmic evolution. The possibility of realizing dynamical dark energy in terms of a light, minimally coupled scalar field, called quintessence, will be addressed in the next section. The proposal of dynamical DE, however, does not solve the puzzle, why the zero-point vacuum energy should be vanishing, and only the classical energy density of a scalar field contributes to the dark energy sector. Indeed it is often quoted, that e.g. quintessence is only meant to address the so called "cosmic coincidence problem", which appears if one reformulates the cosmological constant problem in the following way:

1. *Why* is the vacuum energy density so *small* in comparison to the Planck scale?

2. *Why* has the DE density reached an order of magnitude comparable to that of the dark matter density right *now*, meaning that the onset of acceleration is a recent phenomenon?

Even if dynamical DE provides a satisfying answer to the second question (which is still in doubt), the first part of the problem remains to be addressed. On the other hand, if Λ is really a constant, the coincidence problem is automatically solved, whence the scale of Λ is deduced from some fundamental theoretical principle.

The discovery of supersymmetry in the 1970's opened up the possibility, that the vacuum energy density might be vanishing because of a precise cancellation between the bosonic and fermionic contributions [100]:

$$\langle 0|\mathcal{H}_{b,f}|0\rangle \equiv \int \langle T_{00}\rangle_{vac} = \pm\frac{1}{2}\sum_{\vec{k}} \omega_{\vec{k}}.$$

(The upper sign refers to bosons, the lower to fermions.) But even if supersymmetry (SUSY) is realized by nature, it is necessarily broken at low temperatures, corresponding to the present state of our universe. In this case, the vacuum energy density is expected to receive a contribution at an intermediate scale [82]. On the other hand, in the context of higher-dimensional extensions of standard model physics, supersymmetry can be realized in the bulk spacetime, being broken only on the 3+1-brane where we - the standard model particles - live. Dark energy on the brane then emerges from the Casimir energy of bulk fields, providing the correct energy scale, if the number of extra dimensions is $n = 2$ [29, 70].

2.2 Essentials of quintessence

We consider a classical scalar field theory, minimally coupled to gravity, defined by the action

$$S_\phi = \int d^4x\sqrt{-g}\left(-\frac{1}{2}g^{\mu\nu}\partial_\mu\phi\partial_\nu\phi - V(\phi)\right), \tag{2.11}$$

with energy-momentum tensor

$$T^\phi_{\mu\nu} = -\frac{2}{\sqrt{-g}}\frac{\delta S_\phi}{\delta g^{\mu\nu}} = \partial_\mu\phi\partial_\nu\phi - g_{\mu\nu}\left(\frac{1}{2}\partial^\sigma\phi\partial_\sigma\phi + V(\phi)\right).$$

Taking the field to be homogeneous, we identify its pressure and energy density - in analogy to the perfect fluid case - as:

$$p_\phi = \frac{1}{2}\dot{\phi}^2 - V(\phi), \qquad \rho_\phi = \frac{1}{2}\dot{\phi}^2 + V(\phi).$$

Such a scalar density fluid satisfies the dominant energy condition,

$$\rho \geq |p|,$$

and has a time dependent equation-of-state-parameter,

$$1 \geq w_\phi \geq -1.$$

Since

$$p_\phi = -\rho_\phi + \dot{\phi}^2,$$

the kinetic contribution determines the actual value of w_ϕ. If the field energy density is dominated by the kinetic part, the equation of state is called "stiff" ($w_\phi \approx 1$). If the potential energy dominates, indicating the so-called "slow-roll" regime, the equation-of-state parameter can be close to $w_\phi = -1$. When we refer to a minimally coupled scalar field as quintessence, it is understood that the self-interaction potential allows for a (sufficiently) negative equation of state.

In a FRW cosmological background, the scalar field obeys the following Klein-Gordon equation:

$$\ddot{\phi} + 3H\dot{\phi} + \frac{dV}{d\phi} = 0. \tag{2.12}$$

To realize slow-roll we need $\ddot{\phi} \approx 0$, and the force term to be balanced by Hubble friction:

$$-\frac{dV}{d\phi} \approx 3H\dot{\phi}.$$

Since the latter has become small up to the present, the potential has to be flat. Furthermore, the energy density of the quintessence field (that is, the potential) must be of order H_0^2 at present, corresponding to the critical density:

$$3H^2 = \rho_{crit} \approx \rho_\phi \approx V(\phi).$$

The present field value will then be of order one (Planck mass), since the field mass is of order H_0 or smaller:

$$m_\phi^2 = \frac{d^2V}{d\phi^2} \sim \frac{V(\phi)}{\phi^2}.$$

If the potential has a non-zero minimum,

$$V(\phi_{min}) \neq 0,$$

we get $w_\phi = -1$, whence the field has already reached the minimum, and a cosmological constant $\Lambda = V(\phi_{min})$ is generated dynamically. If the stabilization takes place within a finite period of time, it will typically be preluded by oscillations of the equation-of-state parameter between $w_\phi = -1$ (at the turning points where $\dot{\phi} = 0$), and a value the closer to $w_\phi = 1$, the closer the potential minimum is to zero (when the field passes its minimum value). Since observational evidence points to $w_\phi \simeq const$ around the present, oscillations are potentially dangerous from the phenomenological point of view. Therefore, a promising ansatz of quintessence model building is to assume, that either the scalar field has not yet entered the oscillatory stage, or its potential is of the runaway type.

The invention of quintessence goes back to Wetterich [68, 95, 96], who proposed an exponential potential,

$$V = \Lambda e^{-\lambda\phi},$$

and Ratra and Peebles [69, 77], who discussed in addition an inverse power-law potential,

$$V = \Lambda \phi^{-\alpha},$$

where the field value is measured in Planck units. Both the types of potentials have in common, that they admit so-called "scaling solutions" of the field equations. Liddle and Scherrer [59] provided a "classification of scalar field potentials with cosmological scaling solutions", defining a scaling solution as follows: The corresponding scalar field energy density *scales* as some power of the scale factor,

$$\rho_\phi \sim a^{-n},$$

which is equivalent to the kinetic and potential energy maintaining a fixed ratio [59]:

$$\frac{\dot{\phi}^2}{\rho_\phi} = 1 + w_\phi = \frac{n}{3}.$$

Assuming the expansion of the universe to be driven by a dominating background fluid,

$$\rho_{fluid} \sim a^{-m},$$

where $m = 3(1 + w_{fluid})$, Liddle and Scherrer found scaling behaviour of the scalar density to be possible, if and only if the scalar potential belongs to one of the three following classes:

1. Inverse power-law: scaling with $n < m$ (ρ_ϕ decreases more slowly than ρ_{fluid});

2. Exponential: scaling with $n = m$;

3. Positive power-law: scaling with $n > m$ (ρ_ϕ decreases more rapidly than ρ_{fluid}).

Furthermore, they showed that in case 1 the scaling solution is always an attractor in field space, whereas in case 3 this is only true for sufficiently large powers α:

$$\alpha > 2\,\frac{6+m}{6-m}.$$

(Case 2 will be discussed in detail in chapter 5.)

The interest in scaling solutions was originally motivated by the hope to solve the aforementioned cosmic coincidence problem. The existence of an attractor solution, along which the energy density of the scalar field follows the one of the background fluid, can explain why the respective density parameters are of the same order now. But to become the dominant component, the scalar field must have exited the scaling regime recently. In the inverse power-law case, the scalar field density parameter increases with time along the scaling solution, and will therefore naturally become the dominant component at some instance during cosmic history. But matching the observationally verified onset of acceleration will still require some tuning. (We will reexamine this issue in chapter 5.)

A slightly more general notion was introduced in terms of "cosmological tracking solutions" [88], characterized by the property, that phase-space trajectories of the corresponding system of ordinary differential equations (ODE) converge to a common evolutionary track, from a wide range of initial conditions. The tracker solution need not be a scaling solution, nor an attractor solution characterized by the constancy of specific dynamical quantities. Inverse power-law potentials provide typical examples for this class of models.

In summary, the most appealing feature of dynamical DE in the shape of quintessence is the existence of attractor, or at least "tracker" solutions, which seem to guarantee independence of initial conditions, thereby avoiding the fine tuning problem of the cosmological constant.

2.3 Quintessence candidates

From the phenomenological point of view, the ideal quintessence candidate is a light scalar field, minimally coupled to gravity, lacking any kind of interaction apart from gravitational. A Yukawa type coupling to ordinary matter fermions e.g. would induce a long range force, given the small mass of the scalar particle, and is severely constrained by fifth force experiments and gravity tests [12, 36]. The issue of varying fine structure constant and proton-electron mass ratio within quintessence models is discussed e.g. in [57].

Another consequence of interactions between the matter and the DE sector concerns their respective energy-momentum tensors. The Bianchi identities imply, that the Einstein tensor is covariantly constant,

$$\nabla^\mu G_{\mu\nu} := \nabla^\mu (R_{\mu\nu} - \frac{1}{2} g_{\mu\nu} R) = 0,$$

thus the *total* energy momentum tensor on the RHS is a conserved quantity. But in presence of mutual couplings, the several contributions to the energy momentum tensor in equation (2.1) are not seperately conserved.

2.3.1 Axions

The axion is an example of a light pseudo-Nambu-Goldstone boson, which emerges from a dynamical solution of the strong CP problem. Peccei and Quinn [66, 67] suggested to enlarge the standard model gauge group by an additional global $\mathrm{U}(1)_{PQ}$ chiral symmetry, whose spontaneous breakdown is associated with the appearence of a none-zero vacuum expectation value of a complex scalar field:

$$\langle \Phi \rangle = f_a e^{ia/f_a}.$$

The axion a acquires a mass due to non-perturbative QCD instanton effects, which break the symmetry explicitely down to a discrete subgroup $Z(N)$. The effective potential thereby generated is periodic, with period $\Delta a = 2\pi \frac{f_a}{N}$, and can be written qualitatively as [45, 85]:

$$V(a) \sim m_a^2(1 + \cos(a\frac{N}{f_a})).$$

The axion couples to standard model gauge fields via:

$$\mathcal{L}_c \sim \frac{a}{f_a} Tr(FF^*),$$

where F^* is the dual to the field strength tensor F. In the framework of string theory [89], the terminus axion more generally refers to a pseudoscalar boson with the characteristic shift symmetry

$$a \to a + 2\pi \frac{f_a}{N}.$$

2.3.2 Dilatons

Dimensional reduction of five dimensional Kaluza-Klein theory,

$$S_5 = \frac{1}{2\kappa_5} \int d^5y \sqrt{-g_5} R_5,$$

using the metric ansatz [14],

$$g_{5,ab} = \begin{pmatrix} g_{\mu\nu} + \phi B_\mu B_\nu & \phi B_\mu \\ \phi B_\nu & \phi \end{pmatrix},$$

results in the following low-energy effective action:

$$S_4 = \frac{1}{2} \int d^4x \sqrt{(-g)(-\phi)} (R - \frac{1}{4}\phi F_{\mu\nu}F^{\mu\nu}). \tag{2.13}$$

By conformal transformation (local Weyl rescaling) and field redefinition, this action can be rewritten as follows:

$$S_4 = \frac{1}{2} \int d^4x \sqrt{-g} (R - \frac{1}{4}\Phi F_{\mu\nu}F^{\mu\nu} - \frac{1}{6\Phi^2} g^{\mu\nu}\partial_\mu\Phi\partial_\nu\Phi). \tag{2.14}$$

Here

$$F_{\mu\nu} = \partial_\mu B_\nu - \partial_\nu B_\mu$$

is the electromagnetic field strength, and the field Φ is called dilaton. Being conformally related to the 55-component of the five-dimensional metric tensor g_5, the dilaton is associated with a characteristic length scale of the compactified internal space.

The coupling of the dilaton to the Yang-Mills gauge field gives rise to a time dependence of the effective coupling constant,

$$\frac{1}{\alpha_{eff}^2(\Phi)} = \frac{1}{\alpha_{em,0}^2} + \Phi(t),$$

and thereby to a violation of the Einstein equivalence principle [36]. Since different atoms possess different electromagnetic field contributions to their mass energy, the field dependence of the electromagnetic coupling induces a composition dependence of the gravitational interaction, and thereby a violation also of the weak equivalence principle (cf. universality of free fall).

In string theory, the scalar partner of the graviton, within the 10-dimensional gravity supermultiplet, is called dilaton, whereas the terminus radion has been invoked to denote a scalar field, which represents the size of a compactified internal space, or an inter-brane-distance, in higher-dimensional models [25, 92].

2.3.3 Moduli fields

Within string cosmology [30], scalar degrees of freedom, e.g. corresponding to standard model parameters, receive a geometrical interpretation as "breathing modes" of the compactifying internal manifold (Calabi-Yau threefold), called moduli fields. Apart from the dilaton and an overall volume modulus, different Kähler moduli, e.g. associated with 4-cycle volumes, and "complex structure" or "shape" moduli can be phenomenologically relevant. Complex moduli fields are typically decomposed,

$$T = e^{-\Phi} + i\sigma,$$

into a "dilatonic" part Φ, associated with a (real-valued) volume or length scale, and its axionic partner σ, obeying the characteristic shift symmetry [16].

It is commonly assumed that all those scalar fields become stabilized - together with the geometry of the internal manifold - by flux compactification, before or during the inflationary epoch. (See [16] for an example of "Roulette inflation", featuring a Kähler modulus and its axionic partner.) Since the scalar fields are typically associated with certain fundamental parameters, it is phenomenologically dangerous to permit, that some of the moduli have not yet been stabilized, because resulting e.g. in varying coupling constants. The possibility of exploring moduli fields as quintessence candidates is therefore limited.

The six-dimensional model of Peloso and Poppitz [70] - similar ideas were formulated earlier in [74] - can be regarded as a toy version of the prescribed approach. The authors consider two extra dimensions, compactified on an orbifolded torus T^2/Z_2, whose area (resp. the corresponding volume modulus, called radion) is assumed to be already stabilized. The complex shape modulus instead remains dynamically relevant up to the present, and is regarded as quintessence candidate. (See chapter 6 for a detailed discussion, and [23] concerning the impact on time variation of the electromagnetic fine-structure constant.)

2.3.4 Universal metric coupling

We now consider the possibility, that the quintessence type scalar couples to all standard model fields (which we formally summarize by Ψ) in a universal way, via a factor $A^{-2}(\Phi)$ multiplying the trace of the matter energy-momentum tensor, so that

$$S_{mat} = S_{SM}[\Psi, A^{-2}(\Phi) g^{\mu\nu}].$$

The connection between this ansatz and the form of the coupling, as appearing in the scalar equation of motion, will be made explicit in the next chapter, see equations (3.14) and (3.22).

In this case, the model is no longer faced with the complication of varying α_{em}, since the energy momentum tensor of the electromagnetic field is traceless. Furthermore, we can absorb the scalar coupling into the metric by a conformal transformation,

$$A^2(\Phi)g_{\mu\nu} =: g^{new}_{\mu\nu},$$

thereby avoiding any violation of the Einstein and weak equivalence principles [36]. The resulting theory belongs to the class of scalar-tensor theories of gravity, which will be discussed in general in the next chapter.

To give an example, we refer to Brax and Martin [20], who examined the possibility of obtaining quintessence from a Kähler modulus, within a ten-dimensional supergravity framework. In their "no-scale quintessence" approach, a universal field dependence of the standard model particle masses is predicted. Unfortunately, the coupling strength is in conflict with the bound from the Cassini spacecraft experiment [12]. The authors are led to the conclusion, that quintessence models from supergravity are either experimentally ruled out, or indistinguishable from a cosmological constant. The scalar potential they derived from the superpotential and soft breaking terms,

$$V_{DE} = Ae^{-\alpha\Phi} + Be^{-\beta\Phi},$$

is modified due to the predicted universal coupling,

$$V_{eff} = V_{DE} + \frac{d\ln A(\Phi)}{d\Phi}\rho_{mat},$$

now possessing a minimum, at which the field can be stabilized.

2.3.5 The SUGRA potential

An earlier approach of Brax and Martin [21] to understand quintessence within supergravity, has become quite popular in the literature. They proposed the following, commonly called SUGRA potential,

$$V(\Phi) \sim \Phi^{-\alpha}\exp(\beta\Phi^2),$$

which can be approximately identified with an inverse power-law potential, as long as the exponential correction factor is close to unity, but has a minimum at

$$\Phi_{min} = \sqrt{\frac{\alpha}{2\beta}},$$

which restricts the field to finite values. This potential belongs to the "tracking" class and has the phenomenologically compelling property, that it leads to an equation of state parameter of $w \simeq -0.82$, almost independently of α [19].

2.3.6 K-Essence and phantom fields

A certain relative of quintessence is obtained by introducing a generalized scalar field Lagrangian [5],

$$\mathcal{L} = p(\phi, X), \qquad X := \frac{1}{2}(\nabla\phi)^2,$$

containing - in principle - arbitrary functions of the kinetc term. The issue of scaling solutions in k-essence models was discussed in [3], and Bonvin et al. [17] presented "a no-go theorem for k-essence dark energy", based on the argument that k-essence implies a DE sound speed exceeding the speed of light, but there is ongoing debate on this issue [22, 42].

The so-called phantom DE, which has become popular in recent literature [48], can be regarded as a special case of k-essence, characterized by the choice:

$$p(\phi, X) = X - V(\phi).$$

Here X exhibits the "wrong" sign, corresponding to negative kinetic energy, leading to a "super-negative" equation of state $w_{DE} < -1$. It has been claimed, that a Lagrangian of this type can be derived within quantum cosmology [91]. In the following section we will comment on the observational status of this approach.

2.4 Observational evidence: cosmological constant vs. dynamical dark energy

A revived interest in dynamical models of scalar field DE was triggered by the release of the so called "Gold data set" of luminosity distances to 194 type Ia supernovae in 2004 [81], which seemed to indicate, that the cosmological constant is disfavoured with respect to a dynamical model with time varying equation-of-state parameter, and more, with w_{DE} crossing the "phantom divide line" towards values $w_{DE} < -1$ quite recently. Following a recent publication [1], we will discuss this development below. Our first purpose is to give an overwiew of observational tools and results, which are relevant to the study of dark energy.

2.4.1 Luminosity distance measurements and type Ia supernovae

In a flat FRW spacetime, the Hubble rate can be expressed in terms of the luminosity distance d_L,

$$H(z) = \left[\frac{d}{dz}\frac{d_L(z)}{1+z}\right]^{-1},$$

where z denotes the redshift parameter,

$$1 + z = \frac{a_0}{a},$$

and the luminosity distance can be observationally infered from estimates of both the absolute (M) and apparant magnitude (m) of a source:

$$m - M = 5\log_{10}\left(\frac{d_L}{Mpc}\right) + 25.$$

If the different components of the energy density are characterized by constant equation-of-state parameters w_a, the following identity holds:

$$d_L(z) = \frac{1+z}{H_0}\int_0^z \frac{dz'}{\sqrt{\sum_a \Omega_{a,0}(1+z')^{3(1+w_a)}}}.$$

To include the possibility of varying $w_{DE}(z)$, one has to choose a parametrization of the equation of state, valid in the small redshift regime [1, 33].

Another quantity of diagnostic relevance is the deceleration parameter:

$$q := -\frac{\ddot{a}}{aH^2} = \frac{(1+z)}{H(z)}\frac{dH}{dz} - 1.$$

The zero of $q(z)$ indicates the onset of accelerated expansion, which occurs - according to observations - between $z \approx 0.3$ and $z \approx 1$, depending on the model under consideration.

Type Ia supernovae are regarded as standard candles, characterized by a common absolute magnitude independent of z, presuming not only homogeneity of the progenitor population, but also the existence of a unique explosion mechanism. According to the widely accepted "standard model" of type Ia supernovae [58], they occur in close binaries with at least one white dwarf. Suppose the companion is a red giant star, whose envelope has expanded up to filling his Roche volume, causing a mass flow towards its neighbour. The white dwarf accretes material until his total mass reaches the Chandrasekhar limit. At this point, carbon burning ignites in the stellar core, initializing a thermonuclear explosion. The net reaction,

$$2\,^{12}\mathrm{C} + 2\,^{16}\mathrm{O} \rightarrow {}^{56}\mathrm{Ni},$$

converts around one half of the stellar mass to ^{56}Ni, the total energy release being proportional to the so-called "nickel mass". The radioactive decay,

$${}^{56}\mathrm{Ni} \rightarrow {}^{56}\mathrm{Co} \rightarrow {}^{56}\mathrm{Fe},$$

results in emission of $\gamma-$photons, and in succession Compton and resonant scattering processes transfer the emission to the visual part of the electromagnetic spectrum. So the integrated luminosity of the supernova is proportional to the nickel mass produced by thermonuclear burning, which defines a one parameter family of events. (The variation in this parameter is assumed to be small, because the total mass of the exploding star is bound by the Chandrasekhar mass.) Crucial for observers is the empirical fact, that the peak brightness of the event is linearly correlated to the width of the lightcurve [98]: brighter supernovae evolve more slowly. While the observed peak brightness may be subject to extinction processes, the lightcurve shape is not.

The standard scenario discussed so far does not account for the observed spectral diversity of type Ia supernovae [10], which indicates the existence of different classes of progenitors, supported by the observed dependence of the type Ia supernova rate on redshift and host galaxies [60]. On the other hand, there is ongoing debate on the issue of a second parameter (e.g. metallicity), influencing the lightcurve shape and thereby possibly biasing the luminosity calibration. According to [75], effects of metallicity evolution can be misjudged as indicating an evolution of the DE equation of state.

We want to emphasize one more aspect of the physics of type Ia supernovae. We already mentioned, that scalar-tensor theories of gravity may provide viable DE models. Those theories - as will be discussed in the following chapter - are characterized by the prediction of a varying gravitational constant (or varying particle masses, respectively). This results in a time variation of the Chandrasekhar mass limit, and implies a time dependent modification to supernova luminosities:

$$M - M_0 = \frac{15}{4}\log\left(\frac{G}{G_0}\right).$$

Here M is the absolute magnitude of an event at a given redshift, G the corresponding value of the gravitational constant, and the subscript 0 refers to the local values. As was shown in [51], the effect modifies lightcurve shapes as well, thereby further influencing distance estimates.

2.4.2 Observations of the CMB

The presence of DE affects the CMB temperature anisotropies, expanded in spherical harmonics,

$$\frac{\delta T}{T} = \sum a_{lm} Y_{lm},$$

in at least two ways [33, 63]. First, the position of the acoustic peaks depends on the angular diameter distance to the last scattering shell:

$$D = \int_0^{z_{dec}} \frac{dz'}{\sqrt{\Omega_{mat,0}(1+z')^3 + \Omega_{DE,0} f(z')}},$$

where z_{dec} is the redshift at decoupling and

$$f(z) := \frac{\rho_{DE}(z)}{\rho_{DE,0}} = \exp\left(3\int_0^z dz' \frac{1+w_{DE}(z')}{1+z'}\right)$$

accounts for dynamical variation of the equation of state. Secondly, the CMB spectrum,

$$C_l := \langle |a_{lm}|^2 \rangle = 4\pi \int \frac{dk}{k} P_{init}(k) |\Delta_l(k, \eta_0)|^2,$$

where $P_{init}(k)$ is an initial power spectrum, depends on the transfer function $\Delta_l(k, \eta_0)$ for the l multipole of the k-th wavenumber, at the present (conformal) time η_0. This function receives an additive contribution from the so-called "integrated Sachs-Wolfe (ISW) effect", emerging from variations of the gravitational potential along the line of sight. While the gravitational potential is constant during matter dominated epoch, according to standard ΛCDM cosmology, it becomes time-dependent, if the dark energy component is either dominant or dynamically changing.

2.4.3 Baryon acoustic oscillations

A remarkable confirmation of standard cosmology has been the recent detection of a peak in the power spectrum of galaxy correlation functions, as obtained by the Sloan Digital Sky Survey (SDSS) of luminous red galaxies [41]. Though acoustic oscillations (sound waves) in the tightly coupled, hot baryon-electron-photon plasma cease at decoupling, they leave an imprint in the baryon density disribution. In combination with CMB data, the BAO peak can be used to reduce the number of priors, necessary for parameter estimation, by one, though per se it says nothing about the dynamics of DE at present.

In combination with type Ia supernova observations, the BAO data lead to a significant constraint in the $(\Omega_{mat,0}, w_{DE,0})$-parameter plane. The most recent data release, first results from the ESSENCE supernova survey [97], combined with the results of [41], has provided new estimates of $\Omega_{mat,0}$ and $w_{DE,0}$. Assuming flat FRW geometry, and imposing a prior of constant w_{DE}, the ESSENCE collaboration (applying two different lightcurve fitting procedures to the supernova sample) obtained the following, best fit values:

$$w_{DE,0} = -1.047^{+0.125}_{-0.124}, \qquad \Omega_{mat,0} = 0.274^{+0.032}_{-0.020},$$
$$w_{DE,0} = -0.988^{+0.110}_{-0.109}, \qquad \Omega_{mat,0} = 0.284^{+0.031}_{-0.020}.$$

For comparison, we cite the results of the SDSS large-scale real-space power spectrum measurement [90], combined with CMB data obtained by the Wilkinson Microwave Anisotropy Probe [87]. Assuming flatness and constant w_{DE}, the following parameter estimates were obtained:

$$w_{DE,0} = -0.94 \pm 0.09, \qquad \Omega_{mat,0} = 0.24 \pm 0.02.$$

2.4.4 Cosmological constant vs. phantom DE

In [1] the authors reconstruct the DE equation of state from two complementary supernovae datasets, the newly released "Gold+HST sample" [79], comprised of 135 supernovae up to $z = 1.755$, and data of the SuperNova Legacy Survey (SNLS) [6], including 115 supernovae below $z = 1$. They use the following parametrization of the squared Hubble rate,

$$\frac{H^2}{H_0^2} = \Omega_{mat,0}(1+z)^3 + \sum_{i=0}^{2} A_i (1+z)^i,$$

and marginalize over $\Omega_{mat,0} = 0.28 \pm 0.03$. The best fit results are shown in figures 2.1 and 2.2, which are taken from [1]. As is obvious from figure 2.1, the newly released dataset favours phantom divide line crossing (just like the preceding one [81]), while the SNLS data lead to a contradictory conclusion: the best fit $w_{DE}(z)$, as shown in figure 2.2, exhibits only very mild evolution, with $w_{DE}(z) = -1$ well within 2σ confidence levels. This discrepancy may be a result of the different lightcurve standardization techniques used by the two teams (see [6]), the fact that the Gold+HST sample contains data from two different surveys, or due to systematic bias.

In addition the authors of [1] combine the supernova data with observational results concerning BAO [41] and the CMB (WMAP 3-year [87]), using the marginalization $\Omega_{mat,0} = 0.28 \pm 0.03$ for the entire dataset. As can be observed in figures 2.3 and 2.4, the respective results from the two different supernova samples become "strikingly similar" [1], because the additional CMB and BAO data impose strong constraints. (The authors point out, that the WMAP and BAO data strongly depend on the marginalization value of the matter density, and therefore their use in conjunction with the supernovae data might be questionable.) While now ΛCDM cosmology - as well as weakly time dependent DE - is consistent with the results, the evidence of phantom divide line crossing is significantly reduced. (Compare figures 2.1 and 2.3.)

In summary, following the conclusions of [1], the fundamental question, whether DE is a dynamical quantity or just the cosmological constant, still remains open, though "possible deviation of DE properties from those of Λ is gradually becoming more and more restricted" [1]. Furthermore we want to emphasize, that phantom DE is supported only by one dataset based on supernova observations. Given our yet limited understanding of the physics of type Ia supernovae (as was discussed in a preceding subsection), this evidence has to be treated with the necessary caution. (See also [56] concerning the perspective of future SNe surveys to be capable of discriminating between dynamical DE and Λ.) In this thesis, we will stick to the more conservative interpretation of the data, and consider only scalar fields with positive kinetic energy.

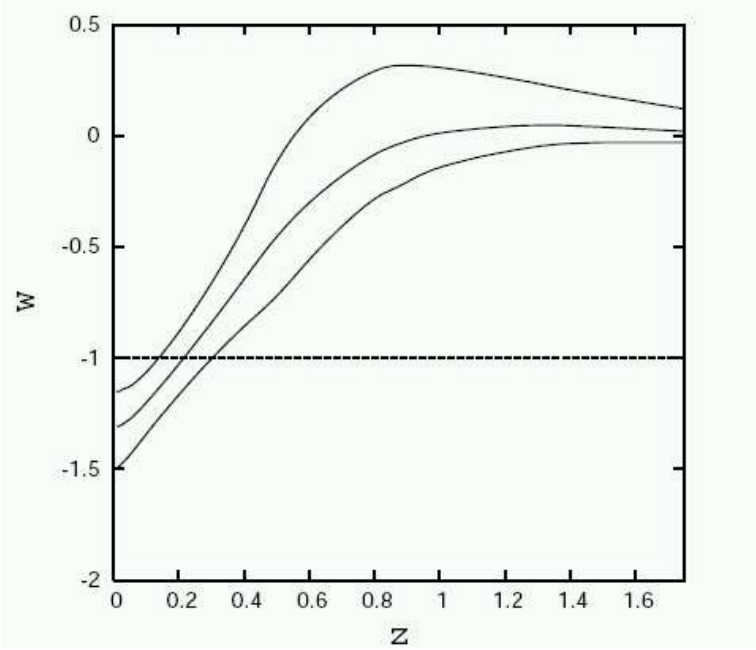

Figure 2.1: Reconstruction of $w_{DE}(z)$ from the Gold+HST dataset, best fit with 2σ confidence levels. Figure taken from [1].

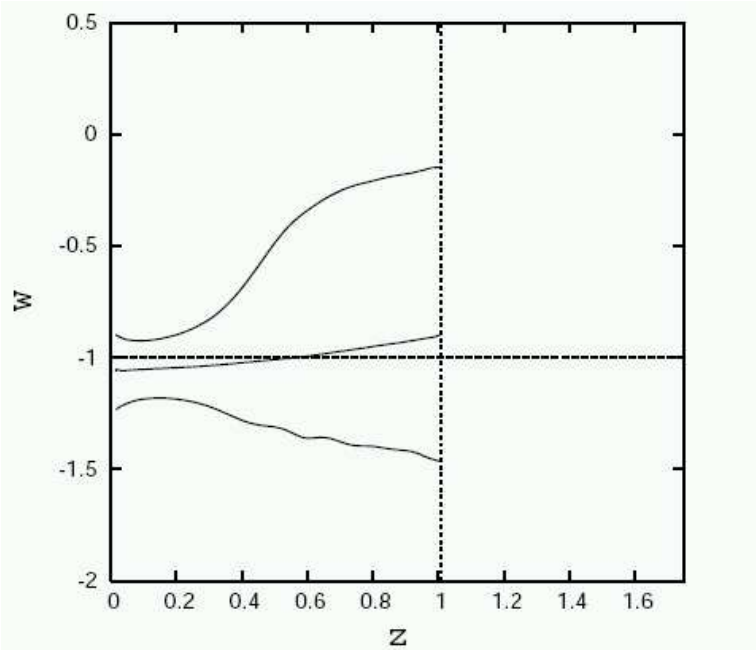

Figure 2.2: Reconstruction of $w_{DE}(z)$ from the SNLS dataset, best fit with 2σ confidence levels. Figure taken from [1].

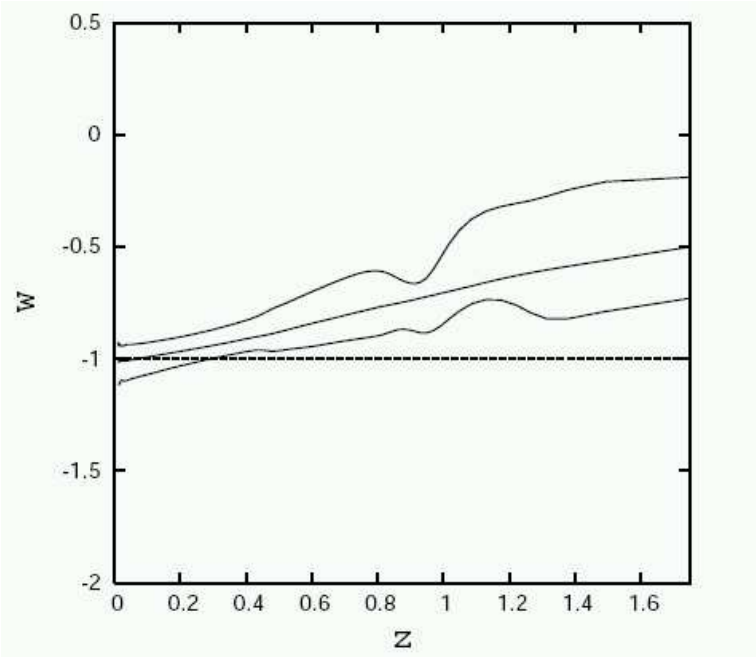

Figure 2.3: Reconstruction of $w_{DE}(z)$ from the Gold+HST dataset, combined with CMB+BAO data, best fit with 2σ confidence levels. Figure taken from [1].

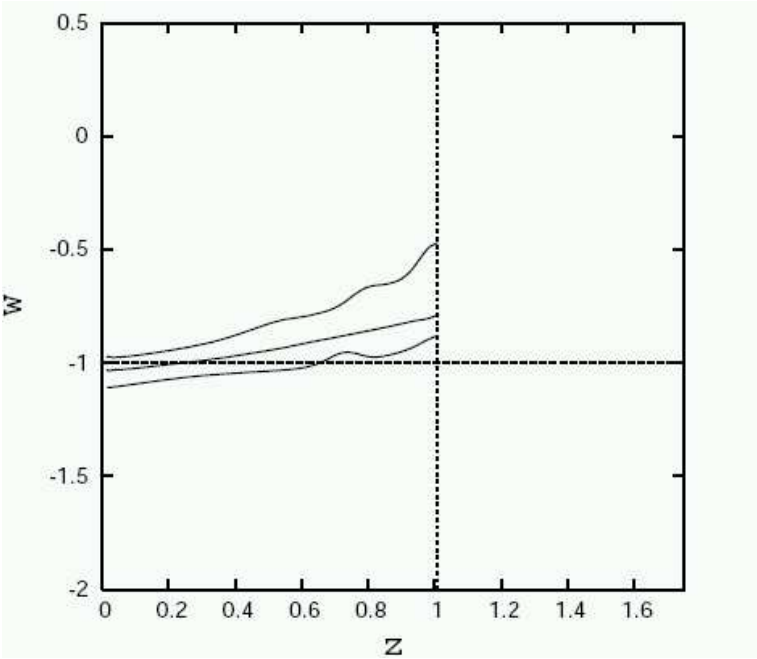

Figure 2.4: Reconstruction of $w_{DE}(z)$ from the SNLS dataset, combined with CMB+BAO data, best fit with 2σ confidence levels. Figure taken from [1].

Chapter 3

Scalar-Tensor Theories of Gravity

As mentioned in the previous chapter, considering a quintessence candidate, which exhibits universal metric coupling, leads us to study scalar-tensor gravity. The Φ-dependent, conformal transformation of the metric results in a new form of coupling between scalar field and Ricci curvature, called non-minimal coupling,

$$\mathcal{L}_{nmc} = F(\phi)R,$$

in the so-called Jordan frame formulation of the theory. The prototype theory, establishing non-minimal coupling, was developed by Jordan [55], Brans and Dicke [18], and will be discussed below.

Many authors distinguish between (particle) "physical" and "geometrical" approaches to understand dark energy, and refer to scalar-tensor theories as example for the latter. There is a certain ambiguity in this classification since, classically, the Jordan frame theory is conformally equivalent to the Einstein frame description, including a scalar field, which universally couples to matter, thereby inducing Φ-dependent masses [28, 44]. So within scalar-tensor theory we recover a property of the cosmological constant, which also can be understood either as "geometrical" (cf. a modification of the LHS of Einstein's equations),

$$G_{\mu\nu} - \Lambda g_{\mu\nu} = T^{mat}_{\mu\nu},$$

or as "physical" vacuum energy, adding to the energy-momentum tensor:

$$G_{\mu\nu} = T^{mat}_{\mu\nu} + T^{vac}_{\mu\nu}.$$

In the following sections, we write down both the Jordan frame field equations of gravity, corresponding to the geometrical interpretation of dark energy, as well as the Einstein frame formulation featuring a scalar field, which is frequently named "extended" or "coupled" quintessence in the literature.

3.1 Brans-Dicke theory

The original motivation to consider a gravity theory, modified by introduction of a scalar field, was Dirac's argument [39], that the gravitational constant should be time dependent. Jordan [55] proposed the following general Lagrangian,

$$\mathcal{L}_J = \sqrt{-g}[\phi_J^\gamma(R - \frac{\omega_J}{\phi_J^2} g^{\mu\nu}\partial_\mu\phi_J\partial_\nu\phi_J) + \mathcal{L}_{mat}(\phi_J, g^{\mu\nu}, \Psi)],$$

with constants γ, ω_J, and Ψ again denoting standard model matter fields in summary, motivated by the embedding of a four-dimensional curved spacetime manifold in five-dimensional Minkowski space. (Compare e.g. the effective four-dimensional action of Kaluza-Klein theory, given in section 2.3.)

In Jordan's Lagrangian, both the non-minimal coupling between scalar field and R, as well as (non-universal) matter couplings are present. To ensure validity of the weak equivalence principle, Brans and Dicke [18] reformulated Jordan's ansatz, demanding S_{mat} to be independent of ϕ:

$$S_{geom} = \frac{1}{2}\int d^4x\sqrt{-g}\phi_{BD}[R - \frac{\omega}{\phi_{BD}^2} g^{\mu\nu}\partial_\mu\phi_{BD}\partial_\nu\phi_{BD}]. \tag{3.1}$$

In this action, the gravitational constant is replaced by the spacetime dependent Brans-Dicke (BD) scalar:

$$\frac{1}{8\pi G} \rightarrow \phi_{BD}.$$

In the original theory (3.1), the scalar field's kinetic term is not written in canonical form. By a redefinition of the field,

$$\phi_{BD} =: \xi\phi^2, \qquad \xi := \frac{1}{2\omega},$$

the action can be rendered into the form:

$$S_{geom} = \int d^4x\sqrt{-g}\frac{1}{2}[\xi\phi^2 R - g^{\mu\nu}\partial_\mu\phi\partial_\nu\phi].$$

In general, a scalar-tensor theory of gravity is characterized by two independent functions, the coupling $F(\phi)$ and a potential $V(\phi)$:

$$S_{geom} = S_{nmc} + S_\phi = \frac{1}{2}\int d^4x\sqrt{-g}F(\phi)R + \int d^4x\sqrt{-g}\left[-\frac{1}{2}g^{\mu\nu}\partial_\mu\phi\partial_\nu\phi - V(\phi)\right]. \tag{3.2}$$

The introduction of a potential term is necessary, if one wishes to allow for a negative equation of state $w_\phi < -\frac{1}{3}$, and therefore a crucial prerequisite to realize models of dynamical dark energy within the framework of scalar-tensor gravity.

3.2 Field equations

By varying the action (3.2) with respect to the metric, we derive the modified LHS of Einstein's equations:

$$\begin{aligned}\delta S_{nmc} &= \frac{1}{2}\int d^4x[F(\phi)R\,\delta\sqrt{-g} + \sqrt{-g}F(\phi)R_{\mu\nu}\delta g^{\mu\nu} + \sqrt{-g}F(\phi)g^{\mu\nu}\delta R_{\mu\nu}] \\ &= \frac{1}{2}\int d^4x(\sqrt{-g}[F(\phi)(R_{\mu\nu} - \frac{1}{2}g_{\mu\nu}R)\delta g^{\mu\nu}] + \sqrt{-g}F(\phi)g^{\mu\nu}\delta R_{\mu\nu}). \end{aligned} \tag{3.3}$$

Apart from the factor $F(\phi)$ multiplying the Einstein tensor $G_{\mu\nu}$, further deviation from GR is determined by the last term: Due to the appearance of $F(\phi)$, it is impossible to recast this part of the integrand into a total divergence. We have to compute $\delta R_{\mu\nu}$ explicitely [25]:

$$\delta R_{\mu\nu} = \nabla_\alpha(\delta\Gamma^\alpha_{\mu\nu}) - \nabla_\nu(\delta\Gamma^\alpha_{\mu\alpha}) = -\nabla_\mu\nabla_\nu(\delta g^{\mu\nu}) + \nabla_\alpha\nabla^\alpha(\delta g_{\mu\nu}g^{\mu\nu}).$$

Integrating twice by parts, we pick up derivatives of $F(\phi)$ and finally get:

$$\delta S_{nmc} = \frac{1}{2}\int d^4x\sqrt{-g}[F(\phi)G_{\mu\nu} - \nabla_\mu\nabla_\nu F(\phi) + g_{\mu\nu}\nabla_\alpha\nabla^\alpha F(\phi)]\delta g^{\mu\nu}.$$

The Jordan frame field equations of gravity thereby obtained read as follows,

$$F(\phi)G_{\mu\nu} - \nabla_\mu\nabla_\nu F(\phi) + g_{\mu\nu}\nabla_\alpha\nabla^\alpha F(\phi) - T^\phi_{\mu\nu} = T^{mat}_{\mu\nu}, \tag{3.4}$$

where we have written

$$T^\phi_{\mu\nu} = \partial_\mu\phi\partial_\nu\phi - g_{\mu\nu}\left(\frac{1}{2}\partial^\sigma\phi\partial_\sigma\phi + V(\phi)\right)$$

on the LHS to emphasize the geometrical interpretation of the scalar field. Since $T^{mat}_{\mu\nu}$ does not depend on ϕ, it is covariantly conserved like in the GR case.

This is not true for $T^\phi_{\mu\nu}$, but we can split the LHS of the field equations as follows,

$$F(\phi)G_{\mu\nu} - \nabla_\mu\nabla_\nu F(\phi) + g_{\mu\nu}\nabla_\alpha\nabla^\alpha F(\phi) - T^\phi_{\mu\nu} =: G_{\mu\nu} - T^{\phi,cons}_{\mu\nu},$$

where we have defined the quantity [72]:

$$T^{\phi,cons}_{\mu\nu} = T^\phi_{\mu\nu} + \nabla_\mu\nabla_\nu F(\phi) - g_{\mu\nu}\nabla_\alpha\nabla^\alpha F(\phi) + (1 - F(\phi))G_{\mu\nu}, \tag{3.5}$$

which is indeed covariantly conserved due to the Bianchi identities.

Since we are interested in applications in cosmology, we specialize to a flat FRW universe, and assume the scalar field to be time dependent only. We find the following Friedmann equations:

$$H^2 = \frac{1}{3F}(\rho_{fluid} + \frac{1}{2}\dot\phi^2 + V(\phi) - 3H\dot F) =: \frac{1}{3}(\rho_{fluid} + \rho^{cons}_\phi), \tag{3.6}$$

$$\dot H = -\frac{1}{2F}(\rho_{fluid} + p_{fluid} + \dot\phi^2 + \ddot F - H\dot F) =: -\frac{1}{2}(\rho_{fluid} + p_{fluid} + \rho^{cons}_\phi + p^{cons}_\phi). \tag{3.7}$$

The quantities ρ^{cons}_ϕ and p^{cons}_ϕ we introduced correspond to $T^{\phi,cons}_{\mu\nu}$ as defined in (3.5).

The simplest way to obtain the scalar field equation of motion is to substitute the FRW metric directly within the action, and integrate over the spatial coordinates:

$$S_{geom} = \mathcal{V} \int dt\, a^3(t) \left[\frac{1}{2}(F(\phi)R + \dot{\phi}^2) - V(\phi) \right].$$

Varying this reduced action with respect to the field renders the Jordan frame Klein-Gordon equation:

$$\ddot{\phi} + 3H\dot{\phi} = -\frac{dV}{d\phi} + \frac{1}{2}\frac{dF}{d\phi}R, \tag{3.8}$$

with $R = (6\dot{H}+12H)$. By replacing this expression explicitely, using the Friedmann equations, we see that the scalar field couples to matter only via gravitational interaction. In other words, in scalar-tensor theories, gravity is mediated not only by the metric tensor field, but also by the BD scalar.

3.3 Biscalar-tensor action, conformal transformation and Einstein frame field equations

As was discussed in chapter 2, several existing approaches to understand DE include two different scalars (e.g. real and imaginary part of some complex field). The purpose of this section is to introduce a class of biscalar-tensor theories, which is sufficiently general to include those specific models from the literature we intend to discuss in detail in chapter 6. We propose the following action:

$$S = \int d^4x\sqrt{-g} \left[\frac{F(\phi)}{2}R - \frac{1}{2}g^{\mu\nu}(\partial_\mu\phi\partial_\nu\phi + G(\phi)\partial_\mu\sigma\partial_\nu\sigma) - V(\phi,\sigma) \right] + S_{mat}[g^{\mu\nu}, \Psi], \tag{3.9}$$

where we again denoted by Ψ the particle content of the standard model.

By a conformal transformation of the metric,

$$g_{\mu\nu} \to g^*_{\mu\nu} = F(\phi)g_{\mu\nu},$$
$$\sqrt{-g} \to \sqrt{-g^*} = F^2(\phi)\sqrt{-g},$$

the Ricci tensor and curvature scalar change according to:

$$R_{\mu\nu} \to R^*_{\mu\nu} = R_{\mu\nu} + \frac{3}{2}\frac{\partial_\mu F\partial_\nu F}{F^2} - \frac{1}{F}(\nabla_\mu\partial_\nu F + \frac{1}{2}g_{\mu\nu}\partial_\rho\partial^\rho F),$$
$$R \to R^* = g^{*\mu\nu}R^*_{\mu\nu} = F^{-1}g^{\mu\nu}R^*_{\mu\nu}.$$

We obtain

$$R = FR^* - \frac{3}{2}\frac{g^{*\mu\nu}\partial_\mu F\partial_\nu F}{F} + 3\partial_\rho\partial^\rho F,$$

to be replaced within the Lagrangian. The last term can be neglected, since it is a total divergence and does not change the equations of motion.

By a redefinition of the scalar field,

$$\left(\frac{d\Phi}{d\phi}\right)^2 = \frac{3}{2F^2}\left(\frac{dF}{d\phi}\right)^2 + \frac{1}{F},$$

we can compensate for the additional terms, and render the field's kinetic term into canonical form:

$$\begin{aligned}\frac{\sqrt{-g^*}}{F^2}&\left(-\frac{3}{4}g^{*\mu\nu}\partial_\mu F\partial_\nu F-\frac{1}{2}Fg^{*\mu\nu}\partial_\mu\phi\partial_\nu\phi\right)\\&=-\sqrt{-g^*}\frac{1}{2}g^{*\mu\nu}\partial_\mu\phi\partial_\nu\phi\left(\frac{3}{2F^2}\left(\frac{dF}{d\phi}\right)^2+\frac{1}{F}\right)\\&=-\sqrt{-g^*}\frac{1}{2}g^{*\mu\nu}\partial_\mu\Phi\partial_\nu\Phi.\end{aligned}\tag{3.10}$$

If we redefine

$$G(\Phi):=[F^{-1}G](\phi(\Phi)),\tag{3.11}$$

$$V(\Phi,\sigma):=F^{-2}(\phi(\Phi))\,V(\phi(\Phi),\sigma),\tag{3.12}$$

$$A(\Phi):=F^{-\frac{1}{2}}(\phi(\Phi)),\tag{3.13}$$

the action takes the following (Einstein frame) form:

$$S=\int d^4x\sqrt{-g}\left[\frac{1}{2}R-\frac{1}{2}g^{\mu\nu}(\partial_\mu\Phi\partial_\nu\Phi+G(\Phi)\partial_\mu\sigma\partial_\nu\sigma)-V(\Phi,\sigma)\right]+S_{mat}[A^{-2}(\Phi)g^{\mu\nu},\Psi],\tag{3.14}$$

where we have suppressed the $*$ identifying the Einstein frame metric. This action is a specific example of the more general case of multiscalar-tensor theories [36], defined by the Einstein frame action

$$S=\int d^4x\sqrt{-g}\left[\frac{1}{2}R-\frac{1}{2}g^{\mu\nu}\gamma_{AB}\partial_\mu\Phi^A\partial_\nu\Phi^B-V(\Phi^1,...\Phi^N)\right]+S_{mat},\tag{3.15}$$

where $\gamma_{AB}(\Phi^1,...\Phi^N)$ is the σ-model metric of the N-dimensional scalar manifold:

$$d\sigma^2=\gamma_{AB}d\Phi^Ad\Phi^B.$$

Varying the action (3.15) with respect to the metric renders the standard Einstein equations:

$$G_{\mu\nu}=T^\Phi_{\mu\nu}+T^{mat}_{\mu\nu},\tag{3.16}$$

where

$$T^{mat}_{\mu\nu}=-\frac{2}{\sqrt{-g}}\frac{\partial}{\partial g^{\mu\nu}}(\sqrt{-g}\mathcal{L}_{mat}),\tag{3.17}$$

and

$$T^\Phi_{\mu\nu}=\partial_\mu\Phi\partial_\nu\Phi+G(\Phi)\partial_\mu\sigma\partial_\nu\sigma-\frac{1}{2}g_{\mu\nu}(\partial^\rho\Phi\partial_\rho\Phi+G(\Phi)\partial^\rho\sigma\partial_\rho\sigma+2V(\Phi,\sigma)),\tag{3.18}$$

equivalent to the minimally coupled, quintessence case.

The scalar field equations of motion are obtained as follows:

$$\begin{aligned}\delta S_\Phi &= \int d^4x\sqrt{-g}(-g^{\mu\nu}\partial_\nu\Phi\delta(\partial_\mu\Phi) \\ &\qquad + \left[-\frac{1}{2}\frac{dG(\Phi)}{d\Phi}g^{\mu\nu}\partial_\mu\sigma\partial_\nu\sigma - \frac{\partial V(\Phi,\sigma)}{\partial\Phi} + \frac{\partial}{\partial\Phi}(\sqrt{-g}\mathcal{L}_{mat})\right]\delta\Phi) \\ &= \int d^4x\left[\partial_\mu(\sqrt{-g}g^{\mu\nu}\partial_\nu\Phi) - \sqrt{-g}\left(\frac{1}{2}\frac{dG(\Phi)}{d\Phi}g^{\mu\nu}\partial_\mu\sigma\partial_\nu\sigma + \frac{\partial V(\Phi,\sigma)}{\partial\Phi}\right)\right. \\ &\qquad \left. - \frac{\partial}{\partial g^{\mu\nu}}(\sqrt{-g}\mathcal{L}_{mat})2Q(\Phi)g^{\mu\nu}\right]\delta\Phi \\ &= \int d^4x\sqrt{-g}\left[\nabla_\mu\partial^\mu\Phi - \frac{1}{2}\frac{dG(\Phi)}{d\Phi}g^{\mu\nu}\partial_\mu\sigma\partial_\nu\sigma - \frac{\partial V(\Phi,\sigma)}{\partial\Phi} + g^{\mu\nu}T^{mat}_{\mu\nu}Q(\Phi)\right]\delta\Phi.\end{aligned} \tag{3.19}$$

In the second step we introduced

$$Q(\Phi) := \frac{1}{A(\Phi)}\frac{dA}{d\Phi}, \tag{3.20}$$

in the last we used the definition of $T^{mat}_{\mu\nu}$.

By varying with respect to σ we get:

$$\begin{aligned}\delta S_\sigma &= \int d^4x\sqrt{-g}(-G(\Phi)g^{\mu\nu}\partial_\nu\sigma\delta(\partial_\mu\sigma) - \frac{\partial V(\Phi,\sigma)}{\partial\sigma}\delta\sigma) \\ &= \int d^4x\left[\partial_\mu(\sqrt{-g}G(\Phi)g^{\mu\nu}\partial_\nu\sigma) - \frac{\partial V(\Phi,\sigma)}{\partial\sigma}\right]\delta\sigma \\ &= \int d^4x\sqrt{-g}\left[G(\Phi)\nabla_\mu\partial^\mu\sigma + \frac{dG(\Phi)}{d\Phi}g^{\mu\nu}\partial_\mu\Phi\partial_\nu\sigma - \frac{\partial V(\Phi,\sigma)}{\partial\sigma}\right]\delta\Phi.\end{aligned} \tag{3.21}$$

As above, we take the metric to be of the flat FRW type,

$$ds^2 = -dt^2 + a^2(t)d\vec{x}^2,$$

where now the time variable and scale factor are related to the Jordan frame quantities by

$$dt = A(\Phi)dt_{JF}, \qquad a = A(\Phi)a_{JF},$$

and assume, that both the scalar fields depend only on time. In this case, the equations of motion take the following form:

$$\ddot{\Phi} + 3H\dot{\Phi} = \frac{1}{2}\frac{dG(\Phi)}{d\Phi}\dot{\sigma}^2 - \frac{\partial V(\Phi,\sigma)}{\partial\Phi} + Q(\Phi)T, \tag{3.22}$$

$$\ddot{\sigma} + 3H\dot{\sigma} = \frac{1}{G(\Phi)}\left(-\frac{dG(\Phi)}{d\Phi}\dot{\Phi}\dot{\sigma} - \frac{\partial V(\Phi,\sigma)}{\partial\sigma}\right). \tag{3.23}$$

Assuming a perfect fluid background, we specify the trace of the energy-momentum tensor to

$$T = -\rho_{fluid} + 3p_{fluid}.$$

This is related to the corresponding Jordan frame quantity by: $T = A^4(\Phi)T_{JF}$.

As a consequence of the coupling between Φ and matter, the matter continuity equation is modified. From the zero component of the Bianchi identity,

$$0 = \nabla^\mu G_{\mu\nu} = \nabla^\mu (T^\Phi_{\mu\nu} + T^{mat}_{\mu\nu}),$$

we get, after using the equations of motion of the Φ-field,

$$\dot{\rho}_{mat} = (-3H + Q(\Phi)\dot{\Phi})\rho_{mat}. \tag{3.24}$$

The corresponding equation for the radiation component,

$$\dot{\rho}_{rad} = -4H\rho_{rad}, \tag{3.25}$$

is unchanged with repect to standard GR, due to the fact that the energy momentum tensor of a perfect fluid with $w = \frac{1}{3}$ is traceless.

The Friedmann equations take their usual form in the Einstein frame:

$$H^2 = \frac{1}{3}(\rho_{mat} + \rho_{rad} + \frac{1}{2}(\dot{\Phi}^2 + G(\Phi)\dot{\sigma}^2) + V(\Phi, \sigma)), \tag{3.26}$$

$$\dot{H} = -\frac{1}{2}(\rho_{mat} + \frac{4}{3}\rho_{rad} + \dot{\Phi}^2 + G(\Phi)\dot{\sigma}^2). \tag{3.27}$$

3.4 Beyond - and back to - general relativity

The predicted deviation from GR - due to the time variability of the gravitational coupling constant, and the existence of a scalar partner to the graviton - has observational consequences, and since we know that GR has so far passed all experimental tests, the possible deviation is severely constrained.

We start with the modification of Newton's law. The Newtonian limit of multiscalar-tensor theory yields the following interaction between two point-like bodies with masses $M_{1,2}$ at distance r [36],

$$\mathcal{L}^N_{int} = \frac{GM_1M_2}{r}\left[1 + \sum_a Q_{a,0}Q^a_0 \exp(-m_a r)\right] A_0^2, \tag{3.28}$$

where the subscript 0 refers to the present value of the respective quantity,

$$Q_a := \frac{d\ln A}{d\Phi_a},$$

and m_a is the mass of scalar field Φ_a. Specializing to only one scalar field, in the zero mass limit the effective Newtonian constant is given by:

$$G_{eff} := GA_0^2(1 + Q_0^2).$$

(Newtonian gravity corresponds to $A_0 = 1, Q_0 = 0$.) The time variation of this quantity is constrained [78]:

$$\left|\frac{\dot{G}_{eff}}{G_{eff}}\right| \leq 6 \times 10^{-12}\, yr^{-1}.$$

We consider now the parametrized post-Newtonian (PPN) approximation. The post-Newtonian corrections can be quantified in terms of Eddington's parameters β, γ [46],

$$-g_{00} \approx 1 - \frac{2M}{r} + \frac{\beta - \gamma}{2}\frac{4M^2}{r^2},$$
$$g_{rr} \approx 1 + \gamma\frac{2M}{r},$$

where $2M$ equals the Schwarzschild radius, and the Schwarzschild solution of Einstein's equations corresponds to

$$\beta = \gamma = 1.$$

In scalar-tensor theory, the parameters can be expressed as follows [36]:

$$\gamma - 1 = -2\frac{Q_0^2}{1 + Q_0^2}, \tag{3.29}$$

$$\beta - 1 = \frac{1}{2}\frac{Q_0^2}{(1 + Q_0^2)^2}\left(\frac{dQ}{d\Phi}\right)_0. \tag{3.30}$$

Current constraints on the PPN parameters from solar system tests, e.g. the Cassini spacecraft experiment [12], imply a bound on the coupling:

$$Q_0^2 < 10^{-3}. \tag{3.31}$$

In addition, we have to take into account constraints from big bang nucleosynthesis (BBN). The introduction of a light scalar field - and a differing value of the gravitational coupling constant - changes the effective number of degrees of freedom of the relativistic particles (g_*), and thereby modifies the Friedmann equation,

$$H^2 = \frac{\pi^2}{90} g_* \left(1 + \frac{\delta g_*}{g_*}\right) T^4,$$

where we have neglected non-relativistic contributions to the energy density, and re-expressed ρ_{rad} in terms of the temperature T. Taking a conservative estimate ($|\frac{\delta g_*}{g_*}| \leq 0.2$), one obtains the bound [78]:

$$0.8 \leq \left|\frac{A_{BBN}^2}{A_0^2}\right| \leq 1.2.$$

The BBN constraint also applies to the minimally coupled, quintessence case [33]:

$$\Omega_{DE}(T \approx 1MeV) < 0.2.$$

Since the BBN bound on the non-minimal coupling is less stringent than the constraints from solar system tests applying to its present value, a larger deviation from GR is admitted in the past. This observation leads us to study the dynamical evolution of the coupling function. For simplicity, we stick to the one field case [9, 35]. Introducing the new variable

$$N := \ln\frac{a}{a_{init}}, \tag{3.32}$$

we rewrite the scalar field equation of motion ($\frac{d}{dt} = H\frac{d}{dN}$):

$$H^2\frac{d^2\Phi}{dN^2} + (\dot{H} + 3H^2)\frac{d\Phi}{dN} = -Q(\Phi)(\rho_{fluid} - 3p_{fluid}) - \frac{dV}{d\Phi}.$$

In the next step we substitute H^2 and $\dot{H}$, using the Friedmann equations:

$$\left(\frac{\rho_{fluid}+V(\Phi)}{3-(\frac{d\Phi}{dN})^2}\right)\frac{d^2\Phi}{dN^2}+\left(\frac{1}{2}(\rho_{fluid}-p_{fluid})+V(\Phi)\right)\frac{d\Phi}{dN}=-Q(\Phi)(\rho_{fluid}-3p_{fluid})-\frac{dV}{d\Phi}.$$

Dividing by ρ_{fluid}, and defining $\nu := \frac{V(\Phi)}{\rho_{fluid}}$, we finally get:

$$\left(\frac{1+\nu}{3-(\frac{d\Phi}{dN})^2}\right)\frac{d^2\Phi}{dN^2}+\frac{1}{2}(1-w_{fluid}+2\nu)\frac{d\Phi}{dN}=-Q(\Phi)(1-3w_{fluid})-\nu\frac{d\ln V}{d\Phi}. \qquad (3.33)$$

Assuming ν and w_{fluid} to be only slowly varying with N, we have obtained the evolution equation of a scalar, "particle-like" dynamical variable with velocity dependent mass [35], in presence of a (quasi-)constant friction parameter and a force term, due to the effective potential:

$$V_{eff} = (1-3w_{fluid})\ln A(\Phi) + \nu \ln V(\Phi).$$

Following [35], we first consider the case of vanishing potential. We have to distinguish three different possibilities:

1. The effective potential has a minimum, given by a zero of $Q(\Phi)$. We can then study the behaviour of the scalar field near this minimum in the quadratic approximation,

$$\ln A(\Phi) \approx (\Phi-\Phi_{min})^2,$$

if Φ is close to Φ_{min}. We introduce $\phi := \Phi - \Phi_{min}$, and neglect the velocity dependence of the mass term (since it is quadratic in $\frac{d\phi}{dN}$) to obtain,

$$\frac{d^2\phi}{dN^2}+\frac{3}{2}(1-w_{fluid})\frac{d\phi}{dN}=-6(1-3w_{fluid})\phi,$$

which is just the equation of motion of a damped harmonic oscillator with frequency

$$\omega^2 := 6(1-3w_{fluid}) > 0,$$

since $w_{fluid} < \frac{1}{3}$, after the first particle species has become non-relativistic. So the field settles to a finite value, corresponding to a zero of $Q(\Phi)$. But as Q measures the deviation from GR, this indicates an attractor mechanism towards Einstein gravity. Indeed Damour and Nordtvedt [35] showed that, whenever the coupling function $Q(\Phi)$ has a zero, an attractor solution exists, which drives the field to its corresponding value, thereby ensuring the scalar-tensor theory to become indistinguishable from GR.

2. The effective potential has no minimum, but $Q(\Phi)$ approaches zero, while the field value runs to infinity. In this case, the theory will approach Einstein gravity asymptotically. As in case 1 this leaves the possibility, that there has been a significant deviation from GR during early stages of cosmic history.

3. If neither case 1 nor case 2 is valid (e.g. if $Q = const$), it is not possible to realize an attractor mechanism towards GR, and observational and experimental constraints cannot be alleviated while extrapolating the value of Q backwards.

We reconsider equation (3.33), now including a non-vanishing potential. Again, $\frac{d\Phi}{dN} = 0$ is a trivial solution if the RHS vanishes, cf. if the effective potential has a minimum, characterized by the equation:

$$Q(\Phi) = -\frac{\nu}{1 - 3w_{eff}} \frac{d \ln V(\Phi)}{d\Phi}.$$

Obviously this minimum does not necessarily correspond with $Q(\Phi) = 0$, and since ν - and in principle even w_{eff} - depends weakly on N, its position changes. So we can only hope for an attractor mechanism towards GR, if the zeroes of $Q(\Phi)$ and $\frac{d \ln V(\Phi)}{d\Phi}$ coincide. Otherwise $Q(\Phi)$ may have a zero, but the field can be driven away from the corresponding value due to the influence of its potential, and the deviation from GR increases with time.

On the other hand, case 2 is still relevant in general, if the potential is of the runaway type. Since we already know that runaway potentials characterize viable quintessence models, this class of theories allows for dynamical DE without conflicting GR precision tests. The late time attractor can be corresponding to either standard Einstein theory or a de Sitter solution, depending on the choice of the potential.

Chapter 4

Scaling Solutions in Scalar-Tensor Cosmology

Lacking robust observational evidence of a time variation of the dark energy equation of state, or even a significant deviation from $w_{DE} = -1$, the cosmological constant seems to be the (mildly) favoured DE candidate. A recent Bayesian model selection approach [84] even claims "substantially" preference of the cosmological constant over dynamical models. Dynamical DE is therefore faced with the challenge to mimic the behaviour of a constant energy density during their late time evolution: The corresponding trajectories in the $(\Omega_{DE}, w_{DE})-$ plane need to approach the line $w_{DE} = -1$ as close as possible, well before reaching $\Omega_{DE} \approx 0.7...0.75$, and within a wide range of initial conditions.

In the quintessence case this challenge is twofold: The scalar field potential has to be extremely flat, in order to provide a quasi-constant energy density and equation of state, and to match the "tracking condition" of [88] to guarantee independence of initial conditions. As already mentioned in chapter 2, inverse power-law potentials,

$$V \sim \phi^{-\alpha},$$

are prototypes of the latter class. In the scaling regime of the tracker solution the equation-of-state parameter is approximately constant and given by:

$$w_{DE} \approx -\frac{2}{\alpha + 2}.$$

Unfortunately, as was demonstrated in numerical studies done by Bludman, the smaller one chooses α, the less trajectories join the tracker solution in time: "Crawling" quintessence potentials are poor trackers [15]. This implies, that the recent behaviour of the DE equation of state becomes sensitive to the choice of initial conditions. (The argument will be illustrated in the next chapter.)

Within the framework of scalar-tensor gravity, the quintessence potential is replaced by an effective potential, including a time dependent term, which results from the non-minimal coupling:

$$V_{eff} = V(\phi) - \frac{1}{2}F(\phi)R.$$

As was argued in [7, 62, 73], the existence of the additional term can lead to an enlargement of the basin of attraction of the tracker solution, even in the case of small potential slope, due

to a mechanism called "R-boost". During the early stages of the radiation dominated epoch, the Ricci scalar,

$$R = \frac{1}{F(\phi)}(\rho_{fluid} - 3p_{fluid} - \dot{\phi}^2 + 4V(\phi) - 3\ddot{F}(\phi) - 9H\dot{F}(\phi)), \tag{4.1}$$

is enhanced stepwise, whenever a new matter species becomes non-relativistic. Photons (and likewise relativistic particles) do not contribute, since their energy-momentum tensor is traceless. Since matter energy density scales as a^{-3}, and the scale factor is small in the early universe, R can be large enough to dominate the scalar field dynamics via the F-dependent term. The field value grows accelerated, and the kinetic energy density of the scalar field increases, until the Hubble friction becomes relevant. The $R-$boost may in principle be effective enough to wash out any dependence on initial conditions, thereby focusing phase-space trajectories towards a common evolutionary track and alleviating the problems of "crawling" quintessence.

The late time evolution of the field is still governed by the runaway potential, because R becomes smaller as the universe expands, and the present value of the coupling $F(\phi) = F_0$ is strongly constrained by precision tests of GR. Assuming - conservatively - that the coupling was already weak in the past (consistent with the bounds on F_0), the authors of [73] proposed the existence of an early time attractor solution characterized by scaling behaviour of the dark energy density, if the coupling $F(\phi)$ belongs to one of three specific classes.

Their work raises two interesting questions we address in the following sections:

1. Does their claim hold, if one relaxes at least some of the several assumptions the authors made prior to and during their calculations?

2. Can the convergence to the early time scaling attractor solution be identified with convergence towards Einstein theory?

4.1 Dynamical evolution equations in the Jordan frame

We recollect the relevant evolution equations from the previous chapter, as derived from action (3.2). We begin with the Friedmann equations,

$$H^2 = \frac{1}{3F}(\rho_{fluid} + \frac{1}{2}\dot{\phi}^2 + V(\phi) - 3H\dot{F}) = \frac{1}{3}(\rho_{fluid} + \rho_\phi^{cons}), \tag{4.2}$$

$$\dot{H} = -\frac{1}{2F}(\rho_{fluid} + p_{fluid} + \dot{\phi}^2 + \ddot{F} - H\dot{F}) = -\frac{1}{2}(\rho_{fluid} + p_{fluid} + \rho_\phi^{cons} + p_\phi^{cons}), \tag{4.3}$$

where the conserved quantities can be expressed as follows:

$$\rho_\phi^{cons} = \frac{1}{2}\dot{\phi}^2 + V(\phi) - 3H(\dot{F} + H(F-1)), \tag{4.4}$$

and

$$p_\phi^{cons} = \frac{1}{2}\dot{\phi}^2 - V(\phi) + \ddot{F} + 2H\dot{F} + (F-1)(2\dot{H} + 3H^2). \tag{4.5}$$

The Klein-Gordon equation of the scalar field takes the following form,

$$\ddot{\phi} + 3H\dot{\phi} = -\frac{dV}{d\phi} + \frac{1}{2}\frac{dF}{d\phi}(6\dot{H} + 12H^2), \tag{4.6}$$

where we replaced $R = (6\dot{H} + 12H^2)$, which can be seen to be equivalent to (4.1) by substituting the Friedmann equations. The continuity equation obeyed by the background fluid,

$$\dot{\rho}_{fluid} = -3H(\rho_{fluid} + p_{fluid}) = -3H(1 + w_{fuid})\rho_{fluid},$$

where w_{fluid} smoothly changes from $\frac{1}{3}$ to zero during the transition from radiation to matter dominated expansion, can be rewritten as:

$$\frac{d\ln\rho_{fluid}}{dt} = -3(1 + w_{fluid})\frac{d\ln a}{dt}. \tag{4.7}$$

Following [73], we are interested in solutions of the scalar field equation of motion, valid during those stages of cosmic evolution, where the Hubble expansion is dominated by the background fluid:

$$H^2 = \frac{\dot{a}^2}{a^2} \approx \frac{1}{3}\rho_{fluid}. \tag{4.8}$$

Since the background energy density scales as

$$\rho_{fluid} \sim a^{-3(1+w_{fluid})} =: a^{-m}, \qquad 3 \leq m \leq 4,$$

according to (4.7), we get

$$\frac{\dot{a}^2}{a^{2-m}} = const \quad \Rightarrow \quad a \sim t^{\frac{2}{m}},$$

and finally:

$$H = \frac{2}{m}t^{-1}.$$

This expression can be substituted into (4.6), together with an approximation of R. We rewrite (4.1), using (4.4) and (4.5),

$$R = \rho_{fluid} - 3p_{fluid} + \rho_{\phi}^{cons} - 3p_{\phi}^{cons} \approx \frac{\rho_{mnr0}}{a^3}, \tag{4.9}$$

in contrast to [73], who replaced

$$R \approx \frac{\rho_{fluid}}{F} = \frac{1}{F}\frac{\rho_{mnr0}}{a^3}, \tag{4.10}$$

where ρ_{mnr0} is the present value of the energy density of the components, which are non-relativistic at the time in which the R-boost occurs. The choice (4.10) reintroduces the explicit dependence on the coupling function F, which on the other hand has already been neglected in the calculation of $H(t)$, see (4.8). In agreement with [48] (see their footnote 4), we regard the two different replacements to be inconsistent. This is potentially dangerous, especially if one intends to solve for the coupling, as we will see in the next section.

By substituting R according to our approximation (given the explicit time dependence of the scale factor), the equation of motion takes the following form,

$$\ddot{\phi} + \frac{6}{m}t^{-1}\dot{\phi} = -\frac{dV}{d\phi} + \frac{C}{2}\frac{dF}{d\phi}t^{-\frac{6}{m}}, \tag{4.11}$$

where we introduced the constant C to account for both ρ_{mnr0} and a proportionality factor in $a(t)$.

4.2 Classification of coupling functions

Motivated by the work of Liddle and Scherrer [59], the authors of [73] classified possible choices of the coupling function $F(\phi)$, which allow for scaling solutions in the background dominated stages of cosmic evolution. They assumed that the DE density is dominated - due to the R-boost - by the kinetic term, and that this term scales as some power of a:

$$\rho_\phi^{cons} \approx \frac{1}{2}\dot{\phi}^2 \sim a^{-n} \sim t^{\frac{2n}{m}}. \tag{4.12}$$

Furthermore they regarded the potential gradient to be negligible in the equation of motion.

Though in the Friedmann equations, the potential energy can be neglected with respect to the background fluid, see (4.8), we will keep the potential force term in the equation of motion. Minimally coupled, quintessence models do as well admit solutions with dominating kinetic energy during early time evolution. Inverse power-law potentials exhibit diverging slopes if $\phi \to 0$, so we do not take it for a priori granted that only the $R-$dependent term is dynamically relevant. On the other hand, there necessarily is a stage of evolution where $\frac{dV}{d\phi}$ and $\frac{dF}{d\phi}R$ contribute to the same order in the RHS of the Klein-Gordon equation.

Since $H \sim t^{-1}$, while $R \sim t^{-\frac{6}{m}}$, which approaches t^{-2} as $m \to 3$, it depends on the effectiveness of the $R-$boost, how long the scalar field remains in the scaling regime. Since we are ultimately interested in attractor solutions, we allow for the scaling behaviour to be maintained during matter dominance, and the potential force term to catch up with $\frac{dF}{d\phi}R$, before the friction term becomes relevant.

Assuming that a scaling solution exists, we can rearrange the equation of motion in order to solve for the coupling function, since we know the time dependence of the scalar field in the scaling regime (specified by choice of n):

$$\frac{dF}{d\phi} = \frac{2}{C}\left(\ddot{\phi} + \frac{6}{m}t^{-1}\dot{\phi} + \frac{dV}{d\phi}\right)t^{\frac{6}{m}}. \tag{4.13}$$

4.2.1 Case $n = m$

If the kinetic energy density of the scalar field scales exactly like the background fluid, we obtain from (4.12):

$$\dot{\phi} = At^{-1} \quad \Rightarrow \quad \phi = A\ln t,$$

where we have set $t_i = 1, \phi_i = 0$. (4.13) then takes the following form:

$$\frac{dF}{d\phi} = \frac{2}{C}\left[A\left(-1 + \frac{6}{n}\right)t^{\frac{2(3-n)}{n}} + \frac{dV}{d\phi}t^{\frac{6}{n}}\right].$$

We plug in $t = \exp\frac{\phi}{A}$ to get

$$\frac{dF}{d\phi} = \frac{2(6-n)}{n}\frac{A}{C}\exp\left(\frac{2(3-n)}{n}\frac{\phi}{A}\right) + \frac{2}{C}\frac{dV}{d\phi}\exp\left(\frac{6}{n}\frac{\phi}{A}\right), \tag{4.14}$$

which differs from the corresponding equation in [73], where the LHS reads

$$\frac{1}{F}\frac{dF}{d\phi} = \frac{d\ln F}{d\phi},$$

because of (4.10), which obviously leads to the wrong result. Equation (4.14) can be integrated to give

$$F(\phi) - F_i = \frac{2}{C}\left[A\phi + \int_0^\phi d\phi' \frac{dV}{d\phi'} \exp\frac{2\phi'}{A}\right], \tag{4.15}$$

if $n = 3$, and else:

$$F(\phi) - F_i = \frac{A^2}{C}\frac{(6-n)}{(3-n)} \exp\left(\frac{2(3-n)}{n}\frac{\phi}{A}\right) + \frac{2}{C}\int_0^\phi d\phi' \frac{dV}{d\phi'} \exp\left(\frac{6}{n}\frac{\phi'}{A}\right). \tag{4.16}$$

If we were interested in a classification of potentials, we could have solved for $V(\phi)$ instead.

To make contact with [59], we choose

$$V = V_0 \exp\left(-2\frac{\phi}{A}\right).$$

The integrations in (4.15) and (4.16) can be performed to simplify the result:

$$F(\phi) - F_i = \frac{2}{C}\left(A - \frac{2V_0}{A}\right)\phi,$$

if $n = 3$, and else,

$$\begin{aligned} F(\phi) - F_i &= \left(\frac{A^2}{C}\frac{(6-n)}{(3-n)} - \frac{4V_0}{C}\frac{n}{2(3-n)}\right) \exp\left(\frac{2(3-n)}{n}\frac{\phi}{A}\right) \\ &= \frac{1}{(3-n)C}(A^2(6-n) - 2n\,V_0) \exp\left(\frac{2(3-n)}{n}\frac{\phi}{A}\right). \end{aligned} \tag{4.17}$$

Remarkably, we obtain the same functional form of $F(\phi)$, whether we neglect the potential at all, like [73], or specify it according to the findings of [59]; only the coefficient discriminates both cases.

We define $\lambda := \frac{2}{A}$, set $V_0 \equiv 1$ and choose $m = 4$ for simplicity. The requirement to keep the coefficient of

$$F(\phi) - F_i = \frac{8}{C}\left(1 - \frac{1}{\lambda^2}\right) e^{-\frac{\lambda}{4}\phi}$$

positive [78], irrespective of F_i, translates to $\lambda \geq 1$. (4.11) now becomes

$$\ddot{\phi} + \frac{3}{2}t^{-1}\dot{\phi} = \lambda\left[e^{-\lambda\phi} - \left(1 - \frac{1}{\lambda^2}\right) e^{-\frac{\lambda}{4}\phi} t^{-\frac{3}{2}}\right].$$

In this case the effective potential has a time dependent minimum, which disappears in the limit $t \to \infty$. The force due to the $R-$term opposes the potential gradient, so the field is driven upward the potential hill, until both terms become equal and the RHS vanishes. Afterwards the potential takes over, and the field starts to slowly roll away to positive infinity. Since the net force is decreasing during the early stage of evolution, the Hubble friction term will become relevant in short time, and the onset of the freezing regime will certainly depend on the initial field velocity. The kinetic energy dominated scaling solution is therefore a transient phenomenon and cannot generally alleviate the need for fine tuning. (These arguments do not only apply to $m = 4$. Whenever $m > 3$, which is assumed, the exponent of the coupling function is negative.)

4.2.2 Case $n \neq m$

From (4.12) we now obtain:

$$\dot{\phi} = At^{-\frac{n}{m}} \quad \Rightarrow \quad \phi = A\frac{m}{m-n}t^{\frac{m-n}{m}}.$$

We have set $t_i = 0$ and $\phi_i = 0$. (4.13) then becomes:

$$\frac{dF}{d\phi} = \frac{2}{C}\left(A\frac{6-n}{m}t^{-\frac{n+m}{m}} + \frac{dV}{d\phi}\right)t^{\frac{6}{m}}.$$

By substitution of

$$t = \left(\frac{m-n}{m}\frac{\phi}{A}\right)^{\frac{m}{m-n}},$$

this takes the form

$$\frac{dF}{d\phi} = \frac{2}{C}\left(\frac{m-n}{m}\frac{\phi}{A}\right)^{\frac{6}{m-n}}\left[A\frac{6-n}{m}\left(\frac{m-n}{m}\frac{\phi}{A}\right)^{-\frac{n+m}{m-n}} + \frac{dV}{d\phi}\right], \tag{4.18}$$

which can be integrated to give:

$$F(\phi) - F_i = \frac{A}{C}\frac{(6-n)(m-n)}{m(3-n)}\left(\frac{m-n}{Am}\right)^{\frac{6-m-n}{m-n}}\phi^{\frac{2(3-n)}{m-n}} + \frac{2}{C}\left(\frac{m-n}{Am}\right)^{\frac{6}{m-n}}\int_0^\phi d\phi' \frac{dV}{d\phi'}\phi'^{\frac{6}{m-n}}. \tag{4.19}$$

Again we wish to combine our result with the corresponding one of [59]. Therefore we specialize to an inverse power law potential,

$$V = V_0\phi^{-\alpha},$$

which admits scaling solutions with $n \neq m$ in the quintessence case, if

$$\alpha = \frac{2n}{m-n}.$$

We find

$$\begin{aligned} F(\phi) - F_i &= \frac{A}{C}\frac{(6-n)(m-n)}{m(3-n)}\left(\frac{m-n}{Am}\right)^{\frac{6-m-n}{m-n}}\phi^{\frac{2(3-n)}{m-n}} - \frac{2}{C}\left(\frac{m-n}{Am}\right)^{\frac{6}{m-n}}\frac{nV_0}{3-n}\phi^{\frac{2(3-n)}{m-n}} \\ &= \frac{1}{(3-n)C}\left[\frac{(6-n)(m-n)A}{m} - 2nV_0\right]\left(\frac{m-n}{Am}\right)^{\frac{6-m-n}{m-n}}\phi^{\frac{2(3-n)}{m-n}}, \end{aligned} \tag{4.20}$$

which gets simplified significantly if $m = 3$:

$$F(\phi) - F_i = \frac{1}{3C}\left[\frac{(6-n)(3-n)}{3} - 2n\frac{V_0}{A}\right]\phi^2. \tag{4.21}$$

Again we observe, that we would have obtained the same functional form by ignoring the potential. If we demand that

$$\xi := \frac{1}{3C}\left[\frac{(6-n)(3-n)}{3} - 2n\frac{V_0}{A}\right] > 0,$$

since otherwise the corresponding force term would oppose the potential gradient (compare subsection 3.2.1), and choose $F_i = 0$, we end up with the coupling function of original Brans-Dicke theory with canonically normalized kinetic term. The case of non-zero F_i we cover, without loss of generality, by setting

$$F_i = \frac{1}{8\pi G} \equiv 1,$$

which corresponds to the "extended quintessence" model of [7]. By inserting the explicit time dependence of the different quanitities into equation (4.4), we realize furthermore, that this choice of coupling is singled out by guaranteeing the same scaling behaviour of all additive components of the conserved energy density. This indicates that our result is consistent, even in case our assumption of kinetic dominance fails during the evolution of the scalar field.

To conclude, we have learned that a BD or extended quintessence coupling, combined with an inverse power-law potential, admits a scaling solution during matter dominated epoch. The scaling regime is maintained, while the the equation of motion changes from being dominated by the $R-$boost, to be governed by the potential. From the phenomenological point of view, this is a promising feature: the later the scalar field exits the scaling regime, the less time remains until the DE density begins to dominate the universe, reducing the possible scatter in (Ω_{DE}, w_{DE}) between different trajectories. It remains to be checked if the scaling solution is also an attractor solution.

4.3 Attractor property

We rewrite equation (4.11) by specifying

$$F(\phi) = \xi\phi^2 + F_i, \qquad V(\phi) = V_0\phi^{-\alpha},$$

and $m = 3$:

$$\ddot{\phi} + 2t^{-1}\dot{\phi} = -\alpha V_0\phi^{-(\alpha+1)} + C\xi\phi t^{-2}. \tag{4.22}$$

Following [94], we define new time and field variables,

$$\tau := \ln t, \qquad u(\tau) := \frac{\phi(t(\tau))}{\phi_s(t(\tau))},$$

where ϕ_s denotes the exact scaling solution discussed in the previous subsection:

$$\phi_s \sim t^{\frac{3-n}{3}}.$$

We introduce the notation

$$u' := \frac{du}{d\tau},$$

and use

$$\dot{\phi} = e^{-\tau}\phi' = e^{-\tau}(u'\phi_s + u\phi_s'),$$
$$\ddot{\phi} = e^{-2\tau}(\phi'' - \phi') = e^{-2\tau}(u''\phi_s + 2u'\phi_s' + u\phi_s'' - u'\phi_s - u\phi_s'),$$

to obtain from (4.20):

$$e^{-2\tau}(u''\phi_s + 2u'\phi_s' + u\phi_s'' - u'\phi_s - u\phi_s' + 2(u'\phi_s + u\phi_s') - C\xi u\phi_s) = -\alpha V_0(u\phi_s)^{-(\alpha+1)}.$$

Since ϕ_s is a solution of the original equation of motion, the following identity holds,

$$e^{-2\tau}(\phi_s'' + \phi_s' - C\xi\phi_s) = -\alpha V_0 \phi_s^{-(\alpha+1)},$$

which we use to eliminate ϕ_s from the potential gradient term,

$$u''\phi_s + 2u'\phi_s' + u\phi_s'' - u'\phi_s - u\phi_s' + 2(u'\phi_s + u\phi_s') - C\xi u\phi_s = u^{-(\alpha+1)}[\phi_s'' + \phi_s' - C\xi\phi_s],$$

where we have already devided by $e^{-2\tau}$. This expression, devided by ϕ_s, can be further simplified to get:

$$u'' + u'(2\frac{\phi_s'}{\phi_s} + 1) = (u^{-(\alpha+1)} - u)\frac{1}{\phi_s}[\phi_s'' + \phi_s' - C\xi\phi_s].$$

Since

$$\phi_s \sim e^{\frac{3-n}{3}\tau},$$

we have

$$\frac{\phi_s'}{\phi_s} = \frac{3-n}{3} = \frac{2}{\alpha+2},$$

where the second equality follows, because

$$\alpha = \frac{2n}{3-n}$$

is necessary to obtain a scaling solution.

Finally the equation of motion reads:

$$u'' + u'\left(\frac{4}{\alpha+2} + 1\right) = (u^{-(\alpha+1)} - u)\left[\frac{4}{(\alpha+2)^2} + \frac{2}{\alpha+2} - C\xi\right]. \tag{4.23}$$

In order to perform a stability analysis, we linearize around the scaling solution by substituting $u = 1 + \delta$:

$$\delta'' + \delta'\left(\frac{4}{\alpha+2} + 1\right) = -\delta(\alpha+2)\left[\frac{4}{(\alpha+2)^2} + \frac{2}{\alpha+2} - C\xi\right]. \tag{4.24}$$

This is a second order, linear ODE with constant coefficients, which is easily solved. The characteristic equation,

$$s^2 + \frac{\alpha+6}{\alpha+2}s + \frac{2(\alpha+4)}{\alpha+2} - (\alpha+2)C\xi = 0,$$

has two roots,

$$s_{1,2} = -\frac{\alpha+6}{2(\alpha+2)} \pm \sqrt{\frac{(\alpha+6)^2}{4(\alpha+2)^2} - \left[\frac{2(\alpha+4)}{\alpha+2} - (\alpha+2)C\xi\right]},$$

which both have negative real parts if

$$\frac{2(\alpha+4)}{\alpha+2} - (\alpha+2)C\xi > 0.$$

This is equivalent to

$$C\xi = \frac{(6-n)(3-n)}{3} - 2n\frac{V_0}{A} < \frac{\frac{4(6-n)}{3-n}}{(\frac{6}{3-n})^2},$$

where we have replaced $\alpha(n)$, and can be recast to

$$\frac{2}{9}\frac{(6-n)(3-n)}{n} < \frac{V_0}{A}.$$

If this condition is fulfilled, the scaling solution is an attractor.

4.4 Einstein frame description

We now turn to the second question we posed at the beginning of this chapter, which is most conveniently addressed in the Einstein frame version of the theory. According to section 3.3, the Einstein frame coupling $Q(\Phi)$ - as defined in (3.20) - can be expressed in terms of the Jordan frame quantity $F(\phi)$ as follows:

$$Q(\Phi) = -\frac{1}{2F(\phi)}\frac{dF}{d\phi}\frac{d\phi}{d\Phi} = -\frac{1}{2F(\phi)}\frac{dF}{d\phi}\left[\frac{3}{2}\left(\frac{d\ln F}{d\phi}\right)^2 + \frac{1}{F}\right]^{-\frac{1}{2}}, \tag{4.25}$$

where $\phi = \phi(\Phi)$. We have found that a Jordan frame coupling function,

$$F(\phi) = F_i + \xi\phi^2, \qquad F_i \,\epsilon\, \{0, 1\},$$

combined with an inverse power-law potential, admits a scaling attractor solution. Substituting this into (4.24), we obtain,

$$Q(\Phi) = \frac{-\xi\phi(\Phi)}{[(6\xi+1)\xi\phi^2(\Phi) + F_i]^{\frac{1}{2}}},$$

which approaches a constant in the limit $\phi \to \infty$, and reduces to

$$Q = -\sqrt{\frac{\xi}{6\xi+1}},$$

in the case $F_i = 0$.

To obtain the explicit form of the Einstein frame quantities we have to solve for $\Phi(\phi)$:

$$\frac{d\Phi}{d\phi} = \sqrt{\frac{6}{\phi^2} + \frac{1}{\xi\phi^2}},$$

where we have chosen the positive sign of the square root, because we wish Φ to increase with ϕ. This can be integrated to give:

$$\Phi = \sqrt{\frac{6\xi+1}{\xi}}\ln\phi = -\frac{1}{Q}\ln\phi.$$

We obtain

$$A(\Phi) = F^{-\frac{1}{2}}(\phi(\Phi)) = \frac{1}{\sqrt{\xi}} e^{Q\Phi},$$

and

$$V(\Phi) = \frac{V}{F^2}(\phi(\Phi)) = \frac{V_0}{\xi^2} \exp((\alpha + 4)Q\Phi).$$

From section 3.4 we already know, that a scalar-tensor theory with constant Q does not admit an attractor mechanism towards Einstein theory. Therefore the coupling function is tightly constrained by present gravity tests, even in the early universe. In this case the effectiveness of the $R-$boost is limited. The constant coupling is furthermore responsible for the different appearence of the potential in the two different frames (which become indistinguishable in the limit $Q \to 0$).

In order to construct a dynamical model of scalar-tensor type DE, which includes convergence to GR, we have to give up the existence of an exact scaling solution, but on the other hand gain the possibility to enhance the effectiveness of the R-boost mechanism by a stronger coupling in the past.

The issue of attractor solutions in DE models can be addressed more systematically in the Einstein frame version of the dynamical evolution equations. In the following chapter we introduce an autonomous system approach with compact phase-space, where attractor solutions with certain phenomenological properties correspond to stationary points of the dynamical system of first order ODE.

Chapter 5

Evolution of the Dark Energy Equation of State

Out of various observational efforts to reveal the nature of dark energy, a model independent reconstruction of the DE equation of state from low redshift data seems to be particularly promising. We presume that this task can be completed within the next few years, and ask, to which extent different dynamical models of dark energy might be discriminated in terms of their small z evolution.

To address this question - and carry on the discussion of scaling and attractor solutions from the previous chapter - we make use of the autonomous system approach introduced by Copeland, Liddle and Wands [31], which we intend to generalize to the case of two scalar fields in the next chapter.

5.1 Dynamical systems terminology

We consider a system of n first order ODE,

$$\dot{x}_i = f_i(x_1, ..., x_n), \tag{5.1}$$

which is called *autonomous*, if none of the n functions f_i explicitly depends on time. A solution of the system is given in terms of a trajectory in the phase-space spanned by the variables x_i, $i \leq n$:

$$t \longmapsto X(t) := (x_1(t), ..., x_n(t)),$$

determined by choice of initial conditions $X(t_{init})$.

A point $X_s := (x_{1,s}, ..., x_{n,s})$ is said to be a *critical* or *fixed point*, if

$$f_i(X_s) = 0 \qquad \forall\, i \leq n,$$

and an *attractor*, if every trajectory entering the vicinity of the fixed point satisfies the following condition:

$$\lim_{t\to\infty} X(t) = X_s.$$

If several attractors coexist in phase-space, their corresponding *basins of attraction* are separated by common boundaries called *separatrices*.

To be able to decide, whether a given fixed point is an attractor or not, one has to evaluate the Jacobi matrix of the vector function $F(X) := (f_1(X), ..., f_n(X))$ at $X = X_s$. Consider small perturbations around the critical point,

$$x_i = x_{i,s} + \delta x_i \,;$$

substituting this into (5.1) and linearizing, we obtain a system of first order ODE *linear* in the perturbations:

$$\frac{d}{dt}\delta x_i = \sum_j M_{ij}\delta x_j, \tag{5.2}$$

where

$$M_{ij} := \left.\frac{\partial f_i(X)}{\partial x_j}\right|_{X=X_s}.$$

The general solution of this system is given by

$$\delta x_i = \sum_{k=1}^{n} C_{ik} e^{\mu_k t},$$

where C_{ik} are integration constants and μ_k the eigenvalues of the *stability matrix* M, which we assume to be distinct for simplicity. Obviously the perturbation will decay if each μ_k has negative real part.

The critical points of a dynamical system can be classified in terms of the eigenvalues of the corresponding stability matrix. An attractor is characterized by the requirement

$$Re[\mu_k] < 0 \qquad \forall\, k \,\leq\, n,$$

and called *stable spiral*, if $det\, M$ is negative, and *stable node* else. Furthermore, we will use the terminus *saddle point*, if and only if M has one eigenvalue with positive real part. Otherwise we call the fixed point *unstable*.

5.2 Autonomous system of scalar field DE models

The Einstein frame evolution equations,

$$\dot{H} = -\frac{1}{2}(\rho_{mat} + \frac{4}{3}\rho_{rad} + \Pi^2), \tag{5.3}$$

$$\dot{\rho}_{mat} = (-3H + Q(\Phi)\Pi)\rho_{mat}, \tag{5.4}$$

$$\dot{\rho}_{rad} = -4H\rho_{rad}, \tag{5.5}$$

$$\dot{\Phi} = \Pi, \tag{5.6}$$

$$\dot{\Pi} = -3H\Pi - \frac{dV}{d\Phi}(\Phi) - Q(\Phi)\rho_{mat}, \tag{5.7}$$

where we have introduced $\Pi := \dot{\Phi}$, and $Q(\Phi)$ was defined in (3.20), already represent an autonomous system. Nonetheless we use a new set of dynamical variables admitting a compact phase-space.

Following [31], we rewrite the Friedmann constraint equation as follows,

$$\Omega_{mat} = 1 - \Omega_{rad} - \frac{\Pi^2}{6H^2} - \frac{V(\Phi)}{3H^2}, \tag{5.8}$$

and define the dynamical variables

$$x^2 := \frac{\Pi^2}{6H^2}, \qquad y^2 := \frac{V(\Phi)}{3H^2}, \qquad z^2 := \Omega_{rad}.$$

The corresponding phase space is isomorphic to the three-dimensional unit ball, though physically relevant is only the quadrant with $y \geq 0$ and $z \geq 0$.

Furthermore we replace the time variable by (3.32),

$$N = \ln \frac{a}{a_{init}} = -\ln(1+z) + \ln \frac{a_0}{a_{init}},$$

where a_{init} is a reference value, defining the initial conditions of the system, and will be specified below. We can now rewrite the second Friedmann equation (5.3),

$$\frac{1}{H}\frac{dH}{dN} = \frac{\dot{H}}{H^2} = -\frac{3}{2}(2x^2 + \frac{4}{3}z^2 + (1 - x^2 - y^2 - z^2)), \tag{5.9}$$

where we have used (5.8) to eliminate ρ_{mat}. From (5.5) and (5.9) we get:

$$\begin{aligned}\frac{dz}{dN} &= \frac{1}{\sqrt{3}H}\frac{d\sqrt{\rho_{rad}}}{dN} - \frac{z}{H}\frac{dH}{dN} \\ &= \frac{1}{2H^2\sqrt{3\rho_{rad}}}(-4H\rho_{rad}) + \frac{3}{2}\,z\,(2x^2 + \frac{4}{3}z^2 + (1 - x^2 - y^2 - z^2)) \\ &= -2z + \frac{3}{2}\,z\,(2x^2 + \frac{4}{3}z^2 + (1 - x^2 - y^2 - z^2)).\end{aligned} \tag{5.10}$$

In the next step we address the scalar field equation of motion (5.7),

$$\frac{1}{H}\frac{d\Pi}{dN} = \frac{1}{H^2}(-3H\Pi + \lambda V - Q\rho_{mat}) = 3(-\sqrt{6}x + \lambda y^2 - Q(1 - x^2 - y^2 - z^2)),$$

where we have introduced the potential slope parameter:

$$\lambda := -\frac{1}{V}\frac{dV}{d\Phi}.$$

Combining with (5.9) we obtain:

$$\frac{dx}{dN} = \frac{1}{\sqrt{6}H}\frac{d\Pi}{dN} - \frac{x}{H}\frac{dH}{dN} = 3x(x^2 + \frac{2}{3}z^2 - 1) + \left(\frac{3}{2}x - \frac{\sqrt{6}}{2}Q\right)(1 - x^2 - y^2 - z^2) + \frac{\sqrt{6}}{2}\lambda y^2.$$

Finally, using $\frac{d\sqrt{V}}{dN} = -\frac{\Pi}{2H}\lambda\sqrt{V}$, we find the evolution equation for y,

$$\frac{dy}{dN} = -\lambda\frac{\Pi}{2H^2}\frac{\sqrt{V}}{\sqrt{3}} - \frac{y}{H}\frac{dH}{dN},$$

where we have to plug in (5.9) once more. We end up with the following dynamical system:

$$\frac{dx}{dN} = 3x(x^2 + \frac{2}{3}z^2 - 1) + \left(\frac{3}{2}x - \frac{\sqrt{6}}{2}Q\right)(1 - x^2 - y^2 - z^2) + \frac{\sqrt{6}}{2}\lambda y^2, \tag{5.11}$$

$$\frac{dy}{dN} = \frac{3}{2}y(1 + x^2 - y^2 + \frac{1}{3}z^2) - \frac{\sqrt{6}}{2}\lambda xy, \tag{5.12}$$

$$\frac{dz}{dN} = \frac{z}{2}(3(x^2 - y^2) + z^2 - 1). \tag{5.13}$$

As long as we regard λ and Q as constants, the system defines a two parameter family of DE models. Choosing e.g. $\lambda = (\alpha + 4)Q$, we find the scaling model from the previous chapter. (Compare section 4.4.) Fixed points of the system correspond to solutions characterized by constant values of the different density parameters, including

$$\Omega_{DE} = x^2 + y^2,$$

and a constant DE equation-of-state parameter:

$$w_{DE} = \frac{p_{DE}}{\rho_{DE}} = \frac{x^2 - y^2}{x^2 + y^2}.$$

We recognize that scaling solutions with $m = n$ are eventually represented by fixed points, as well as any solution corresponding to one fluid component being dominant with $\Omega_{fluid} = 1$.

5.3 Quintessence models

We intend to illustrate the use of the prescribed autonomous system approach by reviewing some of the quintessence models mentioned in chapter 2 or 4. We classify quintessence potentials in terms of the slope parameter λ. To start with, we take $\lambda = const$, and set $Q = 0$ in equation (5.11).

5.3.1 Constant λ: exponential potential

We consider a quintessence field with potential

$$V(\phi) = V_0 e^{\lambda(\phi_0 - \phi)}, \tag{5.14}$$

where ϕ_0 is the present field value and V_0 the scale of the potential - if not exactly equal (because of the finite kinetic contribution to ρ_ϕ), though of the same order as $\rho_\Lambda|_{z=0}$ (corresponding to a cosmological constant).

The dynamical properties of each model, specified by choice of λ, can be represented in terms of the corresponding set of fixed points,

$$X_s = (x_s, y_s, z_s),$$

which we obtain by setting the RHS of the system (5.11) - (5.13) equal to zero, and solving the resulting system of non-linear algebraic equations:

fixed point	**existence**	**stability**	Ω_{DE}	w_{eff}
A	$\forall\lambda$	saddle point	0	0
B_1, B_2	$\forall\lambda$	unstable	1	1
C	$\forall\lambda$	unstable	0	$\frac{1}{3}$
E	$\lambda \geq 2$	saddle point	$\frac{4}{\lambda^2}$	$\frac{1}{3}$
F	$\lambda \geq \sqrt{3}$	stable	$\frac{3}{\lambda^2}$	0
G	$\lambda \leq \sqrt{6}$	stable: $\lambda < \sqrt{3}$	1	$-1 + \frac{\lambda^2}{3}$

Table 5.1: Fixed point properties of the dynamical system (5.11)-(5.13) with $Q = 0$.

$$A: \quad (0,0,0),$$

$$B_1, B_2: \quad (\pm 1, 0, 0),$$

$$C: \quad (0,0,1),$$

$$E: \quad \left(\frac{2\sqrt{2}}{\sqrt{3}\lambda}, \frac{2}{\sqrt{3}\lambda}, \sqrt{1-\frac{4}{\lambda^2}}\right),$$

$$F: \quad \left(\sqrt{\frac{3}{2}}\frac{1}{\lambda}, \sqrt{\frac{3}{2}}\frac{1}{\lambda}, 0\right),$$

$$G: \quad \left(\frac{\lambda}{\sqrt{6}}, \sqrt{1-\frac{\lambda^2}{6}}, 0\right).$$

(A point D does only exist if $Q \neq 0$, see the subceding section.) In table 5.1 we display properties of the critical points we have found. The existence condition can be expressed as follows,

$$x^2 + y^2 + z^2 \leq 1,$$

with x, y, z real. The stability analysis has been performed according to the preceding section. The classification of the critical points given in the table applies of course only provided the existence condition is fulfilled. If the stability condition is violated in a part of parameter space, where the fixed point is allowed to exist (e.g. point G in case $\sqrt{6} \geq \lambda \geq \sqrt{3}$), it is understood to be a saddle point.

We discover two different possible scaling regimes: point E, where the scalar field energy density mimics radiation, and point F, where it acts like dust matter. If existing, F corresponds to the scaling attractor solution of [59]. Fixed points A and C correspond to radiation and matter dominance repectively, while point G approaches the de Sitter solution in the limit $\lambda \to 0$.

Accelerated expansion requires

$$w_{eff} = \frac{p_{tot}}{\rho_{tot}} = \frac{p_{DE} + p_{rad}}{3H^2} = x^2 - y^2 + \frac{z^2}{3} < -\frac{1}{3},$$

which is only possible at G, if $\lambda < \sqrt{2}$. The main result of our fixed point classification happens to be, that there is no way of realizing an epoch of acceleration preceded by a scaling regime, since stability of G excludes existence of E and F.

In a realistic cosmological set-up, we can distinguish two main types of trajectories, depending on choice of λ. Each trajectory will emerge from the vicinity of the critical point C, corresponding to a radiation dominated universe. If $\lambda \gg 2$, we expect a sequence $C \to E \to F$ of scaling regimes, whereas if $\lambda < \sqrt{2}$, the typical path $C \to A \to G$ will lead to an accelerated universe.

The present situation, $(\Omega_{DE}, w_{DE}) \approx (0.7, -1)$, is not represented by a critical point, but can be realized as a transient stage, by choosing λ sufficiently small. Trajectories approaching the final attractor G closely along the $\{x = 0\}$-plane will then generically pass the phase-space region, which provides agreement with current observational data. But to arrange for this coincidence to happen right around the present, the initial value of the variable y has to be precisely adjusted. Fixing y_{init} corresponds to fixing V_0, the scale of the potential. There is no independent freedom of choosing an initial field value, which can be seen by rewriting equation (5.14):

$$V(\phi) = V_0 e^{\lambda(\phi_0 - \phi)} = V_0 e^{\lambda(\phi_0 - \phi_{init})} e^{-\lambda(\phi - \phi_{init})} =: V_0^* e^{-\lambda(\phi - \phi_{init})}.$$

A different choice of ϕ_{init} translates to a redefinition of V_0^*, which thereby can even be adjusted to unity.

Before we present a numerical example, we have to discuss the issue of initial conditions $(x(N_{init}), y(N_{init}), z(N_{init}))$. So far we have avoided to fix the normalization of our "time" variable N. We have to make sure that the basic assumptions,

1. validity of the classical description of the system (that is, validity of classical physics),

2. validity of decoupled continuity equations of the different fluid components (that is, negligibility of interactions),

are justified at N_{init}. A transition of a fermionic matter species from the relativistic to the non-relativistic regime - simply due to cooling of the universe - would have to be simulated by an interaction between the radiation and dust matter fluids, violating the second assumption. To specify initial conditions corresponding to the Planck era within a purely classical approach would be obviously not reasonable. On the other hand, the epoch of big bang nucleosynthesis (BBN) provides constraints on the allowed range of initial conditions (see section 3.4); as we know from the mass estimates of lightest SUSY particles (LSP) representing dark matter candidates, SUSY dark matter would have been already sufficiently cold at BBN to be described as dust matter. (We ignore the baryonic and leptonic contributions to the matter sector.) Therefore we specify $a_{init} = a_{BBN}$, and set

$$\ln(1 + z_{BBN}) \equiv 23,$$

corresponding to an energy scale of $\mathcal{O}(1MeV)$ (see e.g. [49]).

In figure 5.1 we plotted the low redshift evolution of the DE and effective equation-of-state parameters in a model specified by choice of $\lambda = \frac{1}{2}$. We fixed $x_{init} = y_{init} = 1.5 \times 10^{-17}$ to obtain $x^2 + y^2 = 0.72$ at $N = 23$. The numerical results are in agreement with observations (the transition redshift being slightly too large, compare e.g. [1]), but since the scalar field

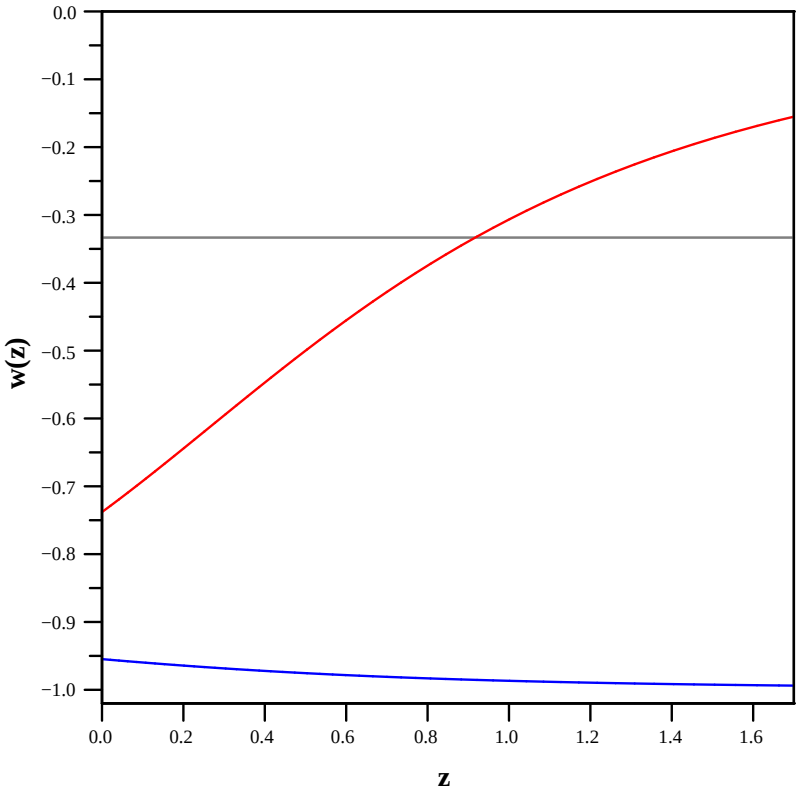

Figure 5.1: Quintessence model with exponential potential, $\lambda = \frac{1}{2}$: small z evolution of w_{eff} (red curve) and w_{DE} (blue curve). The auxiliary line represents the acceleration threshold. At present we find $w_{DE} \approx -0.95$, and a transition redshift $z|_{q=0} \approx 0.93$ (defined by the zero of the deceleration parameter q.)

is frozen to a fixed value during the larger part of cosmic history - thereby mimicking the behaviour of a cosmological constant -, the required amount of relative fine tuning in y_{init} is of the same order as in the cosmological constant case:

$$\frac{\Omega_{DE,BBN}}{\Omega_{\Lambda,BBN}} \approx \mathcal{O}(1).$$

As can be seen in the figure, w_{DE} increases slightly with z approaching zero, indicating the transition from freezing to the slow-roll regime of the attractor G. We can alleviate at least the relative fine tuning by choosing $x_{init} \gg y_{init}$. The bounds from BBN physics ($\Omega_{DE,BBN} \lesssim 0.1$) allow in principle for x_{BBN} up to $x \approx 0.3$, leading to

$$\frac{\Omega_{DE,BBN}}{\Omega_{\Lambda,BBN}} \approx \mathcal{O}(10^{33}),$$

though we have to emphasize that we cannot provide a sound physical motivation of such an extreme inequilibrium between kinetic and potential energy of the scalar field.

In summary, we have to conclude (like many authors before), that a quintessence model with exponential potential fails to solve the coincidence problem. (For a wide range of initial conditions, $y_{init} \approx 10^{-10}$ and larger, a matter dominated epoch does not even exist: The scalar field evolves so fast, that it starts to be the dominant component right after exiting the radiation era.)

Hebecker and Wetterich [53] suggested the following generalization of the potential:

$$V(\phi) = e^{-\lambda(\phi)\phi}.$$

Consider the simple and effective (but certainly not well-motivated) choice of a step function,

$$\lambda(\phi) = \lambda_1 > \sqrt{3}, \qquad \phi \leq \phi^*,$$

$$\lambda(\phi) = \lambda_2 < \sqrt{2}, \qquad \phi > \phi^*,$$

where ϕ^* has to be fixed to match the transition from the matter era to the DE regime. (So one only shifts the necessary tuning to a new "parameter".) During fluid dominance, point F is the relevant attractor, focusing phase-space trajectories and thereby ensuring independence of initial conditions. Then the step in λ initiates the transition to the acceleration epoch, since now fixed point F is no longer stable and G determines the evolution instead. Again we realize - what was already mentioned in chapter 4 -, that a sequence of a scaling attractor and an accelerated attractor solution is a desirable feature of any DE model which addresses the coincidence problem. (In [8] a sequence of the desired kind is obtained by considering a potential given by a sum of two different exponential terms.)

5.3.2 Decreasing λ: tracker potentials

In the spirit of the preceding discussion, we introduce the following choice of the potential slope parameter,

$$\lambda(\phi) = -\frac{1}{V}\frac{dV}{d\phi} = \alpha\,\phi^{-1},$$

which can be seen to correspond to inverse power-law potentials $V \sim \phi^{-\alpha}$. We cover this situation within our autonomous system approach by including λ as a fourth dynamical variable. Its evolution is governed by the following equation:

$$\frac{d\lambda}{dN} = -\sqrt{6}\lambda^2 x(\Gamma - 1), \tag{5.15}$$

where we have defined the constant

$$\Gamma := \frac{V}{(\frac{dV}{d\phi})^2}\frac{d^2V}{d\phi^2}.$$

(See Steinhardt et al. [88], who introduced Γ, not necessarily constant, in a more general set-up. The requirement, $\Gamma > 1$ and nearly constant, is just the aforementioned "tracker condition", compare section 2.3 and chapter 4.) Though the enlarged system, (5.11) - (5.13) and (5.15), is still autonomous in our special case, we do not intend to solve for its fixed points. Instead we adopt the idea of "instantaneous fixed points" [64] and reconsider the fixed point set of the previous subsection as slowly varying with N by replacing $\lambda \to \lambda(N)$.

Thus we gain qualitative understanding of the dynamics in terms of the fixed points moving in phase-space.

We assume an initial field value close to zero, corresponding to large λ. In the limit $\lambda \to \infty$ the saddle point E approaches fixed point C, while the attractor F becomes indistinguishable from point A. A generic trajectory starting near C with $x_{init} = y_{init}$ will at the very beginning be influenced by saddle point E. If x, y are initially small, equations (5.11) and (5.12) can be approximated as follows:

$$\frac{dx}{dN} \approx \frac{x}{2}(z^2 - 3) + \frac{\sqrt{6}}{2}\lambda y^2, \tag{5.16}$$

$$\frac{dy}{dN} \approx \frac{3}{2}y(1 + \frac{1}{3}z^2) - \frac{\sqrt{6}}{2}\lambda xy. \tag{5.17}$$

As long as λ is large enough for the second term, on the RHS of each equation, to determine the sign of $\frac{dx}{dN}$ and $\frac{dy}{dN}$, $x(N)$ increases at the expense of $y(N)$. The resulting, transient increase in w_{DE} can be recognized in figure 5.3. With $z(N)$ and $\lambda(N)$ decreasing, $x(N)$ will soon start to decrease as well, followed by $y(N)$ beginning to grow.

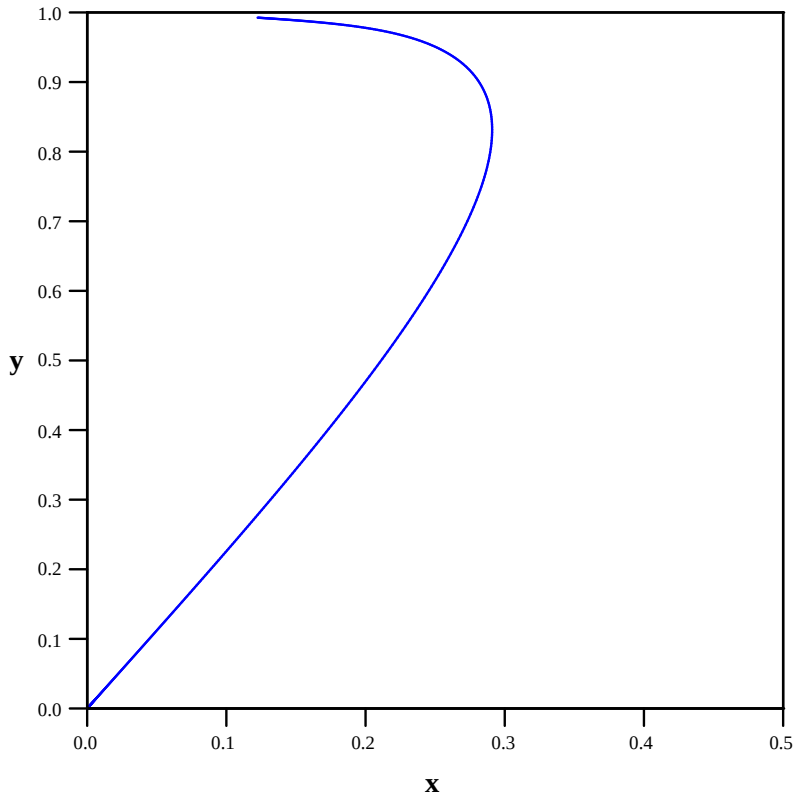

Figure 5.2: Quintessence model with $V \sim \phi^{-1}$: phase-space section (x, y). Evolution of the trajectory specified by $x_{init} = y_{init} = 10^{-11}, \lambda_{init} = 3 \times 10^{12}$, up to the present ($N = 23$).

The system will not remain close to point E, but approach the (spiral) attractor regime of F. Since F moves along the line $\{x = y, z = 0\}$ towards the phase-space boundary as $\lambda(N)$ decreases, the trajectory will be bent towards this line, while $z(N)$ rapidly decreases. As can be seen in figure 5.2, the trajectory does not follow the path of fixed point F with $x(N) = y(N)$, but approximates a straight line $y(N) = c\,x(N)$ with $c = \sqrt{5}$. This corresponds to the $n = 1$ scaling regime with

$$w_{DE} = \frac{x^2 - y^2}{x^2 + y^2} = \frac{1 - c^2}{1 + c^2} = -\frac{2}{3} = \frac{-2 + w_{fluid}\,\alpha}{2 + \alpha},$$

where the last equality is implied by $\alpha = 1$ and $w_{fluid} = 0$ (dust matter). In phase-space, a scaling solution with $n \neq m$ is represented by a straight line instead of a fixed point.

Figure 5.3 shows the evolution of the effective and DE equation-of-state parameters with N. The sequence of radiation, matter and acceleration epoch is evident. The scaling regime is already reached during the radiation dominated stage. Figure 5.4 may be compared with figure 5.1 and the figures in section 2.4. Obviously, to be in good agreement with the observational trend, α should be smaller than one.

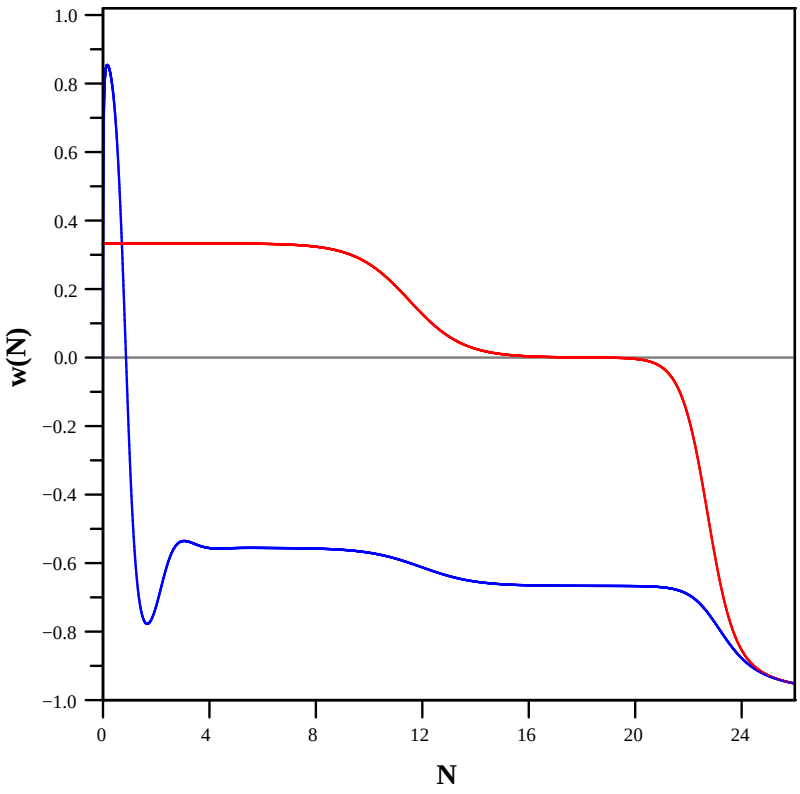

Figure 5.3: Quintessence model with $V \sim \phi^{-1}$: evolution of w_{eff} (red curve) and w_{DE} (blue curve), computed along the trajectory specified in the caption of figure 5.2.

We now turn to the issue of dependence on initial conditions. Since $\alpha = 1$, the scale of the potential is fixed through

$$\frac{V_0}{3H_{init}^2} = \frac{y_{init}^2}{\lambda_{init}},$$

so we can independently vary the initial field value by choosing λ_{init}, while keeping the ratio to y_{init}^2 fixed. In the example of figures 5.2 to 5.4 we have

$$\frac{\Omega_{DE,BBN}}{\Omega_{\Lambda,BBN}} \approx \mathcal{O}(10^{12}),$$

but we can also choose $\Omega_{DE,BBN} \approx 0.1$ corresponding to a ratio of 10^{33}, in contrast to the exponential case even with $x_{init} = y_{init}$.

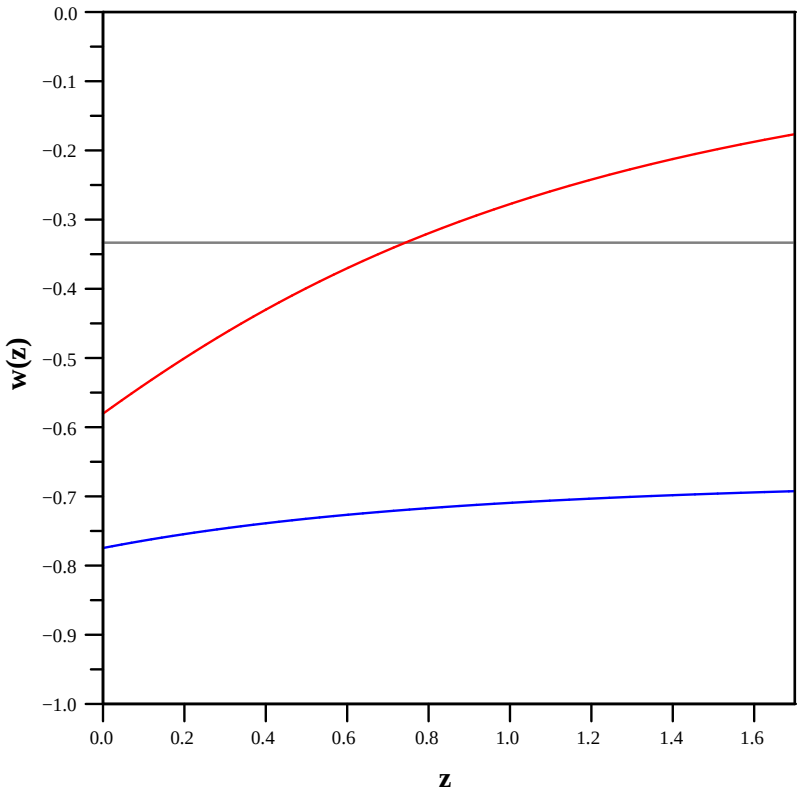

Figure 5.4: Quintessence model with $V \sim \phi^{-1}$: small z evolution of w_{eff} (red curve) and w_{DE} (blue curve), computed along the trajectory specified in the caption of figure 5.2. At present ($\Omega_{DE}|_{N=23} = 0.72$) we find $w_{DE} \approx -0.77$, and a transition redshift $z|_{q=0} \approx 0.75$.

The evolution of the equations of state along a trajectory representative for this case is plotted in figures 5.5 and 5.6, which differ significantly from the corresponding plots in figure 5.3 and 5.4. Now the scalar field equation of state is stiff during radiation epoch and exhibits a

fast transition towards $w_{DE} = -1$ after onset of matter dominance. The scalar field remains frozen afterwards, and the trajectory joins the tracker only recently, without reaching the scaling regime before. As can be read from figure 5.6, the present value of w_{DE} differs from the tracker case (figure 5.4) as well as the predicted transition redshift. Most importantly, if $0 \leq z \leq 1.7$ we find

$$\frac{dw_{DE}}{dz} > 0,$$

along the trajectory from figure 5.6, in contrast to

$$\frac{dw_{DE}}{dz} < 0,$$

along the tracker.

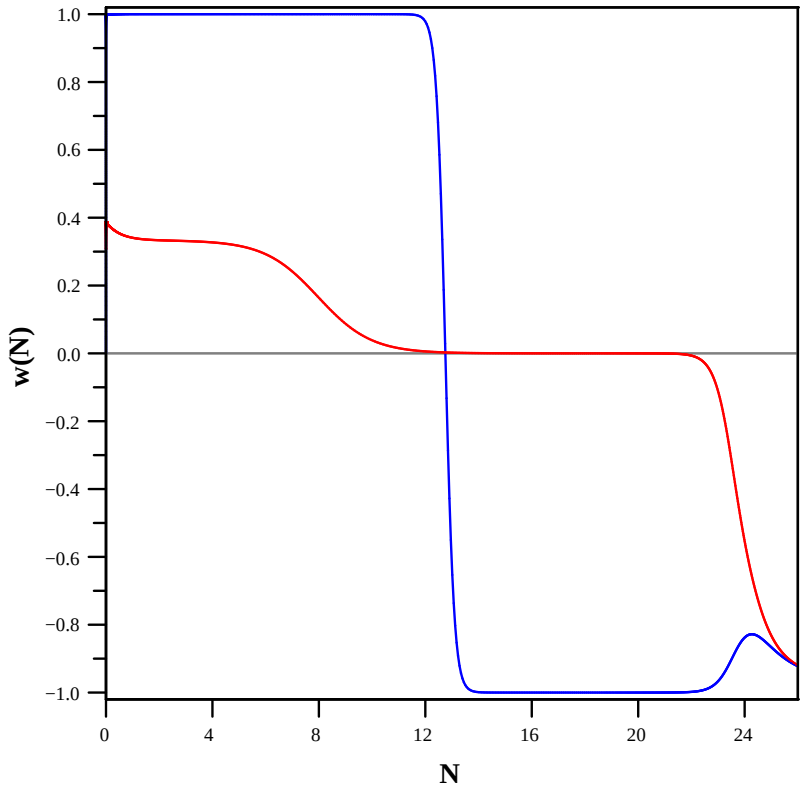

Figure 5.5: Quintessence model with $V \sim \phi^{-1}$: evolution of w_{eff} (red curve) and w_{DE} (blue curve), computed along the trajectory specified by $x_{init} = y_{init} = 0.2, \lambda_{init} = 1.2 \times 10^{33}$.

We have to conclude, that the inverse power-law quintessence model under discussion is not falsifiable by reconstruction of $w_{DE}(z)$ from the data, unless every single trajectory can be ruled out. (According to [15] the situation becomes worse, if one considers $\alpha < 1$ to get a better match with the data. In that case even trajectories are possible, which remain in the freezing regime until now, so being indistinguishable from a cosmological constant.)

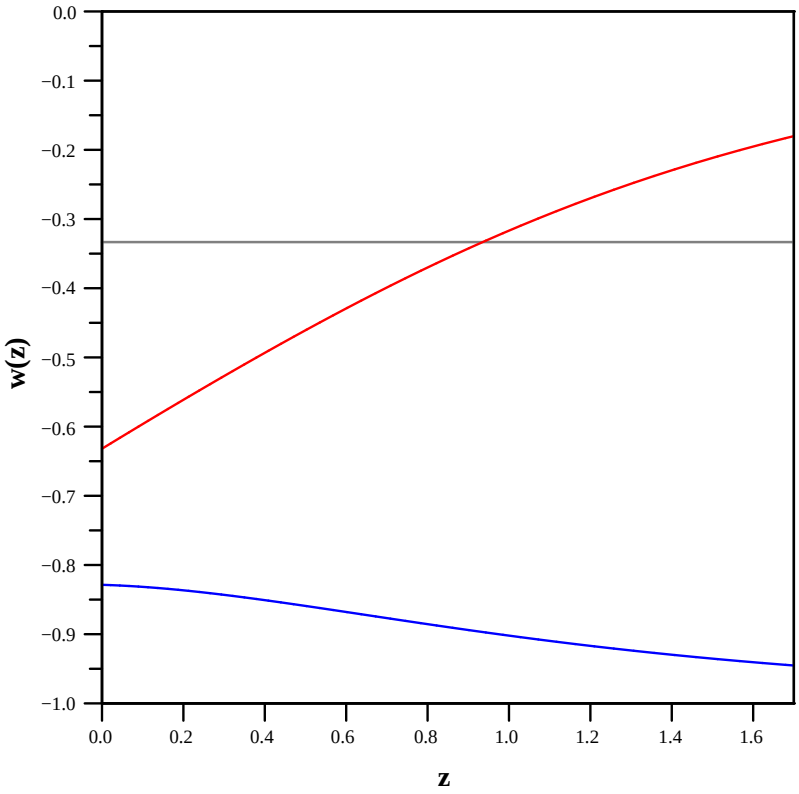

Figure 5.6: Quintessence model with $V \sim \phi^{-1}$: small z evolution of w_{eff} (red curve) and w_{DE} (blue curve), computed along the trajectory specified in the caption of figure 5.5. At present ($\Omega_{DE}|_{N=24.2} = 0.72$, different normalization due to change in z_{init}) we find $w_{DE} \approx -0.83$, and a transition redshift $z|_{q=0} \approx 0.95$.

There is one possible loop-hole in our argument: the model could be modified by some kind of selection mechanism, which reduces the range of allowed initial conditions to the basin of attraction of the scaling tracker solution. This would require a better understanding of the scalar field evolution in the early universe, prior to big bang nucleosynthesis, and therefore lies beyond the viability of our classical dynamical systems approach. (See [83] concerning a possibility of constraining pre-BBN expansion history.)

5.3.3 Increasing λ

We now turn to the case of an increasing potential slope parameter, and consider the simplest possible, namely linear, realization:

$$\lambda(\phi) = c\,\phi.$$

By integration we find the corresponding class of potentials:

$$V(\phi) = V_0 \exp(-\frac{c}{2}\phi^2).$$

Though we do not know how to motivate this from a more fundamental perspective, we will proceed and analyze the phenomenological implications of a Gaussian potential. In section 2.3 we briefly discussed axion fields as quintessence candidates, and we regard the Gaussian as a pre-oscillatory approximation to the typical axion potential (see figure 5.8). This approximation has one, mere technical, advantage: We can represent the Gaussian potential within our autonomous system approach, if we substitute equation (5.15) by

$$\frac{d\lambda}{dN} = \sqrt{6}\, c\, x. \tag{5.18}$$

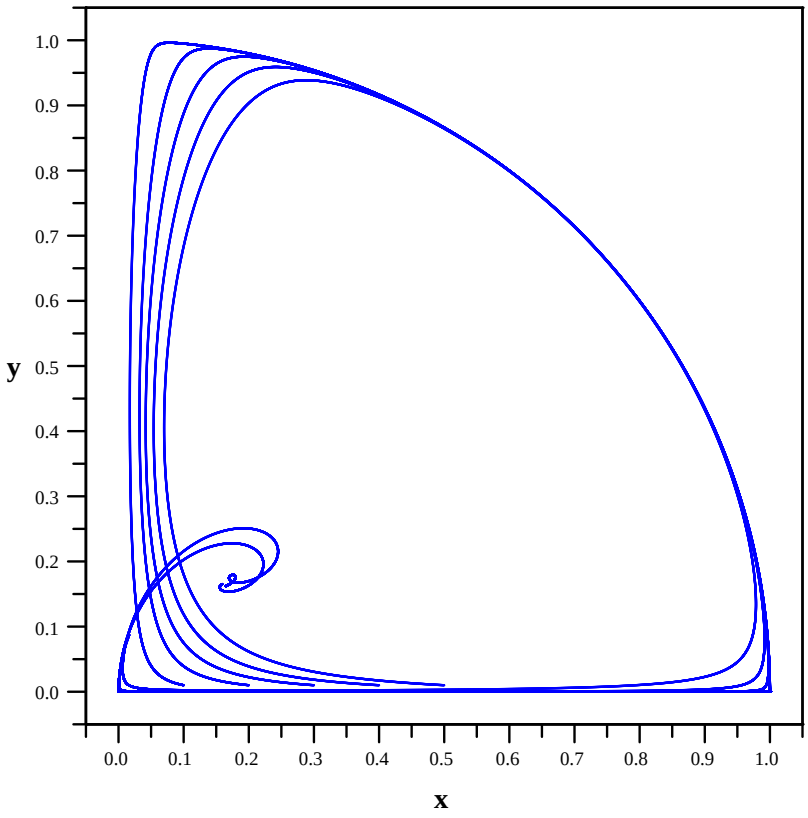

Figure 5.7: Phase-space section (x, y) of a quintessence model with Gaussian potential, $c = \frac{1}{2}$.

As in the previous subsection, we wish to gain qualitative understanding of the dynamics by considering the set of critical points varying with λ. Letting ϕ_{init} be close to zero, we realize that the only stable fixed point is G, drawing the trajectories towards the plane $\{x = 0\}$ and increasing y. (See figure 5.7.)

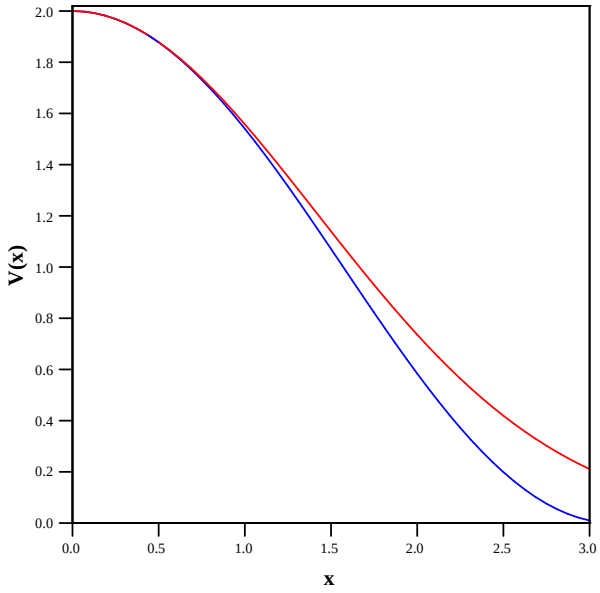

Figure 5.8: Comparison of axionic ($V(x) = 1+\cos x$, lower, blue curve) and Gaussian potential ($V(x) = 2\exp(-\frac{x^2}{4})$, upper, red curve).

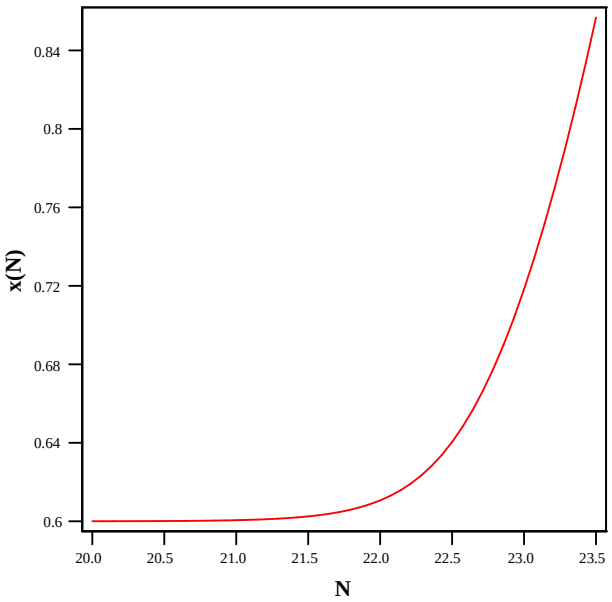

Figure 5.9: Evolution of the field value $x(N)$ in a quintessence model with Gaussian potential, $c = \frac{1}{2}$; to be compared with figure 5.8.

If x, y are also small in the beginning, equations (5.11) and (5.12) can be approximated as follows,

$$\frac{dx}{dN} \approx \frac{x}{2}(z^2 - 3), \tag{5.19}$$

$$\frac{dy}{dN} \approx \frac{3}{2}y(1 + \frac{1}{3}z^2), \tag{5.20}$$

showing that $x(N)$ will rapidly decrease while $y(N)$ grows.

With increasing λ, the attractor G moves, following the phase-space boundary, towards the point $(x, y) = (\frac{1}{\sqrt{2}}, \frac{1}{\sqrt{2}})$, where it becomes a saddle point (at $\lambda = \sqrt{3}$), and further towards the unstable node B_1. The trajectories, focused near the $x-$axis before, remain close to point G and follow its motion, get repelled from the boundary near B_1 and are driven towards point A. (Compare figure 5.7.) Meanwhile the attractor F moves along the straight line $\{x = y\}$ from the boundary towards point A. Since F is a stable spiral, the trajectories are forced to wind around its evolving position, as can be seen in the figure.

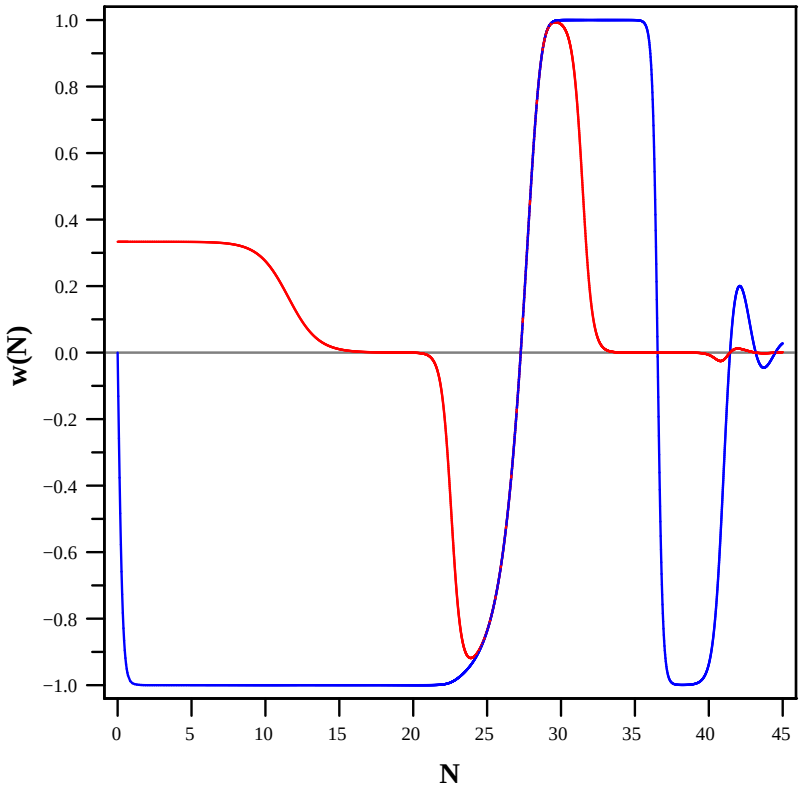

Figure 5.10: Evolution of $w_{DE}(N)$ (blue curve) and $w_{eff}(N)$ (red curve) in quintessence model with Gaussian potential, $c = \frac{1}{2}$.

The Gaussian model therefore provides one very appealing property: its late time evolution is matter dominated, irrespective of initial conditions, and the accelerated stage a transient

phenomenon. So we avoid the future event horizon characterizing the de Sitter like final state of other models we discussed before, thereby reproducing another property of the axionic potential, but without the need of tuning the potential minimum to zero.

We shall give a numerical example. We choose $x_{init} = y_{init} = 10^{-17}$, implying the same amount of relative fine tuning as in the exponential case. Furthermore we set $\lambda_{init} = 0.3$, avoiding to adjust the field value too close to the potential maximum. The evolution of the field value is shown in figure 5.9. At present ($N = 23$) we have $\phi \approx 0.72$, indicating that the Gaussian can still be regarded as an excellent approximation of an axion potential.

In figure 5.10 we plotted the evolution of the DE and effective equation-of-state parameters. The field enters the freezing regime dominated by the Hubble friction very soon, and w_{DE} remains practically constant up to the present ($w_{DE}(z = 0) \approx -0.98$) while the field value "sits and waits". Thus the model is barely distinguishable from a cosmological constant. This property turns out to be quite robust against a change in the initial field value. (We numerically checked values up to $\phi_{init} = 0.6$. In this case w_{DE} has already increased significantly up to the present, leading to $w_{DE}(0) \approx -0.8$. If we choose higher values of ϕ_{init}, the system fails to reach $\Omega_{DE} = 0.7$ at all. We further checked numerically, that the phenomenologically relevant "sit and wait" behaviour is not sensitive to the parameter c, as long as $c \lesssim 4$.)

The most remarkable feature of the model is provided by its future evolution: the accelerated expansion ceases due to the transition to a stiff equation of state. (In our numerical example, acceleration occurs between $N \approx 22.4$ and $N \approx 26.7$, but this period becomes shorter with increasing ϕ_{init}.) Soon after, Ω_{DE} starts to decrease and both the DE and effective equation of state enter an oscillatory period. The final state of the universe is matter dominated with $w_{eff} = w_{DE} = \Omega_{DE} = 0$. (The same qualitative behaviour we expect from an axionic potential with $V(\phi_{min}) = 0$.)

Before summarizing the implications of this section, we have to emphasize that we consider the properties of the examples we presented so far (apart from the Gaussian potential) to be quite well known. Nevertheless it was necessary to go into so much detail, since we are ultimately interested in a comparison with scalar-tensor DE models, in particular with respect to the small redshift evolution of the equation of state. Though it might be a bit premature, given the observational situation, we will comment on the limitations of the simple quintessence models we discussed so far.

Dynamical models of dark energy were proposed to get around the huge amount of fine tuning (relative to the Planck scale) required in setting the cosmological constant to the tiny value that accounts for the observed acceleration. We have learned that exponential and Gaussian quintessence require just the same amount of fine tuning of the potential scale (or a precise fixing of the initial field value in the first case), and our "naturalness" criterion (see [53] for comparison), the ratio

$$\frac{\Omega_{DE,BBN}}{\Omega_{\Lambda,BBN}},$$

in both cases turns out to be of order one. In order to "solve" the coincidence problem, a dynamical DE model derived from a more fundamental theory has to make a precise prediction of the potential scale. Our present situation remains special, in the sense that, instead of being represented by an attractor solution itself, it corresponds to a transition from or towards an attractor regime. (But see [4], where "the present universe as a global attractor" is realized by introducing a dark matter - DE coupling which increases with time.)

Furthermore we have learned, that an inverse power-law potential allows for a value of $\Omega_{DE,BBN}$ as large as given by the BBN bound, corresponding to

$$\frac{\Omega_{DE,BBN}}{\Omega_{\Lambda,BBN}} \approx \mathcal{O}(10^{33}),$$

but only at the expense of predictiveness - due to its sensitivity to $\dot{\phi}_{init}$ (especially if we demand to come close to $w_{DE} = -1$ at present).

Apart from its energy scale, a quintessence model is characterized by a second parameter (λ, α or c) corresponding to the potential slope. We have seen that the allowed range of the parameter is already tightly constrained by observations - and these bounds will tighten the more, the closer the DE equation of state comes to $w_{DE} = -1$ around the present. Furthermore, it will become extremely difficult to discriminate different models by reconstruction of $w_{DE}(z)$ alone.

The next section is devoted to the question, whether DE models based on scalar-tensor theories exhibit more attractive features from the perspective of model building.

5.4 Coupled quintessence models

We turn to the case of non-zero coupling Q. Motivated by our findings from chapter 4, we first consider the exponential potential - now combined with a negative constant Q.

5.4.1 Constant coupling

We redefine the coupling to be positive, $Q := |Q|$, and analyze the two-parameter family of models in terms of the critical points of the corresponding autonomous system (equations (5.11) - (5.13)):

$$A: \quad \left(\sqrt{\frac{2}{3}}Q, 0, 0\right),$$

$$B_1, B_2: \quad (\pm 1, 0, 0),$$

$$C: \quad (0, 0, 1),$$

$$D: \quad \left(\frac{1}{\sqrt{6}Q}, 0, \sqrt{1 - \frac{1}{2Q^2}}\right),$$

$$E: \quad \left(\frac{2\sqrt{2}}{\sqrt{3}\lambda}, \frac{2}{\sqrt{3}\lambda}, \sqrt{1 - \frac{4}{\lambda^2}}\right),$$

$$F: \quad \left(\sqrt{\frac{3 - 2Q(\lambda - Q)}{2(\lambda - Q)^2}}, \sqrt{\frac{3}{2}}\frac{1}{\lambda - Q}, 0\right),$$

$$G: \quad \left(\frac{\lambda}{\sqrt{6}}, \sqrt{1 - \frac{\lambda^2}{6}}, 0\right).$$

fixed point	**existence**	**stability**	Ω_{DE}	w_{eff}
A	$Q \leq \sqrt{\frac{3}{2}}$	stable: $Q < \frac{1}{\sqrt{2}}$ $\wedge \lambda > \frac{3}{2Q} + Q$	$\frac{2}{3}Q^2$	$\frac{2}{3}Q^2$
B_1	$\forall(\lambda, Q)$	saddle point: $\lambda > \sqrt{6} \wedge Q > \sqrt{\frac{3}{2}}$	1	1
B_2		unstable		
C	$\forall(\lambda, Q)$	unstable	0	$\frac{1}{3}$
D	$Q \geq \frac{1}{\sqrt{2}}$	stable: $\lambda > 4Q$	$\frac{1}{6Q^2}$	$\frac{1}{3}$
E	$\lambda \geq 2$ $\lambda \neq 4Q$	stable: $\lambda < 4Q$	$\frac{4}{\lambda^2}$	$\frac{1}{3}$
F	$\frac{3}{2Q} + Q \geq \lambda \geq \frac{Q+\sqrt{Q^2+12}}{2}$ $\wedge Q \leq \sqrt{\frac{3}{2}}$	stable: $\lambda > 4Q$	$\frac{3-Q(\lambda-Q)}{(\lambda-Q)^2}$	$\frac{Q}{\lambda-Q}$
G	$\lambda \leq \sqrt{6}$	stable: $\lambda \leq \sqrt{3}$	1	$-1 + \frac{\lambda^2}{3}$

Table 5.2: Fixed point properties of the dynamical system (5.11)-(5.13)

Properties of the critical points are displayed in table 5.2.

The new features, with respect to the quintessence case, are the modification of fixed point A, and the appearance of a new critical point D. These points have exactly the properties we sought for in chapter 4: They correspond to radiation (D) and matter dominated (A) stages of evolution respectively (depending on the value of Q), and they both exhibit a stiff equation of state: $w_{DE} = 1$. Since they coincide if $Q = \frac{1}{\sqrt{2}}$, and $Q < \frac{1}{\sqrt{2}}$ is necessary to gain $w_{eff} < \frac{1}{3}$ at A, it is not possible to realize a ΛCDM type sequence $D \to A \to G$ of radiation, dust matter and DE dominated expansion respectively. But due to the $R-$boost mechanism mentioned in the previous chapter, either a radiation dominated saddle point D (if $Q \gtrsim 1$), or a matter dominated saddle point A (if $Q < \frac{1}{\sqrt{2}}$), can be followed by the acceleration regime of G.

Let us resume our discussion from section 4.4 and consider the special case $\lambda = (4+\alpha)Q$ with $\alpha \geq 0$ ($\alpha = 0$ corresponds to BD theory with cosmological constant). Applying the observational bound (3.31), we realize that the existence condition of fixed point D cannot be satisfied at all, while the existence conditions of points E and F require very large ($\mathcal{O}(10^3)$ and $\mathcal{O}(10^2)$ respectively) values of α. The resulting subset of models is determined by the coexistence of saddle point A (corresponding to the matter dominated scaling regime we identified in chapter 4) and a late time attractor G. Accelerated expansion in this case requires

$$Q^2 < \frac{2}{(4+\alpha)^2},$$

and if we set $Q = 10^{\frac{3}{2}}$, we get an attractor value of

$$w_{eff} = w_{DE} = -1 + \frac{(4+\alpha)^2}{3000}.$$

Before we can discuss a numerical example and compare to the quintessence case, we have to observe that - in the Einstein frame description of a scalar-tensor theory - the units of time and space have become field dependent, due to the conformal transformation of the metric. Our dynamical variables are dimensionless, and therefore not affected. But our "time" variable N is related to the corresponding Jordan frame quantity by (see (3.32)):

$$\ln \frac{a}{a_{BBN}} = \ln \frac{A(\Phi) a_{JF}}{A(\Phi_{init}) a_{BBN,JF}} = N_{JF} + \ln \frac{A(\Phi)}{A(\Phi_{init})}.$$

If we wish to compare evolution plots of the equation-of-state parameters with those from the preceding subsection, we have to rescale the $N-$axis to N_{JF}. In the case under consideration we have

$$N_{JF} = N_{EF} + Q(\Phi - \Phi_{init}).$$

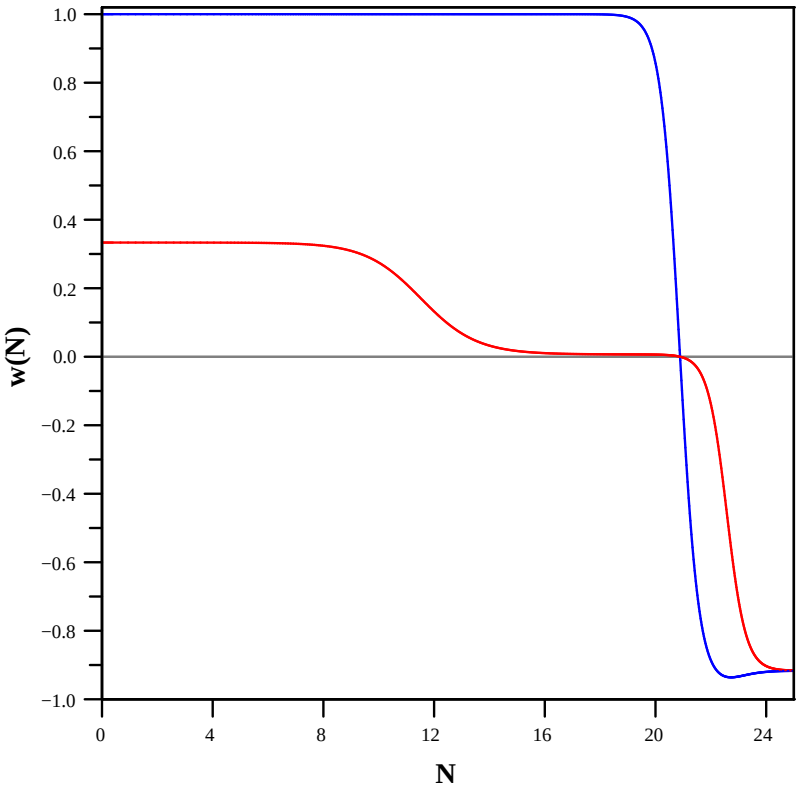

Figure 5.11: Evolution of $w_{DE}(N)$ (blue curve) and $w_{eff}(N)$ (red curve) in a constantly coupled quintessence model with exponential potential, $Q = \frac{1}{10}, \lambda = \frac{1}{2}$ (Initial conditions: see text).

The evolution of w_{eff}, as exhibited by the numerical example of figure 5.11, shows the regime of saddle point A taking over around $N_{JF} \approx 14$, though - due to the smallness of

Q - the effect is barely visible in the plot. We have chosen $Q = \frac{1}{10}$, corresponding to the scaling model of section 4.4, with $\alpha = 1$ and therefore $\lambda = \frac{1}{2}$ (as in the model of figure 5.1). This is about three times the value of the Cassini bound, but still inside the allowed range at BBN (see section 3.4), and small enough not to spoil LSS formation. We may justify our choice by reminding, that the Cassini measurements constrain the coupling between DE and baryonic matter, but not DE and dark matter. (But see [11].) The field dependence of N turns out to be negligible: Given the smallness of Q, Jordan and Einstein frame are practically indistinguishable.

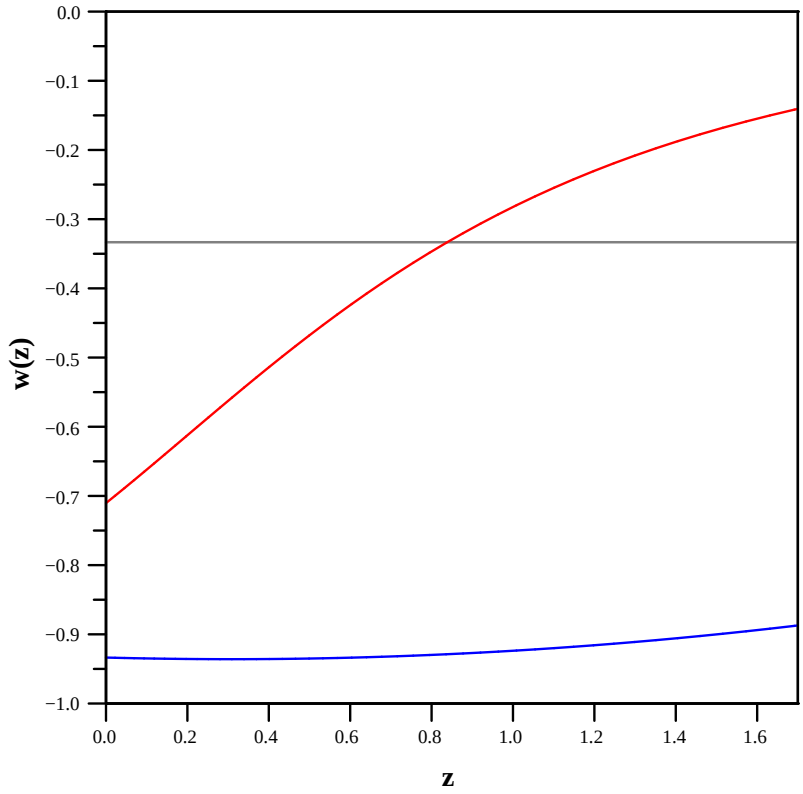

Figure 5.12: Small z evolution of $w_{DE}(N)$ (blue curve) and $w_{eff}(N)$ (red curve) in the constantly coupled quintessence model with exponential potential, $Q = \frac{1}{10}, \lambda = \frac{1}{2}$. At present ($\Omega_{DE} = 0.72$) we have $w_{DE} \approx -0.93$; the transition redshift is at $z \approx 0.84$.

The trajectory has been specified by fixing $y_{init} = 1.5 \times 10^{-17}$ to obtain the proper present value of Ω_{DE} (exactly as in the quintessence case), but $x_{init} = 1.5 \times 10^{-6}$, leading to

$$\frac{\Omega_{DE,BBN}}{\Omega_{\Lambda,BBN}} \approx \mathcal{O}(10^{22}).$$

Since the $R-$boost mechanism will have been active already prior to BBN, it is natural to assume initial conditions exhibiting dominant kinetic energy. The specific value we chose is

singled out by the observation, that larger values lead to a decrease in $x(N)$ in the beginning, which indicates that the effect of the $R-$boost would have been overestimated in that case.

The major difference between the coupled and the corresponding uncoupled quintessence model is the fast transition from a stiff equation of state, exhibited by the former, in recent cosmic history. While the uncoupled quintessence field reaches the freezing regime very soon, the (Einstein frame equivalent of) BD field shows only a very short period of friction dominance, after the equation-of-state parameter has dropped from $w_{DE} = 1$ to a value near -1, and soon afterwards approaches the attractor. As can be seen in figure 5.12, this behaviour (which we have checked to be quite robust against changes in x_{init}) contrasts to the quintessence case shown in figure 5.1. A significantly larger coupling Q between DE and dark matter would shift the transition further towards the present, so that w_{DE} drops from one directly to its attractor value within the observable range of small z. Assuming that the capability of reconstructing $w_{DE}(z)$ will steadily improve during the next few years, it may well become possible to constrain the coupling strength within this type of models.

On the other hand, choosing Q to be in agreement with the Cassini bound shifts the transition in w_{DE} towards larger redshift, rendering the small z evolution practically indistinguishable from the quintessence case shown in figure 5.1. Not surprisingly, the performance of the model depends crucially on the coupling strength, which determines the effectiveness of the $R-$boost. While larger couplings lead to larger values of

$$\frac{\Omega_{DE,BBN}}{\Omega_{\Lambda,BBN}}$$

for a reasonable choice of initial conditions, but may get into conflict with observations, the smaller the coupling, the smaller the deviation from the pure quintessence model and therefore the improvement in the relative fine tuning of $\Omega_{DE,BBN}$.

5.4.2 Inverse power-law potential and exponentially decaying coupling

We will now discuss a model proposed by Bartolo and Pietroni [9], which has - to our knowledge - not yet been explored within the autonomous system approach, nor tested concerning the possibility of the late time equation of state mimicking a cosmological constant. Though not providing exact scaling solutions, the model shares the attractive feature of convergence towards Einstein theory of gravity. (Compare sections 3.4 and 4.4.)

We stick to our redefinition of the coupling Q to be positive. Since we wish to compare the model,

$$V(\Phi) = V_0\Phi^{-\alpha}, \qquad Q(\Phi) := -\frac{d\ln A}{d\Phi} = Be^{-\beta\Phi},$$

with the corresponding quintessence case (subsection 5.3.2), we set $\alpha = 1$, $B = 1$ and $\beta = 13$. The constraint [9]

$$Q_{BBN} - Q_0 \leq 0.08\beta = 1.04,$$

combined with the Cassini bound on Q_0, translates to the initial field value:

$$\Phi_{init} \geq -0.07.$$

This constraint is automatically observed, since the inverse-power law potential restricts us to

$$\Phi_{init} > 0.$$

We have to enlarge the autonomous system (5.11) - (5.13) and (5.15), specified to $\Gamma = 2$, by a fifth equation, governing the evolution of the coupling function:

$$\frac{dQ}{dN} = -\sqrt{6}\,\beta\,Q\,x, \tag{5.21}$$

with $\beta = 13$. Before presenting numerical results, we follow the example of subsection 5.3.2 and try to obtain some qualitative understanding of the dynamics, in terms of the evolution of the critical points with $\lambda(N)$ and $Q(N)$. Since we naturally have $\lambda_{init} \gg Q_{init} \approx 1$, point D is initially a stable attractor, leading to an increase in $x(N)$, while $z(N)$ rapidly decays. (Again we take initial conditions close to the position of fixed point C to be the only reasonable choice.) This is how the $R-$boost manifests itself within the autonomous system description. Since the increase in $x(N)$ triggers the decay of Q (see (5.21)), D will soon - depending on choice of x_{init} - change to be a saddle point, allowing for growth of $y(N)$. The late time attractor G will be approached either via the vicinity of fixed point A or F, and we expect the differences to the quintessence model to vanish in the limit $Q \to 0$.

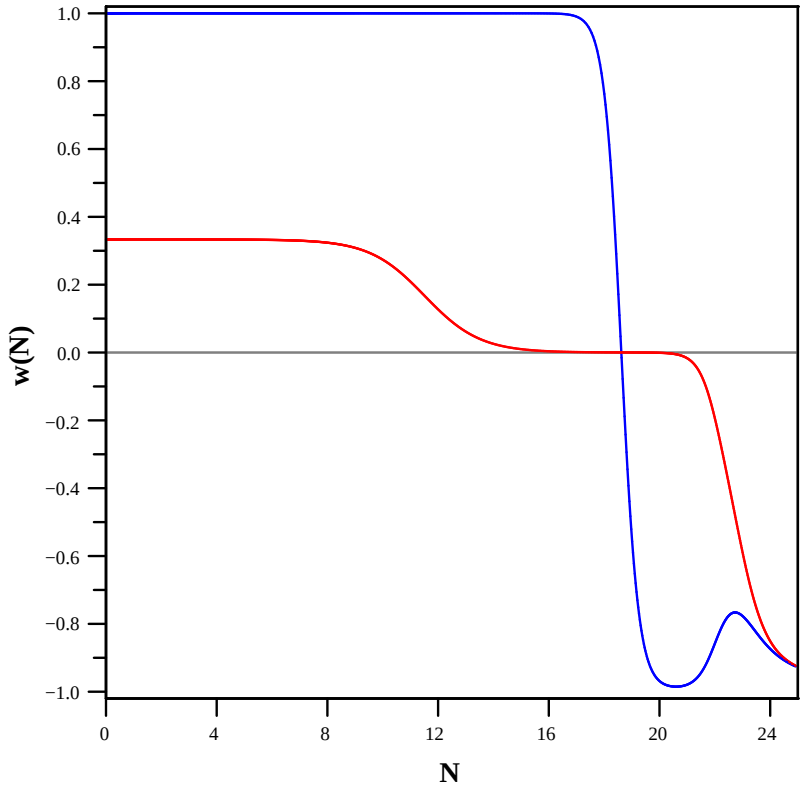

Figure 5.13: Evolution of $w_{DE}(N)$ (blue curve) and $w_{eff}(N)$ (red curve) in a scalar-tensor model with potential $\sim \Phi^{-1}$ and exponentially decaying coupling (initial conditions: $x_{init} = 1.5 \times 10^{-5}, y_{init} = 1.5 \times 10^{-15}, \Phi_{init} = (6 \times 10^4)^{-1}$).

In our numerical example (figures 5.13 and 5.14), we arranged the initial conditions to

realize a trajectory exhibiting increase in the kinetic and potential energy from the beginning, leading to

$$\frac{x_{init}}{y_{init}} = 10^{10},$$

and

$$\frac{\Omega_{DE,BBN}}{\Omega_{\Lambda,BBN}} \approx \mathcal{O}(10^{23}).$$

The energy scale of the potential - as required to match the present DE density - is roughly the same as in the quintessence case. The evolution of the DE and effective equations of state during radiation epoch, as shown in figure 5.13, is very similar to our results concerning a constantly coupled model with exponential potential (see figure 5.11), while the late time evolution resembles the behaviour of the inverse-power law quintessence trajectory displayed in figure 5.5, which fits our expectations.

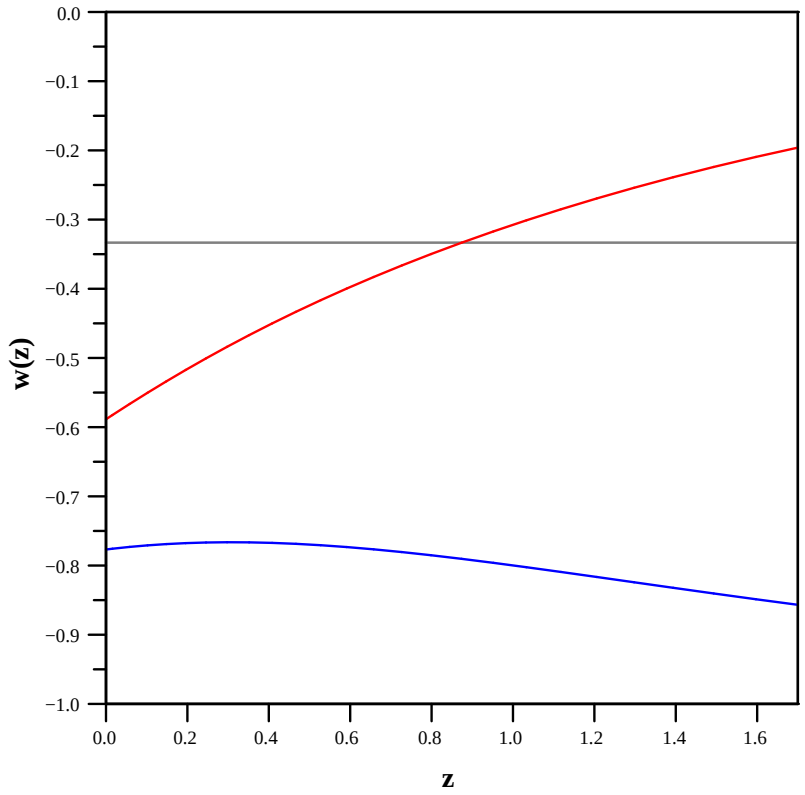

Figure 5.14: Small z evolution of w_{DE} (blue curve) and w_{eff} (red curve) in the scalar-tensor model with potential $\sim \Phi^{-1}$ and exponentially decaying coupling (initial conditions: see above). At present ($\Omega_{DE} = 0.72$) we have $w_{DE} \approx -0.78$; the transition redshift is at $z \approx 0.88$.

Somewhat surprisingly, though the coupled model does not admit a scaling tracker solution like the uncoupled one, the qualitative behaviour of the small z evolution turns out to be less

sensitive to change of initial conditions. (We checked initial conditions up to 10^5 times the values specifying the trajectory we explored in the figures, and found only slight variations in $w_{DE}(0)$ and the transition redshift. Only the transition between $w_{DE} = 1$ and the transient freezing regime occurs at significantly different "times", but well outside the observationally accessible range of z.) While the significant variation of w_{DE} in the small z regime was rather special in the case of figure 5.5, it is a characteristic feature of the coupled model. If the observational trend towards $\frac{dw_{DE}}{dz} = 0$ for $z \lesssim 1$ becomes confirmed in the future, this model could be easily ruled out. On the other hand, changing the potential parameter α towards smaller values is not as dangerous as in the quintessence case, since (in-)dependence on intitial conditions is now determined by the coupling strength around BBN, and not by the tracker property of the potential.

In summary, we finally have found an example that exhibits some of the attractive features, which motivated our analyses in this and the previous chapter: The model converges towards GR, thereby admits a stronger coupling at BBN, as well as a - transiently existing - attractor solution in the radiation epoch, represented by the critical point D. Existence of this fixed point is a genuine property of scalar-tensor theories, and incorporates the $R-$boost mechanism which was proposed to wash out the dependence on initial conditions, as exhibited by quintessence models with shallow slope.

Concluding this chapter, we have to admit that our results are preliminary, in the sense that the efforts to reconstruct the DE equation of state from small redshift data have not yet reached a state of precision and definiteness, which would enable us to discriminate between different models. While the cosmological constant will be clearly ruled out, if the slightest evolution is detected, it remains unclear if any of our model examples could be falsified by this observational tool alone, especially since most of the models principally allow to approximate a cosmological constant gradually by parameter tuning. While we have seen that quintessence models thereby become less attractive, since the parameter tuning also reintroduces dependence on initial conditions, we have rediscovered a scalar-tensor model which is capable to maintain a robust insensitivity to change of initial conditions, due to the $R-$boost mechanism. The specific example we analyzed exhibits a significant small z evolution of the equation-of-state parameter, and is clearly distinguishable from a cosmological constant.

If future equation-of-state reconstructions, based on larger, quality improved data sets still tend to favour the cosmological constant, attempts of model falsification will rely on alternatives, either concerning perturbation growth (to be detected in weak lensing surveys, see e.g. [52]), or variation of α_{em} [61] and gravitational constant in case of quintessence and scalar-tensor models respectively.

The issue of dependence on initial conditions certainly needs to be addressed more systematically, by analyzing large sets of initial values, in order to achieve statistically significant results and discriminate parameter dependencies from variations with change of initial conditions.

Chapter 6

Dark Energy from Biscalar-Tensor Theories

We begin by recollecting the dynamical evolution equations we derived in chapter 3 from the Einstein frame action:

$$S = \int d^4x\sqrt{-g}\left(\frac{1}{2}R - \frac{1}{2}g^{\mu\nu}(\partial_\mu\Phi\partial_\nu\Phi + G(\Phi)\partial_\mu\sigma\partial_\nu\sigma) - V(\Phi,\sigma)\right) + S_{mat}[\Psi, A^{-2}g^{\mu\nu}]. \quad (6.1)$$

The scalar fields obey the following equations of motion,

$$\ddot{\Phi} + 3H\dot{\Phi} = \frac{1}{2}\frac{dG(\Phi)}{d\Phi}\dot{\sigma}^2 - \frac{\partial V(\Phi,\sigma)}{\partial\Phi} + Q(\Phi)\rho_{mat}, \quad (6.2)$$

$$\ddot{\sigma} + 3H\dot{\sigma} = \frac{1}{G(\Phi)}\left(-\frac{dG(\Phi)}{d\Phi}\dot{\Phi}\dot{\sigma} - \frac{\partial V(\Phi,\sigma)}{\partial\sigma}\right), \quad (6.3)$$

with $Q(\Phi)$ defined in (3.20). The Friedmann equations take the following form:

$$H^2 = \frac{1}{3}(\rho_{mat} + \rho_{rad} + \frac{1}{2}(\dot{\Phi}^2 + G(\Phi)\dot{\sigma}^2) + V(\Phi,\sigma)), \quad (6.4)$$

and

$$\dot{H} = -\frac{1}{2}(\rho_{mat} + \frac{4}{3}\rho_{rad} + \dot{\Phi}^2 + G(\Phi)\dot{\sigma}^2). \quad (6.5)$$

The background fluid obeys the modified continuity equation:

$$\dot{\rho}_{fluid} = (-3(1 + w_{fluid})H + (1 - 3w_{fluid})Q(\Phi)\dot{\Phi})\rho_{fluid}, \quad (6.6)$$

with $w_{fluid}\,\epsilon\,[0, \frac{1}{3}]$, the limit values corresponding to pure (dark) matter and pure radiation respectively.

6.1 Two-field models of dark energy

In chapter 2 we gave some examples of theoretical approches to understand dark energy, which naturally involve two real scalar degrees of freedom, e.g. complex structure moduli or Kähler moduli accompanied by axions. Two-field quintessence models, if based on one originally complex scalar field, feature a non-canonical kinetic term just of the kind we introduced in

the biscalar-tensor action above [16, 70]. On the other hand, this non-canonical term can also be viewed as generated by the conformal transformation. Choosing $G(\phi) = 1$ in the Jordan frame theory (3.9) would still lead to a factor

$$G(\Phi) = A^2(\Phi),$$

multiplying the kinetic term of the σ-field. (See section 3.3.)

Within the chosen general framework of biscalar-tensor theories, we can realize three different types of models, which can be interpreted as toy versions of more specific fundamental theories:

1. Both fields run away to infinity and are dynamically relevant as dark energy candidates.

2. One field becomes massive / stabilized at a finite value during cosmic history, the second one enters a period of slow-roll evolution, governed by a flat runaway potential. In this case we get an effective one-field model, with initial conditions dynamically generated by an early period of interaction between the two scalars.

3. Both fields acquire a (small) mass. If the potential is sufficiently flat around its minimum, we can as well get viable dark energy models from this class, assuming that at least one field is still (slowly) rolling, or even frozen to a constant value.

In the following sections, we will discuss examples specified by distinct choices of the functions $A(\Phi), G(\Phi)$, and $V(\Phi, \sigma)$, and their phenomenological implications. To be able to compare with the results of the previous chapter, we generalize the autonomous system approach we already used in the single field case. We start by deriving the general set of dynamical evolution equations, corresponding to the family of models specified by choosing $A(\Phi), G(\Phi)$, and $V(\Phi, \sigma)$ to have exponential form. As in the one-field case, a specific model is defined by a set of constant parameters.

The dynamical variables are:

$$x_1^2 := \frac{\dot{\Phi}^2}{6H^2}, \qquad x_2^2 := \frac{\dot{\sigma}^2}{6H^2},$$

$$y_1^2 := \frac{V_1(\Phi, \sigma)}{3H^2}, \qquad y_2^2 := \frac{V_2(\Phi, \sigma)}{3H^2},$$

$$z^2 := \frac{\rho_\gamma}{3H^2}.$$

We have split the potential into a sum of two terms, to include the possibility of

$$V(\Phi, \sigma) = V_{01} \exp(\lambda_{1\Phi}\Phi) + V_{02} \exp(\lambda_{2\sigma}\sigma).$$

In addition we have to introduce the auxiliary variable

$$G = G(\Phi) = e^{-\gamma\Phi},$$

where the second equality applies only to the special case we are momentarily interested in.

In complete analogy to the one-field case, we use the Friedmann constraint equation to eliminate ρ_{mat}, rewrite the second one,

$$\frac{1}{H}\frac{dH}{dN} = -\frac{3}{2}((1 - x_1^2 - Gx_2^2 - y_1^2 - y_2^2 - z^2) + \frac{4}{3}z^2 + 2(x_1^2 + Gx_2^2)),$$

where we again used N defined in (3.32), and get the following system:

$$\frac{dx_1}{dN} = 3x_1(x_1^2 + Gx_2^2 + \frac{2}{3}z^2 - 1) + \left(\frac{3}{2}x_1 - \sqrt{\frac{3}{2}}Q\right)(1 - x_1^2 - Gx_2^2 - y_1^2 - y_2^2 - z^2)$$
$$+ \sqrt{\frac{3}{2}}(-\gamma G x_2^2 + \lambda_{1\Phi}y_1^2 + \lambda_{2\Phi}y_2^2), \tag{6.7}$$

$$\frac{dx_2}{dN} = 3x_2(x_1^2 + Gx_2^2 + \frac{2}{3}z^2 - 1 + \frac{1}{2}(1 - x_1^2 - Gx_2^2 - y_1^2 - y_2^2 - z^2)) + \sqrt{6}\gamma x_1 x_2$$
$$+ \sqrt{\frac{3}{2}}\frac{1}{G}(\lambda_{1\sigma}y_1^2 + \lambda_{2\sigma}y_2^2), \tag{6.8}$$

$$\frac{dy_1}{dN} = -\sqrt{\frac{3}{2}}(\lambda_{1\Phi}y_1x_1 + \lambda_{1\sigma}y_1x_2) + \frac{3}{2}y_1(1 + x_1^2 + Gx_2^2 - y_1^2 - y_2^2 + \frac{1}{3}z^2), \tag{6.9}$$

$$\frac{dy_2}{dN} = -\sqrt{\frac{3}{2}}(\lambda_{2\Phi}y_2x_1 + \lambda_{2\sigma}y_2x_2) + \frac{3}{2}y_2(1 + x_1^2 + Gx_2^2 - y_1^2 - y_2^2 + \frac{1}{3}z^2), \tag{6.10}$$

$$\frac{dz}{dN} = \frac{z}{2}(z^2 - 1 + 3(x_1^2 + Gx_2^2 - y_1^2 - y_2^2)), \tag{6.11}$$

$$\frac{dG}{dN} = -\sqrt{6}\gamma G x_1. \tag{6.12}$$

We have defined the following quantities, which are constant by assumption:

$$\gamma := -\frac{dG}{d\Phi},$$

$$\lambda_{i\Phi} := -\frac{1}{V_i}\frac{\partial V_i}{\partial \Phi}, \quad \lambda_{i\sigma} := -\frac{1}{V_i}\frac{\partial V_i}{\partial \sigma}, \qquad i \,\epsilon\{1, 2\}.$$

6.2 Dark energy in dilaton-axion-cosmology

Sonner and Townsend [86] discussed a model consisting of an axion and a dilaton coupled to gravity, described by the (Einstein frame) Lagrangian

$$\mathcal{L} = \sqrt{-g}\left[\frac{1}{2}(R - \dot{\Phi}^2 - e^{-\gamma\Phi}\dot{\sigma}^2) - \Lambda e^{-\lambda\Phi}\right], \tag{6.13}$$

which, according to [13], can be "partially motivated from string theory". We do not intend to verify this claim, but to give an alternative motivation. Consider the Jordan frame Lagrangian

$$\mathcal{L} = \sqrt{-g}\left[\frac{1}{2}(\phi^2 R - \dot{\phi}^2 - \dot{\sigma}^2) - \Lambda\phi^{-\alpha}\right],$$

corresponding to Brans-Dicke theory with an additional massless scalar, exhibiting the characteristic shift symmetry of an axion. (Non-gravitational couplings are neglected.) The case

$\alpha = 0$ replaces the inverse-power law potential by a cosmological constant and can be included. The conformally equivalent Einstein frame theory is then just (6.13) with

$$\gamma = \frac{2}{\sqrt{7}}, \qquad \lambda = \frac{\alpha + 4}{\sqrt{7}}.$$

(See section 4.4 for comparison.)

Sonner and Townsend performed a dynamical system analysis on their model, ignoring the matter and radiation content of the universe, and found "recurrent acceleration" within a significant part of the $(\gamma, \lambda)-$parameter space. We are interested in the viability of the model as a DE candidate, and therefore have to take into account the matter and radiation components of the total energy density. The Lagrangian (6.13) coincides with a subset of the class of theories described in the previous section, specified by setting $y_2 = 0$ and the following choice of parameters:

$$\lambda_{1\Phi} := \lambda > 0, \quad \lambda_{1\sigma} = \lambda_{2\Phi} = \lambda_{2\sigma} = 0.$$

As before we redefine $Q = |Q|$ to be positive. Following [86], we allow for γ to take positive and negative values.

If we define the dynamical variable corresponding to the axion kinetic energy - different from the general case - as follows,

$$x_2^2 := \frac{e^{-\gamma\Phi}\dot{\sigma}^2}{6H^2} = \frac{G\dot{\sigma}^2}{6H^2},$$

we can eventually eliminate G completely from the dynamical system. (This is only possible since the axion has no potential; otherwise the variable y_2 would still appear multiplied by a factor $G^{-\frac{1}{2}}$ in the transformed version of (6.8), which corresponds to the axion equation of motion.) The most important advantage of this choice of variables is that it keeps the phase-space compact: $|x_2^2| \leq 1$.

Due to our choice of parameters, and the redefinition of x_2, the equations (6.7) - (6.9) and (6.11) now take the following form:

$$\frac{dx_1}{dN} = 3x_1(x_1^2+x_2^2+\frac{2}{3}z^2-1)+\left(\frac{3}{2}x_1 + \sqrt{\frac{3}{2}}Q\right)(1-x_1^2-x_2^2-y^2-z^2)+\sqrt{\frac{3}{2}}(-\gamma x_2^2+\lambda y^2), \quad (6.14)$$

$$\frac{dx_2}{dN} = 3x_2(x_1^2 + x_2^2 + \frac{2}{3}z^2 - 1 + \frac{1}{2}(1 - x_1^2 - x_2^2 - y^2 - z^2)) + \sqrt{6}\frac{\gamma}{2}x_1x_2, \quad (6.15)$$

$$\frac{dy}{dN} = -\sqrt{\frac{3}{2}}\lambda y x_1 + \frac{3}{2}y_1(1 + x_1^2 + x_2^2 - y^2 + \frac{1}{3}z^2), \quad (6.16)$$

$$\frac{dz}{dN} = \frac{z}{2}(z^2 - 1 + 3(x_1^2 + x_2^2 - y^2)). \quad (6.17)$$

We end up with a three parameter family of models, each characterized by a set of fixed points in four-dimensional compact phase-space. Taking only the solutions with $(y \geq 0, z \geq 0)$, we find the following fixed points $X_s = (x_{1,s}, x_{2,s}, y_s, z_s)$:

$$A: \quad \left(\sqrt{\frac{2}{3}}Q, 0, 0, 0\right),$$

$$B_1, B_2: \quad (\pm 1, 0, 0, 0),$$

$$C: \quad (0, 0, 0, 1),$$

$$D: \quad \left(\frac{1}{\sqrt{6}Q}, 0, 0, \sqrt{1-\frac{1}{2Q^2}}\right),$$

$$E: \quad \left(\frac{2\sqrt{2}}{\sqrt{3}\lambda}, 0, \frac{2}{\sqrt{3}\lambda}, \sqrt{1-\frac{4}{\lambda^2}}\right),$$

$$F: \quad \left(\frac{\sqrt{\frac{3}{2}}}{\lambda - Q}, 0, \sqrt{\frac{2Q(Q-\lambda)+3}{2(\lambda-Q)^2}}, 0\right),$$

$$G: \quad \left(\frac{\lambda}{\sqrt{6}}, 0, \sqrt{1-\frac{\lambda^2}{6}}, 0\right),$$

$$H_1, H_2: \quad \left(\frac{\sqrt{\frac{3}{2}}}{\gamma + Q}, \pm\sqrt{\frac{2Q(\gamma+Q)-3}{2(\gamma+Q)^2}}, 0, 0\right),$$

$$J_1, J_2: \quad \left(\frac{\sqrt{6}}{\gamma+\lambda}, \pm\sqrt{\frac{\lambda(\gamma+\lambda)-6}{(\gamma+\lambda)^2}}, \sqrt{\frac{\gamma}{\gamma+\lambda}}, 0\right).$$

We display properties of the critical points in table 6.1.

The subset of fixed points we get by setting $y = 0$ is identical to the set of fixed points characterizing single field models with exponential potential and constant coupling Q, which we have already extensively discussed in section 5.4. As can be read from the original equation of motion of the axion field, $\dot{\sigma} = 0$ is a trivial solution (and our fixed point analysis shows, that this is indeed a stable configuration in a wide range of parameter space):

$$\ddot{\sigma} + (3H - \gamma\dot{\Phi})\dot{\sigma} = 0.$$

Whence the axion has settled to a constant value, it decouples, while the dilaton alone remains dynamically relevant. The term proportional to $\gamma\dot{\Phi}$ modifies the Hubble friction term (depending on $sgn(\dot{\Phi})$), and can in principle even change its sign if $\gamma > 0$. In a realistic DE model, we can assume the dilaton kinetic energy to be subdominant with respect to the background fluid during early stages of cosmic history; in the original model of Sonner and Townsend the both terms multiplying $\dot{\sigma}$ are naturally of the same order, since then

$$3H = \sqrt{\frac{3}{2}(\dot{\Phi}^2 + G(\Phi)\dot{\sigma}^2) + 3V(\Phi, \sigma)}.$$

f.p.	**existence**	**stability**	Ω_{DE}	w_{eff}
A	$Q \leq \sqrt{\frac{3}{2}}$	stable: $Q^2 < min\{\frac{1}{2}, \frac{3}{2} - \gamma Q, \lambda Q - \frac{3}{2}\}$	$\frac{2}{3}Q^2$	$\frac{2}{3}Q^2$
B_1	$\forall(\gamma, \lambda, Q)$	saddle point: $\lambda > \sqrt{6} \ \wedge \ Q > \sqrt{\frac{3}{2}} \ \wedge \ \gamma < 0$	1	1
B_2		unstable		
C	$\forall(\gamma, \lambda, Q)$	unstable	0	$\frac{1}{3}$
D	$Q \geq \frac{1}{\sqrt{2}}$	stable: $\lambda > 4Q > 2\gamma$	$\frac{1}{6Q^2}$	$\frac{1}{3}$
E	$\lambda \geq 2$ $\lambda \neq 4Q$	stable: $2\gamma < \lambda < 4Q$	$\frac{4}{\lambda^2}$	$\frac{1}{3}$
F	$\frac{3}{2Q} + Q \geq \lambda \geq \frac{Q+\sqrt{Q^2+12}}{2}$ $\wedge Q \leq \sqrt{\frac{3}{2}}$	stable: $Q < \frac{1}{\sqrt{2}}$ $\lambda > max\{4Q, 2Q + \gamma\}$	$\frac{3+Q^2-Q\lambda}{(Q-\lambda)^2}$	$\frac{Q}{\lambda-Q}$
G	$\lambda \leq \sqrt{6}$	stable: $\lambda^2 < min\{4, 3 + Q\lambda, 6 - \gamma\lambda\}$	1	$-1 + \frac{\lambda^2}{3}$
$H_{1,2}$	$\gamma \geq max\{0, \frac{3}{2Q} - Q\}$	stable: $\lambda > \gamma + 2Q$ $\wedge \ \gamma > 2Q$	$\frac{Q}{\gamma+Q}$	$\frac{Q}{\gamma+Q}$
$J_{1,2}$	$\lambda \geq \frac{-\gamma+\sqrt{\gamma^2+24}}{2} \ \wedge \ \gamma \geq 0$ $\lambda \neq \gamma + 2Q$	stable: $\lambda < min\{2\gamma, \gamma + 2Q\}$	1	$\frac{\lambda-\gamma}{\lambda+\gamma}$

Table 6.1: Properties of the fixed points of dynamical system (6.14)-(6.17)

But if γ is sufficiently large, it is possible, even in our version of the model, that $\gamma\dot{\Phi}$ becomes larger than $3H$, thereby causing $\dot{\sigma}$ to diverge. The axion kinetic term $e^{-\gamma\Phi}\dot{\sigma}^2$ can still remain finite, due to the exponentially decreasing dilatonic factor. We identify this situation with the regime of the two pairs of fixed points $H_{1,2}$ and $J_{1,2}$ (the subspace $\{y = 0\}$ defines the separatrix in the stability case), which take the rôle of points A and G in case of large γ. The existence of these points is a genuine property of the two-field model.

The fixed points $H_{1,2}$ and A, F respectively cannot be simultaneously stable: The stability condition $\gamma < \frac{3}{2Q} - Q$ of point A forbids the existence of $H_{1,2}$. On the other hand, stability of $H_{1,2}$ requires

$$\lambda > \gamma + 2Q \geq \frac{3}{2Q} + Q,$$

in conflict with the existence condition of F. Furthermore, stability of G requires $\lambda(\lambda+\gamma) < 6$, and this condition is not compatible with existence of $J_{1,2}$.

By choosing

$$\frac{-\gamma + \sqrt{\gamma^2 + 24}}{2} \leq \lambda < min\{2\gamma, \gamma + 2Q\}, \quad \gamma > max\{2Q, \frac{3}{2Q} - Q\},$$

we can realize a model with late time (possibly de Sitter like) attractors J_1, J_2, preceded by the scaling regime of saddle points H_1, H_2, corresponding to a sequence of matter and DE dominated epochs as in ΛCDM cosmology.

The autonomous system can be reduced to obtain the original Sonner-Townsend model, which enables us to discuss the issue of recurrent acceleration. Setting

$$z = 0, \qquad (1 - x_1^2 - x_2^2 - y^2 - z^2) = 0,$$

and eliminating $y^2 = 1 - x_1^2 - x_2^2$, we end up with a two-dimensional system with compact phase-space like in [86], but spanned by different dynamical variables. Within the full four-dimensional phase-space, trajectories corresponding to the Sonner-Townsend model are confined to the two-dimensional subset of phase-space boundary defined by

$$x_1^2 + x_2^2 + y^2 = \Omega_{DE} = 1.$$

To realize recurrent acceleration, the late time attractor has to be a stable spiral with w_{eff} not too far from $-\frac{1}{3}$. In this case, the trajectories winding around the fixed point can cross both regions corresponding to accelerated and decelerated expansion. This condition cannot be fulfilled if G is the late time attractor, since G is a stable node whenever stable. (The Jacobi matrix at G has four real eigenvalues $\forall(\gamma, \lambda, Q)$.) It remains possible that the effective equation-of-state parameter drops below $-\frac{1}{3}$, before approaching its attractor value, along certain specific trajectories, corresponding to a short period of transient acceleration.

Points J_1, J_2, on the other hand, have two complex eigenvalues if

$$\frac{27}{4}\gamma + 6\lambda - (\gamma + \lambda)(\gamma\lambda + \lambda^2) < 0,$$

and (like G) their position is at the boundary of the compact phase-space, corresponding to $\Omega_{DE} = 1$. Since in a realistic cosmological set-up, Ω_{DE} is monotonically increasing with N (with time) during recent cosmic evolution, and $y > \frac{1}{\sqrt{3}}$ necessary for accelerated expansion, the generic trajectory will reach the boundary soon after passing the phase-space region once, where

$$w_{eff} \approx x_1^2 + x_2^2 - y^2 < -\frac{1}{3},$$

and acceleration is possible. To give an illustrative example, we fix our parameters to $(Q, \gamma, \lambda) = (0, 4, 2)$. In this case $J_{1,2}$ are stable spirals with $w_{eff} = -\frac{1}{3}$. Figure 6.1 shows the phase-portrait of the Sonner-Townsend model, while figure 6.2 displays the corresponding phase-space section of our realistic version. We plotted only one trajectory in each case, which exhibits the characteristic features.

We discuss figure 6.1 first. Accelerated expansion occurs in the phase-plane region with $x_1^2 + x_2^2 < \frac{1}{3}$.

(1) The trajectory starts near the repeller $B_1 : (x_1, x_2) = (1, 0)$, and follows the boundary of the phase-plane until it reaches the vicinity of $B_2 : (-1, 0)$, which is a saddle point in the two-dimensional case. During this first stage we have $x_1 + x_2 \approx 1$, and therefore $w_{DE} = w_{eff} \approx 1$. The evolution of the fields is entirely determined by interaction via the non-canonical kinetic term: the "friction" term in the axion equation of motion is initially sign reversed,

$$\gamma\dot{\Phi} > 3H \approx \sqrt{\frac{3}{2}}\dot{\Phi},$$

which causes the rapid increase in $x_2 \sim \dot{\sigma}$. When $x_1 \sim \dot{\Phi}$ drops below zero (due to the effective force term $\sim \dot{\sigma}^2$), the axion is subject to enhanced friction, and its velocity decreases again.

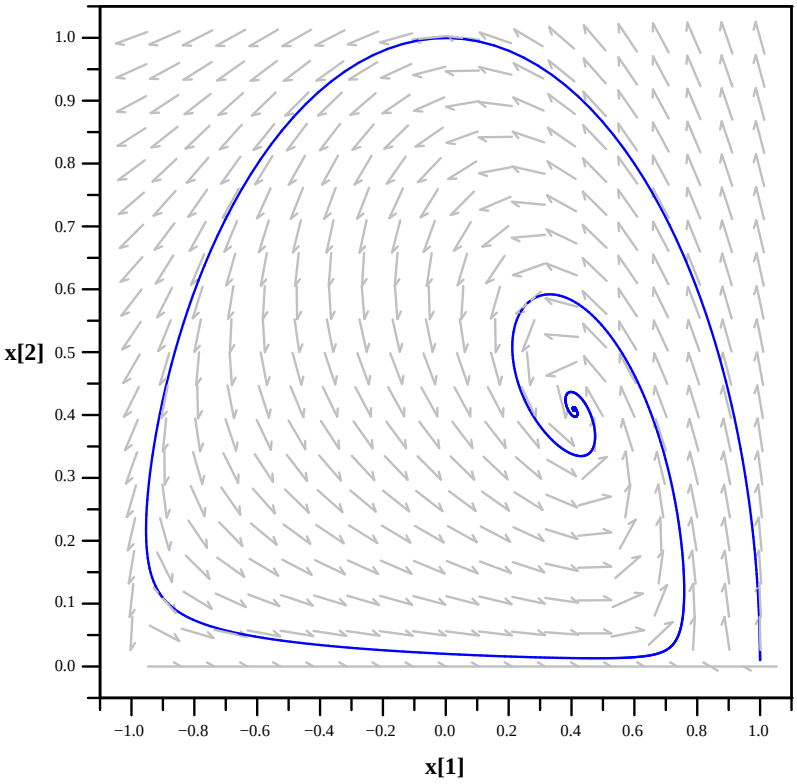

Figure 6.1: Phase-portrait of Sonner-Townsend model, $\gamma = 4, \lambda = 2$.

(2) When the modified friction term has grown sufficiently to force the axion into slow-roll, the dilaton evolves nearly undisturbed and its kinetic and potential energy increase. When the trajectory, which is now driven towards the saddle point G, passes $x_1 \approx -\frac{1}{\sqrt{3}}$, it enters the region where accelerated expansion occurs. Since there is now a significant contribution from the potential to H, the dilaton's velocity increases up to $x_1 \approx \frac{1}{\sqrt{3}}$, where the trajectory exits the accelerated regime, before the friction term in the axion field equation gets sign reversed again.

(3) Approaching the saddle point $G = (\sqrt{\frac{2}{3}}, 0)$, the trajectory is again bent towards increasing x_2.

(4) Now it enters the regime of the attractor, and re-enters the subspace with $w_{eff} < -\frac{1}{3}$, soon after $x_2(N)$ has passed a local maximum. Since the attractor is located exactly at the boundary between accelerated and decelerated expansion, $w_{eff} = w_{DE}$ oscillates around $-\frac{1}{3}$, while the trajectory approaches the fixed point.

Now we turn to the model version with background fluid, where

$$y^2 < 1 - x_1^2 - x_2^2,$$

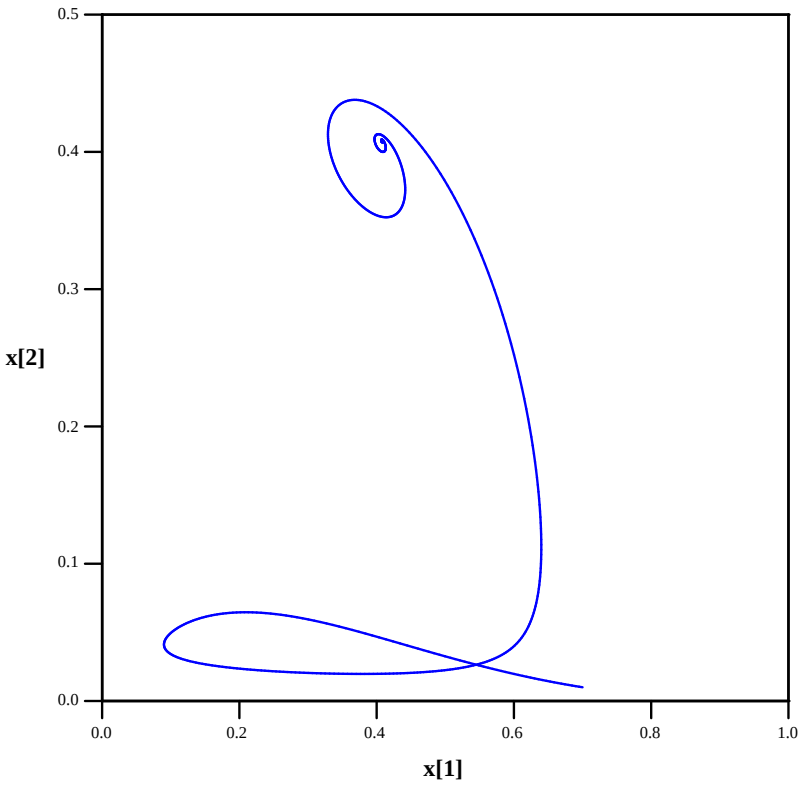

Figure 6.2: Phase-space section (x_1, x_2) of the extended model version, parameters as above.

before the final attractor is reached. We let our trajectory start close to $(x_1, x_2, y, z) = (0.7, 0, 0, 0.7)$, which is of course not very realistic ($\Omega_{DE} = \Omega_{rad}$), but makes it easier to recognize the qualitative features in the phase-space plot. The discussion follows the steps (1) to (4), corresponding to the $(x_1, x_2)-$section of figure 6.2, in analogy to the former case. In figure 6.3 we show the evolution of w_{eff} and w_{DE} with y.

(1) Due to our extreme choice of $x_{1,init}$, the axion's velocity is initially enhanced by "negative friction". But the trajectory stays close to the x_1-axis, indicating background fluid dominance. Ω_{DE} decreases.

(2) The turning point is already reached around $(x_1, x_2) = (0, 0)$. The axion gets nearly frozen. No acceleration occurs, since the potential energy is, though increasing, still negligible with respect to the background. As can be seen in figure 6.3, w_{DE} approaches -0.8, but w_{eff} decreases only slowly.

(3) Since the background energy density is decreasing, the axion can enter the "negative friction" regime, leading to a rapid increase in x_2. Now the potential energy remains approximately constant (as in the Sonner-Townsend case), thereby allowing for w_{eff} and w_{DE} to grow towards zero again. (See figure 6.3.)

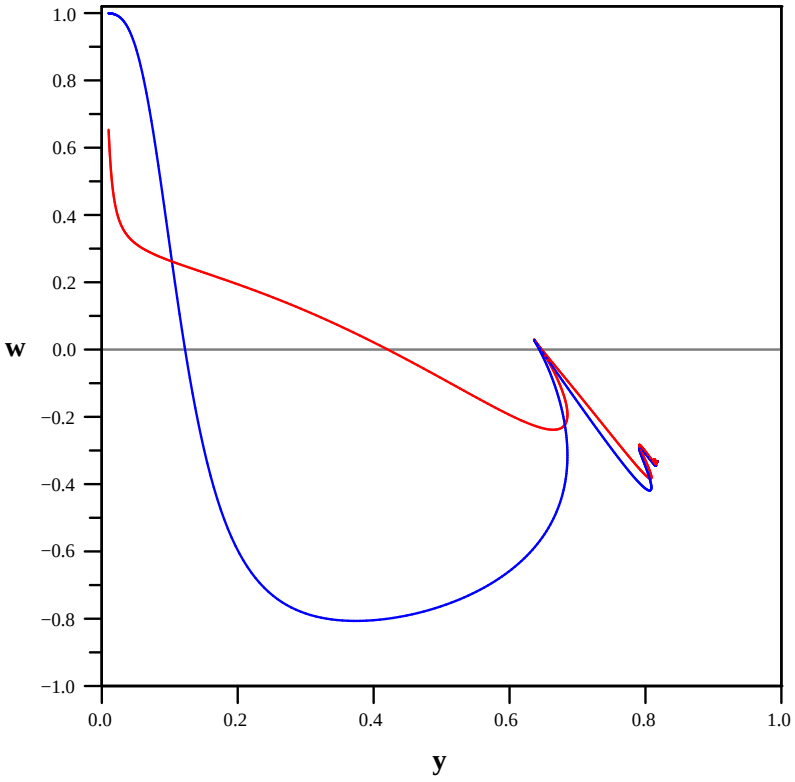

Figure 6.3: The same trajectory as in figure 6.2, plotted in $(y, w_{eff})-$ (red curve) vs. $(y, w_{DE})-$plane (blue curve).

(4) In approaching the attractor, the trajectory's behaviour as shown in figure 6.2 is very similar to what we observed in figure 6.1. A short period of transient acceleration begins when $y \approx 0.8$ is reached, but afterwards w_{eff} increases again and the attractor value $w_{eff} = w_{DE} = -\frac{1}{3}$ is approached from above.

In summary, the main difference between the two models is the absence of the first enduring stage of accelerated expansion (2) in our extended version, due to the difference between w_{DE} and w_{eff} resulting from background fluid dominance. We have to emphasize, that a more realistic choice of initial conditions would only further suppress the scalar field dynamics, since then $\Omega_{DE} \ll \Omega_{rad}$ initially. During the matter dominated epoch we have

$$w_{eff} = w_{DE}(1 - \Omega_{mat}).$$

None of the other fixed points exhibits negative values of w_{eff}. If the stationary point corresponding to acceleration is a saddle point, and another fixed point stable, an early period of transient acceleration is possible. This can be achieved by choice of parameters, but duration and even existence of this period depend on initial conditions. So we have

to conclude, that recurrent acceleration - in contrast to the simpler model of [86] - is not a generic feature of our modified approach. This class of models does not provide a DE candidate, realizing an equation of state close to $w_{DE} \approx -1$ at present, without the side-effect of a future event horizon due to eternal acceleration.

6.3 Periodic interaction potential

In the previous section, we discussed a family of DE models with at least one field, the dilaton, running to infinity. Depending on the choice of parameter γ, the second, axionic field could either become stabilized at a fixed value or stay dynamically relevant and show runaway behaviour as well. For completeness, we will now construct a simple toy model, where both fields are (in principle) allowed to settle down to fixed values, corresponding to minima of the interaction potential.

We consider the following (Jordan frame) action:

$$S = \int d^4x\sqrt{-g}\left[\frac{1}{2}(\xi\phi^2 R - g^{\mu\nu}\partial_\mu\phi\partial_\nu\phi - g^{\mu\nu}\partial_\mu\sigma\partial_\nu\sigma) - V_1(\phi) - V_2(\sigma)\right] + S_{mat}[g^{\mu\nu}, \Psi], \tag{6.18}$$

containing the BD scalar (which we keep calling dilaton for convenience) and a second, minimally coupled scalar field. We specify the dilaton potential to be a polynomial $P(\phi)$ with at least one minimum, and

$$V_2(\sigma) = \Lambda(C + \cos(k\sigma)),$$

which is the natural choice of potential for an axion type field. (The replacement $1 \to C > 1$ is for later convenience.) By assumption the BD field couples universally, so there can be no interaction term in the total scalar potential. (Furthermore we neglect any coupling of the axion to the matter sector.)

Performing a conformal transformation, we find the corresponding Einstein frame action,

$$S \supset \int d^4x\sqrt{-g}\left[\frac{1}{2}(R - g^{\mu\nu}\partial_\mu\Phi\partial_\nu\Phi - A^2(\Phi)g^{\mu\nu}\partial_\mu\sigma\partial_\nu\sigma) - V(\Phi) - A^4(\Phi)\Lambda(C + \cos(k\sigma))\right], \tag{6.19}$$

where $\kappa := \sqrt{\frac{\xi}{6\xi+1}}$ and

$$A(\Phi) = \frac{1}{\sqrt{\xi}}e^{-\kappa\Phi} = \frac{1}{\sqrt{\xi}}e^{-Q\Phi}.$$

The Einstein frame, dilaton potential is now a sum of exponentials:

$$V(\Phi) := A^4(\Phi)P(e^{\kappa\Phi}) = \sum_i a_i e^{b_i Q\Phi}.$$

(Potentials of this type have frequently been discussed in the literature, see [8], or [32] for an example in the context of supergravity. A dilaton potential of the type

$$V(\Phi) \sim f(\Phi)[e^{k_1\Phi} + Be^{-k_2\Phi}],$$

with $k_{1,2} > 0$, can be found in [50], compare (6.20). A Jordan frame phase-space study of a single field BD model with potential $V(\phi) = \lambda\phi^n$ was done in [24].) For simplicity we restrict ourselves to the case

$$V(\phi) \sim \phi^\alpha \quad \Longrightarrow \quad V(\Phi) \sim \exp((\alpha - 4)Q\Phi),$$

with $\alpha > 4$.

As before, we fix the geometry by inserting the flat FRW metric, and assume the scalar fields to be homogeneous. Setting $\xi = 1$ for simplicity, we obtain the following Lagrangian:

$$\mathcal{L} = \sqrt{-g}\left[\frac{1}{2}(R - \dot{\Phi}^2 - e^{-\gamma\Phi}\dot{\sigma}^2) - \Lambda(C + \cos(k\sigma))e^{-\lambda\Phi} - V_0 e^{\beta\Phi}\right], \tag{6.20}$$

where now

$$\gamma = 2Q, \qquad \lambda = 4Q, \qquad \beta = (\alpha - 4)Q.$$

Obviously, we could have obtained this Lagrangian directly from the Sonner-Townsend model by replacing

$$\Lambda \longrightarrow \Lambda(C + \cos(k\sigma)),$$

and introducing the additive potential term

$$V_1(\Phi) = V_0 e^{\beta\Phi}$$

for the dilaton. In the following, we assume the different parameters to be independent, in order to cover a more general class of models.

The total potential is periodic in $\sigma-$direction, with period $\Delta\sigma = \frac{2\pi}{k}$, and has saddle points at

$$(\Phi_s, \sigma_s) = \left(\frac{1}{\beta + \lambda}\ln\left(\frac{\Lambda}{V_0}(C+1)\frac{\lambda}{\beta}\right), 0 \pm n\Delta\sigma\right), \qquad n \,\epsilon\, \mathbb{N}_0, \tag{6.21}$$

and minima at

$$(\Phi_m, \sigma_m) = \left(\frac{1}{\beta + \lambda}\ln\left(\frac{\Lambda}{V_0}(C-1)\frac{\lambda}{\beta}\right), \frac{\pi}{k} \pm n\Delta\sigma\right). \tag{6.22}$$

The choice $C > 1$ we made above guarantees the existence of the minima.

We already know that, for the axion to be a viable quintessence candidate, its potential has to be fine tuned in order to match the present DE density: The axion remains frozen near the maximum of the potential (realizing an effective cosmological constant), and starts to slowly roll down towards the minimum just around the present. In analogy to the one-field case we assume that only the region around a saddle point is phenomenologically relevant. Following our considerations in section 5.3, we replace the axion potential by a Gauss function:

$$V_2(\sigma) = \Lambda(C+1)\exp(-\frac{k^2}{2(C+1)}\sigma^2).$$

The dynamical evolution equations then take the following form:

$$\begin{aligned}\frac{dx_1}{dN} &= 3x_1(x_1^2 + Gx_2^2 + \frac{2}{3}z^2 - 1) + \left(\frac{3}{2}x_1 + \sqrt{\frac{3}{2}}Q\right)(1 - x_1^2 - Gx_2^2 - y_1^2 - y_2^2 - z^2) \\ &\quad + \sqrt{\frac{3}{2}}(-\gamma G x_2^2 + \lambda y_1^2 - \beta y_2^2), \end{aligned} \tag{6.23}$$

$$\begin{aligned}\frac{dx_2}{dN} &= 3x_2(x_1^2 + Gx_2^2 + \frac{2}{3}z^2 - 1 + \frac{1}{2}(1 - x_1^2 - Gx_2^2 - y_1^2 - y_2^2 - z^2)) \\ &\quad + \sqrt{6}\gamma x_1 x_2 + \sqrt{\frac{3}{2}}\frac{1}{G}\mu y_1^2, \end{aligned} \tag{6.24}$$

$$\frac{dy_1}{dN} = -\sqrt{\frac{3}{2}}y_1(\lambda x_1 + \mu x_2) + \frac{3}{2}y_1(1 + x_1^2 + Gx_2^2 - y_1^2 - y_2^2 + \frac{1}{3}z^2), \tag{6.25}$$

$$\frac{dy_2}{dN} = \sqrt{\frac{3}{2}}\beta y_2 x_1 + \frac{3}{2}y_2(1 + x_1^2 + Gx_2^2 - y_1^2 - y_2^2 + \frac{1}{3}z^2), \tag{6.26}$$

$$\frac{dz}{dN} = \frac{z}{2}(z^2 - 1 + 3(x_1^2 + Gx_2^2 - y_1^2 - y_2^2)), \tag{6.27}$$

$$\frac{dG}{dN} = -\sqrt{6}\gamma G x_1, \tag{6.28}$$

$$\frac{d\mu}{dN} = \sqrt{6}\eta x_2. \tag{6.29}$$

We introduced the new parameter

$$\eta := \frac{k^2}{C+1}.$$

The corresponding phase-space is non-compact, since the variables μ (which is proportional to the axion field value), G and x_2 are unbound ($Gx_2^2 \leq 1$ is still valid of course). But a solution, where any of these variables diverge, would be an artefact of deleting the minima of the potential by the substitution of $V_2(\sigma)$ with a Gaussian. A stationary point of the full system requires stationarity of both field values, as can be read from the last two equations, and therefore corresponds to "sit and wait" behaviour of both fields. For each value of G (and therefore of the dilaton field Φ), there are two solutions $P^* = (x_1, x_2, y_1, y_2, z, \mu)$ of the corresponding system of nonlinear algebraic equations (in fact we have "stationary lines" in phase-space):

$$C^* = (0, 0, 0, 0, 1, 0),$$

$$G^* = \left(0, 0, \sqrt{\frac{\beta}{\beta+\lambda}}, \sqrt{1 - \frac{\beta}{\beta+\lambda}}, 0, 0\right).$$

Points of C^* correspond to the usual radiation dominated repeller, while points of G^* have $\Omega_{DE} = 1$ and $w_{eff} = w_{DE} = -1$, so they represent a de Sitter solution. Those points are saddle points, the Jacobi matrix having one real positive eigenvalue. The corresponding physical situation is realized, if the axion field is initially precisely fixed at the saddle point of the potential. This configuration is of course unstable with respect to perturbations in the axion field value, but insensitive to changes in the background fluid or the second field. A deviation from $(\mu, x_2) = (0, 0)$ in the initial conditions will cause the axion to slowly roll, away from the saddle point. Otherwise it will remain fixed, until all background energy density is diluted away, while the dilaton is stabilized in the limit $\rho_{mat} \to 0$. In this case, we again have effectively a single field model, which generates a cosmological constant dynamically, due to a non-zero potential minimum.

To discuss this in more detail, we consider the original dilaton field equation,

$$\ddot{\Phi} + 3H\dot{\Phi} = -\frac{\gamma}{2}e^{-\gamma\Phi}\dot{\sigma}^2 - \beta V_0 e^{\beta\Phi} + \lambda\Lambda(C + \cos(k\sigma))e^{-\lambda\Phi} + Q(\Phi)\rho_{mat} \tag{6.30}$$

(Q redefined to be positive), which reduces to

$$\ddot{\Phi} + 3H\dot{\Phi} = -\beta V_0 e^{\beta\Phi} + Ke^{-\lambda\Phi} + Q\rho_{mat}$$

(with a new (quasi-)constant K), if the axion is assumed to be frozen. Though the dilaton potential has a minimum for each fixed value of σ, the field will settle to a fixed value only

in the limit $\rho_{mat} \to 0$, since the effective potential is time dependent. Due to the constant coupling Q the dilaton can evolve, even if the axion does not.

On the other hand, we face modifications with respect to an axionic quintessence model where the dilaton is absent: Considering how the axion field equation is influenced by the presence of the second field,

$$\ddot{\sigma} + (3H - \gamma\dot{\Phi})\dot{\sigma} = k\sin(k\sigma)e^{(\gamma-\lambda)\Phi}, \tag{6.31}$$

we observe that the "sit and wait" mechanism will be relevant as long as $\gamma\dot{\Phi} < 3H$. The freezing regime of the axion can be prolonged, and the need for fine tuning alleviated, if either

1. the dilaton field value (assumed to be positive) decreases, while $\gamma > 0$, or

2. the dilaton field value increases, while $\gamma < 0$.

In both cases the friction term is enhanced, whenever the dilaton field value changes. (We assume that $e^{(\gamma-\lambda)\Phi}$ is of order unity, and therefore the modification of the force term negligible.)

In the next section, we intend to discuss an example, specified by $Q = 0$. In that case, the dilaton potential has a time independent minimum, for each value of σ. If the axion sits and waits exactly at its saddle point value, the dilaton will be stabilized at the saddle point. Otherwise both fields will be dynamically relevant, and ultimately reach the minimum of the total potential. The axion kinetic energy acts as an additional force term in the dilaton Klein-Gordon equation, equivalent to $Q\rho_{mat}$, but quadratic in the small deviation from $\dot{\sigma} = 0$, and will therefore be negligible. If we assume

$$\Phi_{init} > \Phi_s > \Phi_m > 0,$$

while $\sigma_{init} \approx \sigma_s$, and furthermore $\gamma > 0$, condition 1 (see above) is satisified, and a single field model with Gaussian potential, as discussed in section 5.3, will provide a phenomenologically viable approximation.

6.4 Dark energy from shape moduli

Following Peloso and Poppitz [70], we consider a 6-dimensional product manifold, consisting of a non-compact 4-dimensional (e.g. FRW) spacetime and a toroidal compactification space. Let the torus be parametrized by

$$(y_1, y_2)\,\epsilon\,(-\pi r_1, \pi r_1] \times (-\pi r_2, \pi r_2],$$

and carry an action of the group $\mathbb{Z}_2$, defined by the map

$$S : (y_1, y_2) \mapsto -(y_1, y_2).$$

The torus has four fixed points under this map,

$$P_1 = (0,0), \quad P_2 = (\pi r_1, 0), \quad P_3 = (0, \pi r_2), \quad P_4 = (\pi r_1, \pi r_2),$$

and the resulting space (homeomorphic to $\mathbb{S}^2$) contains four conical singularities placed at the fixed points, each with deficit angle π, corresponding to the tension of the $3+1$-branes located at the positions of the singularities.

The volume of the extra space is determined by the expectation value of a scalar field, called radion, which couples to the trace of the energy-momentum tensor of matter fields localized on (one of) the branes. Peloso and Poppitz assume, that the radion can be stabilized by the interplay between a 6-dimensional negative cosmological constant - energetically favouring the extra space to shrink - and a U(1) gauge field in the bulk, with quantized magnetic flux,

$$\Phi_{mag} = \frac{2\pi N}{e},$$

where e is the gauge coupling, and $N \epsilon \mathbb{N}$ [70]. The magnetic energy is proportional to the inverse of the surface volume, and contrasts the effect of the negative cosmological constant Λ_6. After minimizing the total energy, the volume modulus is expected to be stabilized at [70]:

$$\langle \mathcal{A} \rangle = \frac{\pi N}{\sqrt{-2\Lambda_6}}.$$

Let us now generalize the geometry of the torus by introducing a *shift* parameter θ [38], and a complex shape modulus:

$$\tau = \tau_1 + i\tau_2 := \frac{r_2}{r_1} e^{i\theta}.$$

In agreement with Peloso and Poppitz, we regard the area of the torus,

$$\mathcal{A} = r_1 r_2 \sin\theta,$$

as fixed. The torus is now parametrized by a complex variable z with periodic identifications [38]:

$$z \to z + \sqrt{\frac{\mathcal{A}}{\tau_2}} = z + 2\pi r_1,$$

$$z \to z + \tau\sqrt{\frac{\mathcal{A}}{\tau_2}} = z + 2\pi r_2(\cos\theta + i\sin\theta).$$

Deformations of the extra space are associated with dynamical evolution of the two shape moduli τ_1 and τ_2, which do not - in contrast to the radion - couple to the standard model fields on the brane, but only to the Kaluza-Klein spectrum of bulk fields [70]. The Casimir energy of the bulk fields generates a potential, and therefore a possible stabilization mechanism for the moduli.

6.4.1 Action and field equations

We consider the block-diagonal metric ansatz of [70]:

$$ds^2 = G_{IJ} dx^I dx^J = g_{\mu\nu} dx^\mu dx^\nu + g_{ab} dx^a dx^b,$$

where

$$I, J \epsilon \{0, ...5\}, \quad \mu, \nu \epsilon \{0, ..., 3\}, \quad a, b \epsilon \{4, 5\},$$

and G_{IJ} depends only on coordinates with Greek indices. The metric on the torus is given by

$$g_{ab} = \frac{1}{\tau_2}\begin{pmatrix} 1 & \tau_1 \\ \tau_1 & |\tau|^2 \end{pmatrix}, \tag{6.32}$$

and has determinant one. The 6-dimensional Ricci tensor obtained from the metric ansatz reads as follows,

$$R_{IJ} = R_{\mu\nu} + \Gamma^{\rho}_{ab}\Gamma^{c}_{\rho c} - \Gamma^{c}_{a\rho}\Gamma^{\rho}_{cb} - \Gamma^{\rho}_{ac}\Gamma^{c}_{\rho b},$$

where we already skipped a total divergence, with

$$\Gamma^{\rho}_{ab} = \frac{1}{2}g^{\rho\sigma}\partial_\sigma g_{ab},$$

$$\Gamma^{c}_{a\rho} = \frac{1}{2}g^{cd}\partial_\rho g_{ad},$$

while any other Christoffel coefficients with mixed or Latin indices vanish.

The resulting 6-dimensional Ricci scalar is given by:

$$R[G] = R[g_{\mu\nu}] + \frac{1}{4}g^{ab}g^{cd}g^{\mu\nu}(\partial_\mu g_{ab}\partial_\nu g_{cd} - \partial_\mu g_{ac}\partial_\nu g_{bd} - \partial_\mu g_{ad}\partial_\nu g_{bc}).$$

We substitute

$$\partial_\mu g_{44} = -\frac{1}{\tau_2^2}\partial_\mu \tau_2,$$

$$\partial_\mu g_{45} = \frac{1}{2}(\tau_2\partial_\mu\tau_1 - \tau_1\partial_\mu\tau_2),$$

$$\partial_\mu g_{55} = \frac{2\tau_1}{\tau_2}\partial_\mu\tau_1 + \left[1 - \left(\frac{\tau_1}{\tau_2}\right)^2\right]\partial_\mu\tau_2,$$

and integrate over the extra dimensions to finally obtain the 4-dimensional effective action,

$$S_{geom} = M_6^4\int d^6x\sqrt{-G}\,R[G] = \frac{1}{2}\int d^4x\sqrt{-g}[R - \frac{g^{\mu\nu}}{2\tau_2^2}\partial_\mu\tau\partial_\nu\overline{\tau}], \tag{6.33}$$

where we have set

$$2M_6^4\langle\mathcal{A}\rangle \equiv M_p^2 \equiv 1.$$

Assuming FRW geometry on the brane, and homogeinity of the scalar fields, we introduce

$$\Phi := \frac{1}{\sqrt{2}}\ln\tau_2, \qquad \sigma := \frac{1}{\sqrt{2}}\tau_1,$$

and find the reduced action

$$S_\Phi = -\mathcal{V}\int dt\, a^3(t)\left[\frac{1}{2}(\dot\Phi^2 + e^{-2\sqrt{2}\Phi}\dot\sigma^2) + V(\Phi,\sigma)\right], \tag{6.34}$$

with yet unspecified potential. The kinetic part of this action corresponds to the Lagrangian (6.20), if we choose

$$\gamma = 2\sqrt{2}.$$

6.4.2 The Casimir potential

The Casimir energy of bulk fields, which obey periodic boundary conditions in the extra space coordinates x^4, x^5, generates a potential for the shape moduli which is naturally related to the size of the extra dimensions [70]. If the bulk fields belong to supersymmetric multiplets, and furthermore the brane-localized breakdown of SUSY is communicated to the bulk with gravitational strength, the mass splitting within the bulk multiplets is of order $10^{-3}eV$ and induces a non-vanishing Casimir potential. The contribution of a 1/4 hypermultiplet with massless fermion and scalar of mass M, given by

$$V^* = \frac{M^2}{(2\pi L^2)}[\frac{\pi^3\tau_2^2}{45} - \sum_{p=1}^{\infty}\frac{1}{p^2}(\frac{2\pi(1-\cosh(2\pi p\tau_2)\cos(2\pi p\tau_1))}{[\cosh(2\pi p\tau_2)-\cos(2\pi p\tau_1)]^2} - \frac{1}{p\tau_2}\frac{\sinh(2\pi p\tau_2)}{\cosh(2\pi p\tau_2)-\cos(2\pi p\tau_1)})], \tag{6.35}$$

where $L := \langle\mathcal{A}\rangle^{1/2}$ is the characteristic length scale of the internal space, is plotted in figure 6.4. Contributions of other multiplets with SUSY breaking mass splittings are easily obtained from (6.35), and the total potential can be written as a power series in ML with a leading contribution given by (6.35), multiplied by some overall constant factor [70, 76]. The scale of the potential is of the same order as the present energy density in the universe if $L \lesssim 6\mu m$, meaning that indeed shape moduli in correspondingly large extra dimensions can provide a viable quintessence candidate.

The Casimir potential is invariant under $SL(2,\mathbb{Z})$ transformations,

$$\tau \to \frac{a\tau + b}{c\tau + d},$$

with $a, b, c, d \,\epsilon\, \mathbb{Z}$ and $ad - bd = 1$. The two values,

$$\tau_s = i, \qquad \tau_m = e^{\frac{2\pi i}{3}},$$

are fixed points of the special transformations,

$$\tau \to -\frac{1}{\tau}, \qquad \tau \to -\frac{1}{\tau+1},$$

respectively, and correspond to saddle point and minimum in the fundamental domain of the torus in the complex plane [70].

The Casimir potential can be approximated within the general framework of the preceding section. Consider the following choice of parameters:

$$\gamma = 2\sqrt{2}, \quad \lambda = 6, \quad \beta = 12.$$

The remaining parameters C and $\frac{V_0}{\Lambda}$ can be adjusted (taking values of order unity) to match the positions of the Casimir potential extrema (compare (6.21) and (6.22)) at

$$(\Phi_s, \sigma_s) = (0, \pm n), \qquad n \,\epsilon\, \mathbb{N}_0,$$

$$(\Phi_m, \sigma_m) = \left(\ln\left(\frac{\sqrt{3}}{2}\right), \frac{1}{2} \pm n\right).$$

The resulting potential contour is shown in figure 6.5.

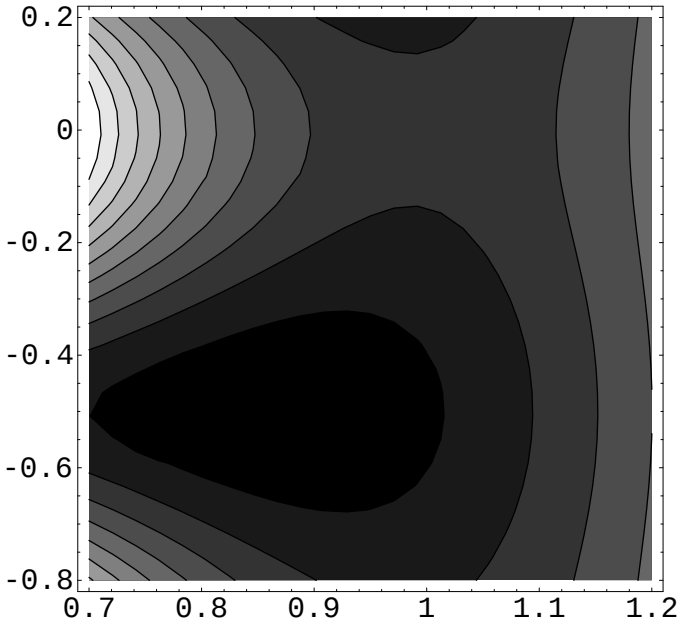

Figure 6.4: Contourplot of the shape moduli potential according to [70].

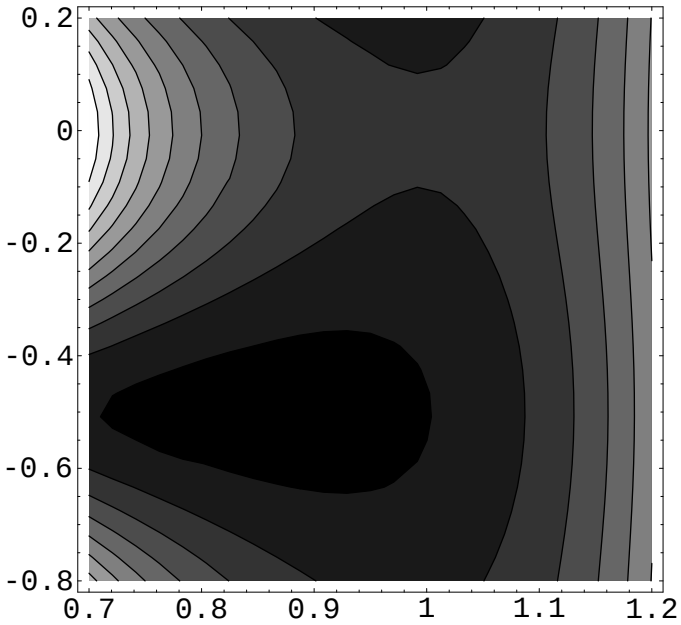

Figure 6.5: Contourplot of the potential $V(\sigma, x) = \Lambda(C + \cos(2\pi\sigma))x^{-6} + V_0 x^{12}, x := e^{\sqrt{2}\Phi}$.

In quadratic approximation, our model potential does not precisely coincide with the Casimir potential: We find

$$\frac{m_{2,s}}{m_{1,s}} \approx -5.9, \quad \frac{m_{2,m}}{m_{1,m}} \approx 0.6,$$

instead of the values, -5.0 and 1.0 respectively, given by Peloso and Poppitz. We could compensate for this discrepancy, if we allow β and λ to take non-integer values. The comparison of figures 6.4 and 6.5 shows, that our toy model matches the qualitative features of the Peloso-Poppitz potential quite well.

In summary, the shape moduli approach infers the right potential scale and field masses to obtain a viable DE model - provided a SUSY bulk field content. As Peloso and Poppitz have already mentioned, only the behaviour of the axionic field, in the vicinity of the saddle point, is phenomenologically relevant. We have covered this situation already by the numerical example given in section 5.3.3. In the previous section, we presented qualitative arguments to justify the assumption, but we have also seen, that the success of the model crucially depends on the choice of initial conditions. As was disussed in subsection 5.3.3, the initial value of the axionic field must not deviate from the saddle point value by too much. The question remains open, whether this choice is natural in the shape moduli case.

An interesting issue of further investigation might be the interplay between the volume and shape moduli during the stabilization of the radion. The compactification process may serve as a mechanism, which dynamically generates initial conditions for the shape moduli, thereby helping to avoid the fine tuning problem of common axion-type quintessence models.

Chapter 7

Summary and conclusion

Incorporating a dynamical realization of dark energy within particle physics or gravity theory remains to be a formidable task to be addressed in the future. Many proposals have been published during the course of the last decade, including dark energy candidates like radions, dilatons, or axions, motivated from higher-dimensional supergravity or other extensions of the standard model, phantom field k-essence, which has been claimed to be inferable from quantum loop cosmology, and more elaborate or exotic approaches we have not even mentioned in our thesis. Instead of testing every single proposal against available observational data, we have followed a different course. As low-energy effective field theories, scalar-tensor theories of gravity are characterized by a few free functions of (in our case) one or two scalar fields, including the simpler case of minimally coupled, quintessence fields. We have investigated the possibility to constrain the choice of those functions by phenomenological considerations. In order to provide a viable dark energy model, a quintessence potential has to belong to one of the following classes:

1. The potential exhibits at least one non-zero, local minimum at a finite field value, and the scalar field has already been stabilized at this minimum. The set-up constitutes a dynamically generated cosmological constant, and is therefore observationally indistingiushable from the case of constant vacuum energy. In order to match the present dark energy density, the actual value of the potential minimum is subject to fine tuning, but the corresponding energy density could have been significantly larger in the past. Fine tuning of initial conditions is therefore unnecessary.

2. The scale of the potential is low enough, for the Hubble friction to keep the scalar field frozen at a position close to its initial value, where it "sits and waits", until the Hubble rate is sufficiently reduced to allow for slow roll. A prototype of this class is the axion potential. If the potential has a zero minimum, the accelerated expansion will be a transient phenomenon, in which case a future event horizon is avoided. (In chapter 5 we have introduced a Gaussian model potential, which shares these properties without exhibiting any minima.) Models of this class generically require not only fine tuning of the potential scale, but also of the initial field value, depending on the specific shape of the potential.

3. The potential is of the runaway type, and (at least locally) sufficiently flat to admit slow-roll during the present stage of cosmic history. This corresponds to an extremely light

scalar field, establishing a new long range interaction - in addition to standard model physics -, which is phenomenologically dangerous and represents the major obstacle against a realization within particle physics. The dilaton e.g. is characterized by an exponential potential, which is commonly considered to be modified by perturbative corrections [50]; the resulting theory would rather belong to the first class.

While the cosmological constant requires one single fine tuning, dynamical models featuring scalar fields are possibly subject to different kinds of tuning, even in the simplest, minimally coupled, case of quintessence. The *dark energy density* is the adequate quantity to be compared with the cosmological constant, interpreted as vacuum energy. Any dynamical model, to be preferable over the cosmological constant, is at least required to allow for a significantly larger contribution to the energy density in the past. In chapter 5 we introduced the following criterion:

$$\left.\frac{\Omega_{DE}}{\Omega_\Lambda}\right|_{BBN} \gg 1.$$

We have seen that some of the quintessence models we discussed already fail to match this criterion, if not refering to an unreasonable choice of initial conditions.

Secondly, the *energy scale of the potential* determines the present dark energy density. The deviation of the two quantities corresponds to the deviation of the equation of state from $w_{DE} = -1$ at present. Together with a second parameter, determining its slope (or the field mass, respectively), the potential scale has to be infered from more fundamental principles, within a general theoretical framework. But the margin of both parameters becomes smaller and smaller, the more the model is required to mimic the late time behaviour of a cosmological constant.

Finally, the "initial" (in our case: BBN) value of the dark energy density is determined not only by the potential scale, but also by *initial conditions* on field value and velocity. The main issue in dynamical model building is the search for attractor solutions, which can reproduce the observed late time evolution of the dark energy sector, being independent of initial conditions. To realize the present universe as a global attractor, quintessence models are forced to refer to the introduction of additional parameters [4, 8]. Instead, late time attractors of runaway models are typically characterized by $\Omega_{DE} = 1$ and

$$-\frac{1}{3} > w_{DE} > -1.$$

In the attempt to solve or at least alleviate the coincidence problem, inverse power-law, "tracking" potentials have been regarded as exceptionally promising. The tracker solution corresponds to a sequence of radiation and matter dominated scaling regimes, in agreement with standard ΛCDM cosmology, followed by a period of accelerated expansion. Though, during earlier stages of cosmic history, the evolution of the scalar field is quite sensitive to the choice of initial conditions, the - observable - late time behaviour should be entirely determined by the tracker solution. Unfortunately, as has been noticed lately [15], this advantage disappears, if the model is required to mimic the behaviour of a cosmological constant around the present - which seems necessary to stay in agreement with observations. As we have seen in chapter 5, this leads to the loss of predictiveness: A quintessence model with $V \sim \phi^{-1}$ is not falsifiable by reconstruction of its equation of state.

The main purpose of our thesis has been to investigate, whether modifications with respect to the single field, quintessence case can help to alleviate - or even avoid - the fine

tuning problems of model building. Within the framework of scalar-tensor theories, we explored consequences of the non-minimal coupling between scalar field and Ricci curvature, and of the introduction of a second, minimally or non-minimally coupled scalar field. In both cases the increase in complexity - in the number of model parameters - is soundly motivated. Though we have given some examples, how to improve the situation gradually, we have to conclude, that the problem of dependence on initial conditions remains far from being solved. Since none of the simple effective models we discussed in this thesis realizes the present stage of the universe as a global attractor, some dependence on initial conditions is inevitable.

In detail, we have followed the "$R-$boost" proposal of [7, 62, 73] and provided a classification of (Jordan frame) coupling functions admitting cosmological scaling solutions. In particular, we have found that models with $F(\phi) = \xi\phi^2 + const$, including original Brans-Dicke theory, allow for scaling attractor solutions during matter dominated epoch, if either the potential force term is subdominant in the equation of motion, or the potential is of the inverse power-law type and matching, or dominating, the strength of the coupling term. We have investigated the corresponding class of models in the Einstein frame as well, using a dynamical systems method, and verified both the existence of the $R-$boost, and the fact that it can reduce dependence on initial conditions. Unfortunately, scalar-tensor theories with constant (Einstein frame) coupling do not share the attractive property of convergence to general relativity. The effectiveness of the $R-$boost is therefore limited due to experimental and observational constraints on the coupling strength.

Alternatively, we have considered a model proposed by Bartolo and Pietroni [9], which incorporates an attractor mechanism to general relativity, due to an exponentially decaying (Einstein frame) coupling. In this case, the late time attractor is indistinguishable from inverse-power law quintessence, but the coupling is allowed to be significantly stronger in the early universe. Since now model building relies on two independent functions, the potential parameters can be adjusted to mimic a cosmological constant around the present, while the dependence on initial conditions is reduced due to the enhanced $R-$boost. However, in our numerical example we have found significant evolution at low redshift, allowing the model to be distinguished from a cosmological constant, as soon as observational data permit an improved reconstruction of the equation of state.

Though dark energy models featuring a second scalar field rely on a larger number of free parameters, the examples we have investigated in chapter 6 do not exhibit additional qualitative features. On the contrary, regarding their phenomenological implications, they can be approximated within a single field set-up under some very general and natural conditions. In our extended version of the Sonner-Townsend axion-dilaton model, the dilaton turns out to be the relevant dynamical ingredient in a wide (and reasonable) range of parameter space, while the axion is fastly stabilized to a fixed value, only due to enhanced friction. The resulting family of models, effectively featuring only one field, is conformally equivalent to Brans-Dicke theory with inverse-power law potential, and corresponds to the class of models identified in chapter 4.

On the other hand, we have reproduced the relevant features of the shape moduli proposal of Peleso and Poppitz within a class of two-field models, which share the phenomenological properties of an axion type, single field model. Under certain assumptions concerning initial field values, the presence of the second field has a stabilizing effect on the relevant "sit and wait" behaviour, again because of enhanced friction.

None of our model examples unites all the different attractive features we discussed in

the preceding chapters, like convergence to Einstein theory, existence of subceding scaling solutions, corresponding to the evolutionary sequence of standard cosmology, or an effective $R-$boost mechanism to reduce dependence on initial conditions. Furthermore it remains unclear, to which extent the model parameters can be infered from more fundamental theories.

In the shape moduli proposal of Peloso and Poppitz, the phenomenologically relevant model parameters are directly related to geometrical and field theoretical considerations: The properties of the Casimir potential are deduced from the length scale of two "large" extra dimensions, and the assumption of a Planck suppressed communication of brane-localized SUSY breakdown to the bulk field content. The model still has one significant disadvantage: initial field values have to be chosen close to a saddle point of the Casimir potential - otherwise the shape moduli fail to provide a quintessence candidate at all.

On the other hand, the authors only assumed, that the internal orbifold volume can be stabilized by the interplay between a negative cosmological constant, and the magnetic flux of a gauge field in the bulk. An interesting issue of further research would be to explore the dynamical interaction between volume and shape moduli during the compactification regime. Within this generalized set-up, it might be possible to derive constraints on the allowed range of "initial" conditions for the shape moduli, acting as quintessence. Though this consideration is entirely speculative, the idea of dynamical generation of "initial" conditions is worthwile to be kept in mind. (In principle, the $R-$boost mechanism can be interpreted in the same spirit, as we have already remarked in chapter 5.)

Given the fact, that none of our simple models is capable to completely avoid dependence on initial conditions, it seems to be a promising objective to search for a physically motivated, dynamical selection mechanism to complement the conventional conception of a basin of attraction. On the other hand, this is yet an additional requirement model building efforts are challenged with, and not so very different from the introduction of additional parameters. But as long as the predicted redshift evolution of the equation-of-state parameter, $w_{DE}(z)$, changes from trajectory to trajectory, a dynamical model is definitely incomplete. On the other hand, the reconstruction of the equation of state from supernovae and other available data has to be supplemented by additional information - e.g. concerning the possible evolution of electromagnetic fine structure and gravitational constant on cosmological time scale -, to improve our capability of model selection.

We have not yet taken into account possible deviations from the assumed homogeinity of the scalar field(s), and the resulting effects on perturbation growth and large scale structure formation. It is commonly assumed, that future weak lensing surveys of cosmic shear will provide complementary information on the nature of dark energy [52]. A combined effort to reconstruct not only the expansion history but also the growth history of the universe might be able to decide, whether dark energy is a dynamical quantity or not, hopefully within the forthcoming decade.

In summary, we have learned that scalar field dynamical models of dark energy are, in principle, capable to mimic a cosmological constant around the present. But the closer the equation of state has to approach $w_{DE} = -1$, the less attractive they become; not only because the allowed range in parameter space is reduced, but also since the late time evolution develops an increasing sensitivity to initial conditions. On the other hand, it is still possible that the cosmological constant will be definitely ruled out by observations one day. In that case, sound knowledge of dynamical alternatives will turn out to be crucial, in order to understand the origin of dark energy.

Acknowledgements

I am very grateful to my supervisor, Prof. Wilfried Buchmüller, who gave enjoyable leeway to me, but, whenever it came to the point, prevented me from hunting phantoms.

Thanks to Prof. Jan Louis for co-supervising this thesis.

Futhermore, I wish to thank Riccardo Catena for his advice, helpful discussions, and for proofreading of the manuscript.

Bibliography

[1] Ujjaini Alam, Varun Sahni, and Alexei A. Starobinsky. Exploring the properties of dark energy using type Ia supernovae and other datasets. *JCAP*, 0702:011, 2007. [astro-ph/0612381].

[2] Luca Amendola. Coupled quintessence. *Phys. Rev.*, D62:043511, 2000. [astro-ph/9908023].

[3] Luca Amendola, Miguel Quartin, Shinji Tsujikawa, and Ioav Waga. Challenges for scaling cosmologies. *Phys. Rev.*, D74:023525, 2006. [astro-ph/0605488].

[4] Luca Amendola and Domenico Tocchini-Valentini. Stationary dark energy: The present universe as a global attractor. *Phys. Rev.*, D64:043509, 2001. [astro-ph/0011243].

[5] C. Armendariz-Picon, Viatcheslav F. Mukhanov, and Paul J. Steinhardt. Essentials of k-essence. *Phys. Rev.*, D63:103510, 2001. [astro-ph/0006373].

[6] Pierre Astier et al. The SuperNova Legacy Survey: Measurement of Ω_m, Ω_Λ and w from the first year data set. *Astron. Astrophys.*, 447:31–48, 2006. [astro-ph/0510447].

[7] Carlo Baccigalupi, Sabino Matarrese, and Francesca Perrotta. Tracking extended quintessence. *Phys. Rev.*, D62:123510, 2000. [astro-ph/0005543].

[8] T. Barreiro, Edmund J. Copeland, and N. J. Nunes. Quintessence arising from exponential potentials. *Phys. Rev.*, D61:127301, 2000. [astro-ph/9910214].

[9] Nicola Bartolo and Massimo Pietroni. Scalar tensor gravity and quintessence. *Phys. Rev.*, D61:023518, 2000. [hep-ph/9908521].

[10] J. Berian James, Tamara M. Davis, Brian P. Schmidt, and Alex G. Kim. Spectral diversity of type Ia supernovae. *Mon. Not. Roy. Astron. Soc.*, 370:933–940, 2006. [astro-ph/0605147].

[11] Orfeu Bertolami, F. Gil Pedro, and M. Le Delliou. Dark energy-dark matter interaction and the violation of the equivalence principle from the abell cluster a586. astro-ph/0703462, 2007.

[12] B. Bertotti, L. Iess, and P. Tortora. A test of general relativity using radio links with the Cassini spacecraft. *Nature*, 425:374, 2003.

[13] Andrew P. Billyard, Alan A. Coley, and James E. Lidsey. Cyclical behaviour in early universe cosmologies. *J. Math. Phys.*, 41:6277–6283, 2000. [gr-qc/0005118].

[14] Milutin Blagojević. *Gravitation and Gauge Symmetries*. Institute of Physics Publishing, 2002.

[15] Sidney Bludman. Tracking quintessence would require two cosmic coincidences. *Phys. Rev.*, D69:122002, 2004. [astro-ph/0403526].

[16] J. Richard Bond, Lev Kofman, Sergey Prokushkin, and Pascal M. Vaudrevange. Roulette inflation with Kähler moduli and their axions. hep-th/0612197.

[17] Camille Bonvin, Chiara Caprini, and Ruth Durrer. A no-go theorem for k-essence dark energy. *Phys. Rev. Lett.*, 97:081303, 2006. [astro-ph/0606584].

[18] C. Brans and R. H. Dicke. Mach's principle and a relativistic theory of gravitation. *Phys. Rev.*, 124:925–935, 1961.

[19] P. Brax, J. Martin, and A. Riazuelo. Quintessence model building. hep-th/0109207.

[20] Philippe Brax and Jerome Martin. Moduli fields as quintessence and the chameleon. hep-th/0612208.

[21] Philippe Brax and Jerome Martin. Quintessence and supergravity. *Phys. Lett.*, B468:40–45, 1999.

[22] Jean-Philippe Bruneton. On causality and superluminal behavior in classical field theories. Applications to k-essence theories and MOND-like theories of gravity. gr-qc/0607055.

[23] Mark Byrne and Christopher Kolda. Quintessence and varying α from shape moduli. hep-ph/0402075.

[24] S. Carloni, S. Capozziello, J.A. Leach, and P.K.S. Dunsby. Cosmological dynamics of scalar-tensor gravity. gr-qc/0701009.

[25] Sean M. Carroll. *Spacetime and Geometry*. Addison Wesley, 2004.

[26] Riccardo Catena, N. Fornengo, A. Masiero, Massimo Pietroni, and Francesca Rosati. Dark matter relic abundance and scalar-tensor dark energy. *Phys. Rev.*, D70:063519, 2004. [astro-ph/0403614].

[27] Riccardo Catena, M. Pietroni, and L. Scarabello. Dynamical relaxation of the dark matter to baryon ratio. *Phys. Rev.*, D70:103526, 2004. [astro-ph/0407646].

[28] Riccardo Catena, Massimo Pietroni, and Luca Scarabello. Einstein and Jordan reconciled: a frame-invariant approach to scalar-tensor cosmology. astro-ph/0604492.

[29] Pisin Chen. Dark energy and the hierarchy problem. hep-ph/0611378.

[30] James M. Cline. String cosmology. hep-th/0612129, 2006.

[31] Edmund J. Copeland, Andrew R. Liddle, and David Wands. Exponential potentials and cosmological scaling solutions. *Phys. Rev.*, D57:4686–4690, 1998. [gr-qc/9711068].

[32] Edmund J. Copeland, N. J. Nunes, and Francesca Rosati. Quintessence models in supergravity. *Phys. Rev.*, D62:123503, 2000. [hep-ph/0005222].

[33] Edmund J. Copeland, M. Sami, and Shinji Tsujikawa. Dynamics of dark energy. *Int. J. Mod. Phys.*, D15:1753–1936, 2006. [hep-th/0603057].

[34] T. Damour, G. W. Gibbons, and C. Gundlach. Dark matter, time varying G, and a dilaton field. *Phys. Rev. Lett.*, 64:123–126, 1990.

[35] T. Damour and K. Nordtvedt. Tensor - scalar cosmological models and their relaxation toward general relativity. *Phys. Rev.*, D48:3436–3450, 1993.

[36] Thibault Damour. Gravitation, experiment and cosmology. gr-qc/9606079.

[37] Thibault Damour, Federico Piazza, and Gabriele Veneziano. Runaway dilaton and equivalence principle violations. *Phys. Rev. Lett.*, 89:081601, 2002. [gr-qc/0204094].

[38] Keith R. Dienes. Shape versus volume: Making large flat extra dimensions invisible. *Phys. Rev. Lett.*, 88:011601, 2002. [hep-ph/0108115].

[39] Paul A. M. Dirac. New basis for cosmology. *Proc. Roy. Soc. Lond.*, A165:199–208, 1938.

[40] Albert Einstein. Cosmological considerations in the general theory of relativity. *Sitzungsber. Preuss. Akad. Wiss. Berlin (Math. Phys.)*, 1917:142–152, 1917.

[41] Daniel J. Eisenstein et al. Detection of the baryon acoustic peak in the large-scale correlation function of SDSS luminous red galaxies. *Astrophys. J.*, 633:560–574, 2005. [astro-ph/0501171].

[42] George Ellis, Roy Maartens, and Malcolm MacCallum. Causality and the speed of sound. gr-qc/0703121, 2007.

[43] G. Esposito-Farese and D. Polarski. Scalar-tensor gravity in an accelerating universe. *Phys. Rev.*, D63:063504, 2001. [gr-qc/0009034].

[44] Valerio Faraoni and Shahn Nadeau. The (pseudo)issue of the conformal frame revisited. *Phys. Rev.*, D75:023501, 2007. [gr-qc/0612075].

[45] Joshua A. Frieman, Christopher T. Hill, Albert Stebbins, and Ioav Waga. Cosmology with ultralight pseudo Nambu-Goldstone bosons. *Phys. Rev. Lett.*, 75:2077–2080, 1995. [astro-ph/9505060].

[46] Yasunori Fujii and Kei-Ichi Maeda. *The Scalar-Tensor Theory of Gravitation*. Cambridge University Press, 2003.

[47] George Gamov. *My world line*. New York, 1970.

[48] Radouane Gannouji, David Polarski, Andre Ranquet, and Alexei A. Starobinsky. Scalar-tensor models of normal and phantom dark energy. *JCAP*, 0609:016, 2006. [astro-ph/0606287].

[49] Carl L. Gardner. Quintessence and the transition to an accelerating universe. *Nucl. Phys.*, B707:278–300, 2005. [astro-ph/0407604].

[50] M. Gasperini. Dilaton cosmology and phenomenology. hep-th/0702166.

[51] E. Gaztañaga, E. Garcia-Berro, J. Isern, E. Bravo, and I. Dominguez. Bounds on the possible evolution of the gravitational constant from cosmological type Ia supernovae. *Phys. Rev.*, D65:023506, 2002. [astro-ph/0109299].

[52] A. F. Heavens, Thomas D. Kitching, and A. N. Taylor. Measuring dark energy properties with 3d cosmic shear. *Mon. Not. Roy. Astron. Soc.*, 373:105–120, 2006. [astro-ph/0606568].

[53] A. Hebecker and C. Wetterich. Natural quintessence? *Phys. Lett.*, B497:281–288, 2001. [hep-ph/0008205].

[54] Edwin Hubble. A relation between distance and radial velocity among extra–galactic nebulae. *Proc. Nat. Acad. Sci.*, 15:168–173, 1929.

[55] Pascual Jordan. *Schwerkraft und Weltall*. Vieweg, Braunschweig, 1955.

[56] Lawrence M. Krauss, Katherine Jones-Smith, and Dragan Huterer. Dark energy, a cosmological constant, and type Ia supernovae. astro-ph/0701692.

[57] Seokcheon Lee. Time variation of fine structure constant and proton - electron mass ratio with quintessence. astro-ph/0702063.

[58] Bruno Leibundgut. Type Ia supernovae. *Astron. Astrophys. Rev.*, 10:179, 2000. [astro-ph/0003326].

[59] Andrew R. Liddle and Robert J. Scherrer. A classification of scalar field potentials with cosmological scaling solutions. *Phys. Rev.*, D59:023509, 1999. [astro-ph/9809272].

[60] Filippo Mannucci, M. Della Valle, and N. Panagia. Two populations of progenitors for type Ia SNe. *Mon. Not. Roy. Astron. Soc.*, 370:773–783, 2006. [astro-ph/0510315].

[61] C. J. A. P. Martins. Astrophysical probes of fundamental physics. astro-ph/0610665.

[62] Sabino Matarrese, Carlo Baccigalupi, and Francesca Perrotta. Approaching Lambda without fine-tuning. *Phys. Rev.*, D70:061301, 2004. [astro-ph/0403480].

[63] Viatcheslav Mukhanov. *Physical Foundations of Cosmology*. Cambridge University Press, 2005.

[64] S. C. C. Ng, N. J. Nunes, and Francesca Rosati. Applications of scalar attractor solutions to cosmology. *Phys. Rev.*, D64:083510, 2001. [astro-ph/0107321].

[65] John A. Peacock. *Cosmological Physics*. Cambridge University Press, 1999.

[66] R. D. Peccei and Helen R. Quinn. Constraints imposed by CP conservation in the presence of instantons. *Phys. Rev.*, D16:1791–1797, 1977.

[67] R. D. Peccei and Helen R. Quinn. CP conservation in the presence of instantons. *Phys. Rev. Lett.*, 38:1440–1443, 1977.

[68] R. D. Peccei, J. Sola, and C. Wetterich. Adjusting the cosmological constant dynamically: Cosmons and a new force weaker than gravity. *Phys. Lett.*, B195:183, 1987.

[69] P. J. E. Peebles and Bharat Ratra. Cosmology with a time variable cosmological constant. *Astrophys. J.*, 325:L17, 1988.

[70] Marco Peloso and Erich Poppitz. Quintessence from shape moduli. *Phys. Rev.*, D68:125009, 2003. [hep-ph/0307379].

[71] S. Perlmutter et al. Discovery of a supernova explosion at half the age of the universe and its cosmological implications. *Nature*, 391:51–54, 1998. [astro-ph/9712212].

[72] Francesca Perrotta and Carlo Baccigalupi. On the dark energy clustering properties. *Phys. Rev.*, D65:123505, 2002. [astro-ph/0201335].

[73] Valeria Pettorino, C. Baccigalupi, and F. Perrotta. Scaling solutions in scalar-tensor cosmologies. *JCAP*, 0512:003, 2005. [astro-ph/0508586].

[74] Massimo Pietroni. Brane worlds and the cosmic coincidence problem. *Phys. Rev.*, D67:103523, 2003. [hep-ph/0203085].

[75] Philipp Podsiadlowski, Paolo A. Mazzali, Pierre Lesaffre, Christian Wolf, and Francisco Forster. Cosmological implications of the second parameter of type Ia supernovae. astro-ph/0608324.

[76] Eduardo Ponton and Erich Poppitz. Casimir energy and radius stabilization in five and six dimensional orbifolds. *JHEP*, 06:019, 2001. [hep-ph/0105021].

[77] Bharat Ratra and P. J. E. Peebles. Cosmological consequences of a rolling homogeneous scalar field. *Phys. Rev.*, D37:3406, 1988.

[78] Alain Riazuelo and Jean-Philippe Uzan. Cosmological observations in scalar-tensor quintessence. *Phys. Rev.*, D66:023525, 2002. [astro-ph/0107386].

[79] Adam G. Riess et al. New hubble space telescope discoveries of type Ia supernovae at $z > 1$: Narrowing constraints on the early behavior of dark energy. astro-ph/0611572.

[80] Adam G. Riess et al. Observational evidence from supernovae for an accelerating universe and a cosmological constant. *Astron. J.*, 116:1009–1038, 1998. [astro-ph/9805201].

[81] Adam G. Riess et al. Type Ia supernova discoveries at $z > 1$ from the hubble space telescope: Evidence for past deceleration and constraints on dark energy evolution. *Astrophys. J.*, 607:665–687, 2004. [astro-ph/0402512].

[82] Varun Sahni. The cosmological constant problem and quintessence. *Class. Quant. Grav.*, 19:3435–3448, 2002. [astro-ph/0202076].

[83] Mia Schelke, Riccardo Catena, Nicolao Fornengo, Antonio Masiero, and Massimo Pietroni. Constraining pre big-bang nucleosynthesis expansion using cosmic antiprotons. *Phys. Rev.*, D74:083505, 2006. [hep-ph/0605287].

[84] Paolo Serra, Alan Heavens, and Alessandro Melchiorri. Bayesian evidence for a cosmological constant using new high-redshift supernovae data. astro-ph/0701338.

[85] Pierre Sikivie. Axion cosmology. astro-ph/0610440.

[86] Julian Sonner and Paul K. Townsend. Recurrent acceleration in dilaton-axion cosmology. *Phys. Rev.*, D74:103508, 2006. [hep-th/0608068].

[87] D. N. Spergel et al. Wilkinson microwave anisotropy probe (WMAP) three year results: Implications for cosmology. astro-ph/0603449.

[88] Paul J. Steinhardt, Li-Min Wang, and Ivaylo Zlatev. Cosmological tracking solutions. *Phys. Rev.*, D59:123504, 1999. [astro-ph/9812313].

[89] Peter Svrcek. Cosmological constant and axions in string theory. hep-th/0607086.

[90] M. Tegmark et al. Cosmological constraints from the SDSS luminous red galaxies. *Phys. Rev.*, D74:123507, 2006. [astro-ph/0608632].

[91] Thomas Thiemann. Solving the problem of time in general relativity and cosmology with phantoms and k-essence. astro-ph/0607380.

[92] A. J. Tolley, C. P. Burgess, C. de Rham, and D. Hoover. Scaling solutions to 6d gauged chiral supergravity. *New J. Phys.*, 8:324, 2006. [hep-th/0608083].

[93] Diego F. Torres. Quintessence, super-quintessence and observable quantities in Brans-Dicke and non-minimally coupled theories. *Phys. Rev.*, D66:043522, 2002. [astro-ph/0204504].

[94] Jean-Philippe Uzan. Cosmological scaling solutions of non-minimally coupled scalar fields. *Phys. Rev.*, D59:123510, 1999. [gr-qc/9903004].

[95] C. Wetterich. Cosmology and the fate of dilatation symmetry. *Nucl. Phys.*, B302:668, 1988.

[96] Christof Wetterich. The cosmon model for an asymptotically vanishing time dependent cosmological 'constant'. *Astron. Astrophys.*, 301:321–328, 1995. [hep-th/9408025].

[97] W. Michael Wood-Vasey et al. Observational constraints on the nature of the dark energy: First cosmological results from the ESSENCE supernova survey. astro-ph/0701041.

[98] S. E. Woosley, Daniel Kasen, S. Blinnikov, and E. Sorokina. Type Ia supernova light curves. astro-ph/0609562.

[99] Y. B. Zeldovich. Cosmological constant and elementary particles. *JETP Lett.*, 6:316, 1967.

[100] Bruno Zumino. Supersymmetry and the vacuum. *Nucl. Phys.*, B89:535, 1975.

Erklärung

Ich versichere, dass ich diese Arbeit selbständig verfasst, und keine anderen als die angegebenen Hilfsmittel und Quellen benutzt habe. Ausserdem bin ich mit einer Ausleihe bzw. Veröffentlichung einverstanden.

Hamburg,